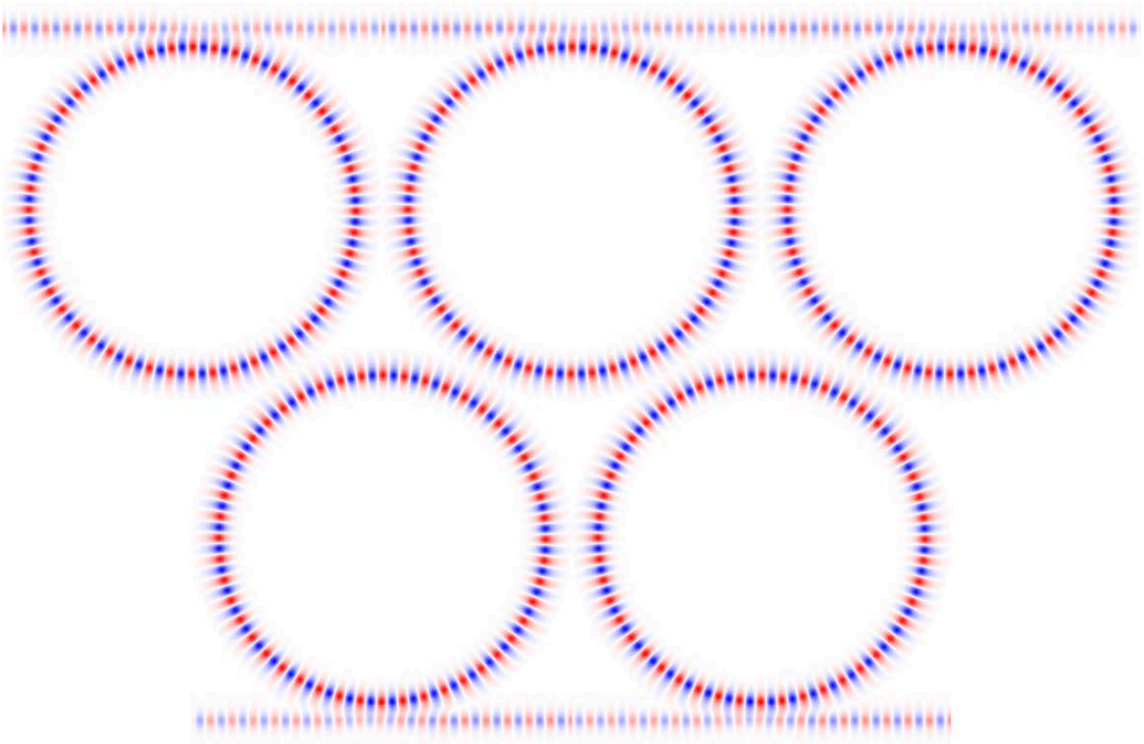

XXXII International Workshop on Optical Wave & Waveguide Theory and Numerical Modelling

April 8-10, 2026 – Lausanne, Switzerland

Conference guide and book of abstracts

Workshop program

Wednesday, April 8	
8:00	Registration
9:00	Workshop opening
	Numerical methods 1 Chair: Carsten Rockstuhl
9:15	**Metasurface modelling using GSTC method** Karim Achouri, *Swiss Federal Technology Institute of Lausanne (EPFL), Switzerland*
9:45	**Computational nanophotonics with the boundary elements method and mesoscopic boundary conditions** Ulrich Hohenester, *University of Graz, Austria*
10:15	Group photo, coffee & posters
	Numerical methods 2 Chair: Felix Binkowski
11:15	**Modelling Photonic Crystal Surface-Emitting Lasers Using the Time-Domain Unstructured Transmission Line Method** Ana Vukovic, *University of Nottingham, United Kingdom*
11:45	**Finite element method based frameworks for efficient simulations and optimizations in nano-photonics** Sven Burger, *Zuse Institute Berlin, Germany*
12:15	Lunch & posters
	Quantum nanophotonics Chair: Stefan Rotter
13:30	**Quantum Dynamics in Nanoplasmonic Cavities** Ortwin Hess, *Trinity College Dublin, Ireland*
14:00	**Fully atomistic modelling of plasmonic nanostructures** Chiara Cappelli, *Scuola Normale Superiore, Italy*
14:30	**Nonreciprocal plasmons in one-dimensional carbon nanostructures** Álvaro Rodriguez Echarri, *AMOLF, The Netherlands*
15:00	Coffee & posters
	Electromagnetism fundamentals Chair: Alain Dereux
15:45	**The flow of Fisher information in electromagnetism** Stefan Rotter, *Vienna University of Technology, Austria*
16:15	**Multipole analysis of the resonant electromagnetic response of particle clusters and metasurfaces** Andrey Evlyukhin, *Leibniz University Hannover, Germany*
16:45	**Bias-free optical nonreciprocity and directional dichroism** Viktar Asadchyi, *Aalto University, Finland*
17:15	Posters, beers & nibbles
21:00	End of day 1

Thursday, April 9	
	Device design and optimization 1 Chair: Ulrich Hohenester
9:00	**Inverse design of free-form metadevices** Carsten Rockstuhl, *Karlsruhe Institute of Technology, Germany*
9:30	**Simulation and Optimization of Large-Scale Metasurfaces** Jens Niegemann, *Synopsis, Inc., Vancouver, Canada*
10:00	Coffee & posters
	Device design and optimization 2 Chair: Pavel Peterka
11:00	**Modelling high-NA EUV lithography** Peter Evanschitzky, *Fraunhofer Institute for Integrated Systems and Device Technology, Germany*
11:30	**Future directions and needs for the modelling of optical structures in research and industry** Round-table discussion
12:15	Lunch & posters
	Applied numerical modelling in nanophotonics Chair: Ana Vukovic
13:30	**Cavity-resonator-integrated grating filters for second harmonic generation** Anne-Laure Fehrembach, *Fresnel Institute, France*
14:00	**Nanoparticles Identification from Scattering Data** Alexander A. Iskandar, *Bandung Institute of Technology, Indonesia*
14:30	**Numerical modelling of fiber lasers based on active fibers with structured cores** Pavel Peterka, *Institute of Photonics and Electronics of the Czech Academy of Sciences, Czechia*
15:00	**Semi-analytical modeling of feedback trapping in optical nanocavities** Martijn Wubs, *Technical University of Denmark, Denmark*
15:45	Coffee & posters
16:15	Excursion & conference dinner & best poster awards
22:00	End of day 2

Friday, April 10	
	Numerical methods 3 Chair: Anne-Laure Fehrembach
9:00	**Optimized Principal Volume in the Green Dyadic Method** Alain Dereux, *University of Burgundy Europe, France*
9:30	**Computing resonance modes and resonance expansions using AAA rational approximation** Felix Binkowski, *Zuse Institute Berlin, Germany*
10:00	Coffee & posters
	ML and AI for nanophotonics Chair: Karim Achouri
10:45	**Numerical modelling and shaping of nanoscale light-matter interactions with Discontinuous Galerkin methods and machine learning algorithms** Stéphane Lanteri, *Côte d'Azur University, France*
11:15	**Photonic reservoir computing on a system with hysteresis** Sendy Phangl, *University of Nottingham, United Kingdom*
11:45	Final remarks
12:00	Lab tour (optional)

Reaching venue

OWTNM26 will take place on the campus of the Swiss Federal Institute of Technology Lausanne (EPFL).

The EPFL campus is connected to the city by the M1 Subway, which has two end stations: Flon in downtown Lausanne, or Renens. Flon is a short subway train ride away (M2 line, 1 stop) from Lausanne railway station; Renens is another major stop on many train lines from Geneva airport, Zurich and Bern.

The workshop takes place in the lecture theatre ELA-1 in the electrical engineering buildings. Campus map can be found online: https://plan.epfl.ch
Follow this instruction to get to the venue from the metro stop:

- Leave the Metro station EPFL and take the underpassage towards the south (i.e. walk in the same direction as your train if you come from Flon and take the stairs down, or walk in the opposite direction as your train if you come from Renens and take the ramp down)
- On the other side of the underpassage, take the monumental stairs up
- Walk toward the south along the BM building (where the EPFL center for micro- and nanotechnology is located)
- Aim slightly towards the right to reach the EL building;
- Enter the building marked ELA1 in red, you've reach the venue!

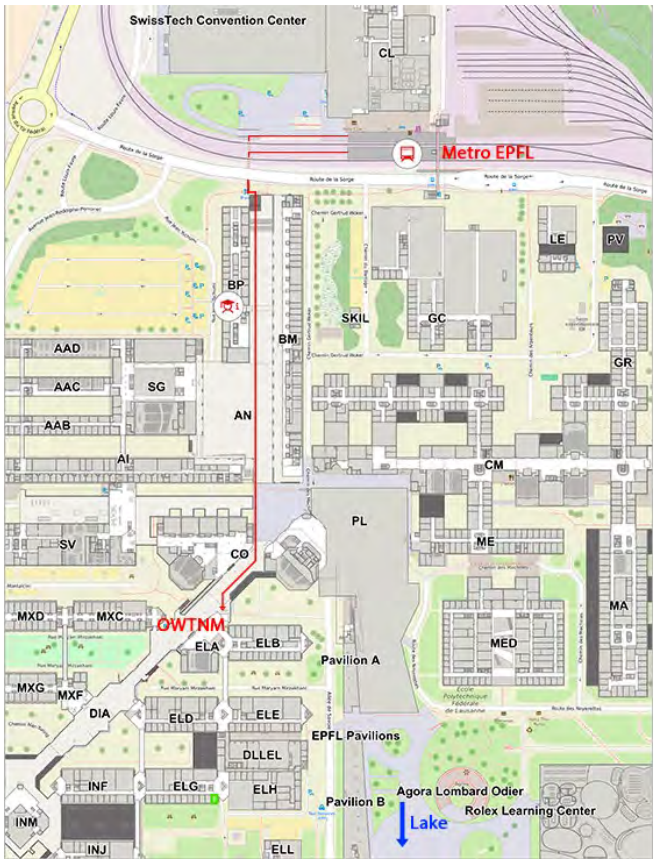

Sponsors

Swiss National Science Foundation

OPTICA

Ansys part of SYNOPSYS®

SWISS PHOTONICS

EPFL

iOptics

Excursion and conference dinner

The social activity and conference dinner are scheduled for Thursday evening (9th of April, 16:15–22:00).

Following a short ride from the venue and a scenic walk along the lake, participants will enjoy a guided tour of the Olympic Museum, located at Quai d'Ouchy 1, 1006 Lausanne, Switzerland (www.olympics.com/museum/). The evening will conclude with a banquet featuring stunning views of Lake Geneva and the best poster awards ceremony.

Pictures taken from https://www.lausanne-tourisme.ch/en/explore/the-olympic-museum/

Invited speakers

Karim Achouri
Metasurface modelling using GSTC method
Swiss Federal Technology Institute of Lausanne (EPFL), Switzerland

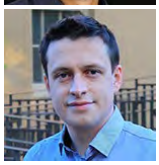

Viktar Asadchyi
Bias-free optical nonreciprocity and directional dichroism
Aalto University, Finland

Felix Binkowski
Computing resonance modes and resonance expansions using AAA rational approximation
Zuse Institute Berlin, Germany

Sven Burger
Finite element method based frameworks for efficient simulations and
optimizations in nano-photonics
Zuse Institute Berlin, Germany

Chiara Cappelli
Fully atomistic modelling of plasmonic nanostructures
Scuola Normale Superiore, Italy

Alain Dereux
Optimal large-scale radiative cooling devices
University of Burgundy Europe, France

Álvaro Rodriguez Echarri
Nonreciprocal plasmons in one-dimensional carbon nanostructures
AMOLF Institute, The Netherlands

Peter Evanschitzky
Modelling high-NA EUV lithography
Fraunhofer Institute for Integrated Systems and Device Technology, Germany

Andrey Evlyukhin
Multipole analysis of the resonant electromagnetic response of particle clusters and metasurfaces
Leibniz University Hannover, Germany

Anne-Laure Fehrembach
Cavity-resonator-integrated grating filters for second harmonic generation
Fresnel Institute, France

Ortwin Hess
Quantum Dynamics in Nanoplasmonic Cavities
Trinity College Dublin, Ireland

Ulrich Hohenester
Computational nanophotonics with the boundary elements method and mesoscopic boundary conditions
University of Graz, Austria

Alexander A. Iskandar
Controlling scattered light with symmetry and structure
Bandung Institute of Technology, Indonesia

Stéphane Lanteri
Numerical modelling and shaping of nanoscale light-matter interactions with Discontinuous Galerkin methods and machine learning algorithms
Côte d'Azur University, France

Jens Niegemann
Simulation and Optimization of Large-Scale Metasurfaces
Synopsis, Inc., Vancouver, Canada

Pavel Peterka
Numerical modelling of fiber lasers based on active fibers with structured cores
Institute of Photonics and Electronics of the Czech Academy of Sciences, Czechia

Sendy Phang
Photonic reservoir computing on a system with hysteresis
University of Nottingham, United Kingdom

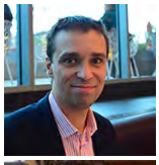

Carsten Rockstuhl
Inverse design of free-form metadevices
Karlsruhe Institute of Technology, Germany

Stefan Rotter
The flow of Fisher information in electromagnetism
Vienna University of Technology, Austria

Ana Vukovic
Implementation of laser gain models in the numerical Unstructured Time Domain Transmission Line (UTLM) method
University of Nottingham, United Kingdom

Martijn Wubs
Nanophotonic trapping
Technical University of Denmark, Denmark

List of posters

#	Title and presenting author
P1	**Compact angular filtering with metagratings** Mahmoud A. A. Abouelatta, EPFL - LEAP
P2	**Efficient Metasurface Modeling via Optimal Multipolar Decomposition of Bianisotropic Metasurfaces** Hossein Allahverdizadeh, EPFL - LEAP
P3	**Machine learning-driven inverse design of plasmonic metasurfaces** Amirmostafa Amirjani, KU Leuven, Belgium
P4	**Modulational instability recurrence in second-harmonic generation** Andrea Armaroli, University of Ferrara, Department of Engineering
P5	**Environmental Effects on Emitter–Plasmon Strong Coupling** Stavros Athanasiou, EPFL - NAM
P6	**Fabrication tolerance analysis of modal phase matching for second-harmonic generation in MgO-doped LNOI waveguides** Gaetano Bellanca, University of Ferrara
P7	**Inverse Design of InP Nanocavities for Photonic-Crystal-Based Random Lasing Networks** Enrico Bianco, EPFL - PSI
P8	**Electro-optical simulation of an integrated Ge-Si photodetector** Mariona Bonàs Vera, EPFL - PSI
P9	**Tricks and traps in the eigenmode analysis of periodic metal nanostructures** Sergejs Boroviks, EPFL - NAM
P10	**Multiscale computation of optical properties of soot nanoparticles: Coupling between atomistic DADI model and SIE method** Nicolas Brosseau-Habert, Université Maris et Louis Pasteur
P11	**Far-Field Patterns of Different Second-Harmonic Sources in Plasmonic Nanostructures** Ebru Buhara, EPFL - NAM
P12	**Transfer Matrix Modeling of Strong Light-Matter Coupling in the THz Range** Noureddine Charrouj, Institute of High Pressure Physics
P13	**High Quality factor Whispering Gallery Mode Microsphere Resonator Coupled to an On-Chip Waveguide** Naresh Choudhary, Indian Institute of Technology Madras
P14	**GPU accelerated tool for analysis of large scale diffractive optical elements** Adria Cobos Concha, Universitat Politècnica de Catalunya
P15	**Resonance prediction for plasmonic metal-insulator-metal waveguide filters** Shafaq Ejaz, Paderborn University Germany

P16	**Mittag-Leffler expansion of the scattering matrix for spherical particles via rescaled scattering channels** Elias Fösleitner, University of Graz
P17	**Mie Void Resonators for Programmable Quantum Emission Control** Yuchao Fu, EPFL - NAM
P18	**Physics-Informed Neural Networks for Confocal Fluorescence Imaging Under Wave-Optics Constraints** Fatima Zohra Goffi, Leibniz Institute of Photonic Technology
P19	**Momentum-related orthogonality of modes in dielectric optical waveguides** Manfred Hammer, Paderborn University
P20	**Multi-Photon Dynamics without Mode Decomposition** Bernd Levent Inci, Chair for Micro- and Nanoelectronics, TU Dortmund
P21	**A generalized perturbative approach for the computation of nonlinear scattering problems** Jérémy Itier, Institut Fresnel
P22	**PyMieDiff: Enabling differentiable Mie scattering through PyTorch** Oscar Jackson, University of Southampton
P23	**2D/3D FDTD Modeling of Coaxial Waveguide with Magnetized Nonlinear Ferrite and Slow-Wave Structure** Serhii Karelin, Kharkiv Institute of Physics and Technology
P24	**Inverse-designed Si-Sb2S3 tunable multi-mode interference coupler** Peter Kepič, Central European Institute of Technology, Brno University of Technology
P25	**Photonic structures in transition metal dichalcogenides for integrated quantum photonics** Anita Kohlwes, TU Dortmund Universtity
P26	**Decoupling nonlinear excitation and emission using dual bound states in the continuum** Changliang Li, EPFL - NAM
P27	**Self-Consistent Optical-Thermal Modeling of VO2 Nanoparticles for Tunable Photonic Applications** Filip Ligmajer, Brno University of Technology
P28	**Intelligent Multimodal Meta-lens Imaging and Perception** Xiaoyuan Liu, EPFL - NAM
P29	**A framework for modelling scattering of polarization-entangled photons** Ivan Lopushenko, University of Oulu
P30	**Structural perturbation theory for bound states in the continuum** Ya Yan Lu, City University of Hong Kong
P31	**Numerical Analysis of Finite-Difference PML Modes in Free-Space Problems** Hannes Lüder, VPIphotonics GmbH

P32	**Insights into the fluorescence and energy transfer simulations of periodic structures** Ilia Lykov, EPFL
P33	**Simulation of InP electro-optic modulator based on Pockels and Kerr effects** Cristina Garcia Marcilla, Paul Scherrer Institute
P34	**A surface integral equation framework for light scattering in layered media** Parmenion Mavrikakis, EPFL - NAM
P35	**Imaging of degenerate and hybridized plasmonic modes by cathodoluminescence spectroscopy** Viktor Myroshnychenko, Paderborn University
P36	**All-Dielectric Photo-thermo-optical Metasurfaces for Thermal Landscaping at the Nanoscale** Gopal Narmada Naidu, EPFL - STI
P37	**Extraction of intrinsic chiral effects via Mueller matrix polarimetric decomposition** Jeeban Kumar Nayak, NAM-EPFL
P38	**How to Build a Scattering Code with Mathematically Guaranteed Convergence** Alexander Nosich, Laboratory of Micro and Nano Optics, Institute of Radio-Physics and Electronics NASU, Kharkiv, Ukraine
P39	**Utilization of a Pair of Matched Dielectric Mirrors for Modes Filtering in Open Resonators** Vadym Pazynin, Technical University of Berlin, Berlin, Germany
P40	**A model of a quasi-single-mode Fabry-Perot resonator incorporating a tilted high-k frequency-selective dielectric plate** Vadym Pazynin, Technical University of Berlin, Berlin, Germany
P41	**Bound states in the continuum for guiding light** Jiří Petráček, Brno University of Technology, Brno, Czech Republic
P42	**GPU-Accelerated Graph-Based Maxwell Solver for Large-Scale Nanophotonic Simulations** Lorenzo Piatti, Harvard University
P43	**Optical Magnetic-Field-Gated Criticality in Photon Avalanching Processes** Benoît Reynier, University of Fribourg
P44	**A Magnetic Monopole Antenna** Benoît Reynier, University of Fribourg
P45	**Magnetoelectric Nonreciprocal Metasurfaces with Spontaneous Magnetization: Measurements and Analysis** Shadi Safaei Jazi, Aalto University
P46	**Enhanced Molecular Chiral Response Driven by Crosstalking Quasi-Bound States in the Continuum** Diana Shakirova, Institute of Physics, University of Graz

P47	**From Maxwell to Effective Hamiltonians: a Reduced-Order Framework for Layered Photonic Cavities** Jacek Szczytko, Faculty of Physics, University of Warsaw
P48	**Freeform light routing in photonic integrated circuits using hyperuniform disordered structures** Ali P. Vafa, University of Surrey
P49	**Fano resonances in deep subwavelength gratings** Steven Verwer, AMOLF
P50	**Passive and Active Plasmonic Metafiber Devices** Jiyong Wang, Hangzhou Dianzi University
P51	**Opto-mechanical analogue of Peierls transition** Torgom Yezekyan, University of Southern Denmark
P52	**Angle-Invariant Scattering in Metasurface** Mustafa Yucel, EPFL - LEAP
P53	**Low-frequency electromagnetic forces for bio-nanoparticle manipulations** Siarhei Zavatski, EPFL - NAM
P54	**Designing optical metagrating for total internal reflection** Vladimir Zenin, University of Southern Denmark

Invited talk abstracts

Metasurface modelling using the GSTC method

Karim Achouri

Institute of Electrical and Microengineering, École Polytechnique Fédérale de Lausanne (EPFL), Laboratory for Advanced Electromagnetics and Photonics, Lausanne, Switzerland
karim.achouri@epfl.ch

Metasurfaces have been a major topic of interest and scientific research of the past 15 years. In order to provide a physical understanding of the interaction between electromagnetic waves and metasurfaces, and to enable their efficient design, we have developed a theoretical and numerical framework to model, analyze, and synthesize these complex structures. Our approach is based on generalized sheet transition conditions (GSTC), which correspond to extended boundary conditions that we use to model metasurfaces as zero-thickness sheets harboring electric and magnetic multipolar responses [1].

This GSTC method now incorporates various numerical schemes [2], may be applied to nonlinear structures [3] and spatially nonlocal systems [4]. Finally, we are also able to connect the spatial symmetries of the metasurface structure to its scattering response [5].

At the conference, I will present some of our most recent developments, which cover the concepts of angle invariant scattering [6], the modelling of multipolar metasurfaces with different substrate and superstrate [7] and the design of metagratings performing the Fourier-filtering operations of step function in momentum space [8] and of a meta-pinhole [9].

This work is supported by the Swiss National Science Foundation (project TMSGI2_218392).

References

[1] K. Achouri and C. Caloz, *Electromagnetic Metasurfaces: Theory and Applications*. Hoboken, NJ: Wiley-IEEE Press, 2021.

[2] Y. Vahabzadeh, N. Chamanara, K. Achouri, and C. Caloz, "Computational Analysis of Metasurfaces," *IEEE J. Multiscale Multiphys. Comput. Tech.*, vol. 3, pp. 37–49, 2018.

[3] K. Achouri, G. D. Bernasconi, J. Butet, and O. J. F. Martin, "Homogenization and Scattering Analysis of Second-Harmonic Generation in Nonlinear Metasurfaces," *IEEE Trans. Antennas Propagat.*, vol. 66, pp. 6061–6075, Nov. 2018.

[4] K. Achouri and O. J. F. Martin, "Extension of Lorentz reciprocity and Poynting theorems for spatially dispersive media with quadrupolar responses," *Phys. Rev. B*, vol. 104, p. 165426, Oct. 2021.

[5] K. Achouri, V. Tiukuvaara, and O. J. F. Martin, "Spatial symmetries in nonlocal multipolar metasurfaces," *Adv. Photon.*, vol. 5, June 2023.

[6] M. Yücel, F. S. Cuesta, and K. Achouri, "Angle-invariant scattering in metasurfaces," *Physical Review B*, vol. 111, June 2025.

[7] H. Allahverdizadeh and K. Achouri, "Multipolar angular scattering of substrated metasurfaces," *Physical Review B*, vol. 112, Dec. 2025.

[8] M. A. A. Abouelatta, S. Boroviks, O. J. F. Martin, and K. Achouri, "Step function in momentum space by a metagrating," *Advanced Optical Materials*, Sept. 2025.

[9] M. A. Abouelatta and K. Achouri, "Metapinhole: Planar fourier optics without lenses," *arXiv preprint arXiv:2509.05555*, 2025.

Nanophotonic simulations using the boundary element method

U. Hohenester[1,*]
[1]*Institute of Physics, University of Graz, Universitätsplatz 5, 8010 Graz, Austria*
*ulrich.hohenester@uni-graz.at

Computational Maxwell solvers based on the boundary element method (BEM) enable fast and accurate simulations of sufficiently small scatterers. Over the last few years, we have developed our own BEM Maxwell solver termed nanobem, and have implemented the computation of T-matrices for scatterers with arbitrary geometries [1].

The combination of BEM and T-matrices has allowed us to develop two add-ons to the nanobem toolbox dealing with optical tweezers and optical interference microscopies, which have been used for life science applications. In this talk I will first present our simulation approach for optofluidic force induction, a novel nanoparticle characterization scheme based on optical and fluidic forces [2]. I will then discuss interference scattering microscopy, allowing for the label-free localization of proteins and other nanoparticles, and how it can be efficiently simulated with our toolbox. An outlook to future developments will summarize the talk.

References

[1] N. Asadova et al., JQSRT 333, 109310 (2025).
[2] M. Šimić et al., Nano Letters 25, 8805 (2025).
[3] F. Hitzelhammer et al., ACS Photonics 11, 2745 (2024).

Modelling Photonic Crystal Surface-Emitting Lasers (PCSELs) Using the Time-Domain Unstructured Transmission Line Method (UTLM)

Ana Vukovic*, Phillip Sewell

Faculty of Engineering, University of Nottingham, Nottingham, United Kingdom

*ana.vukovic@nottingham.ac.uk

Abstract

Photonic Crystal Surface-Emitting Lasers (PCSELs) are promising candidates for the realization of single-mode, high-power, and high-brightness lasers [1,2]. PCSELs of different sizes can be fabricated to suit particular applications. Large-area PCSELs (~3 mm emission diameter) have demonstrated continuous-wave lasing at 50 W with highly collimated output beams and a divergence of only 1/20th of a degree. In contrast, smaller-area PCSELs (~9 μm emission diameter) offer the possibility of rapid on–off switching for communication purposes.

PCSELs feature a sophisticated epitaxial structure composed of active and passive layers, highly reflective mirrors, and a photonic crystal (PC) lattice layer [1,2]. The lasing power depends on a number of factors, including the cavity length, the epitaxial structure, the separation between the PC layer and the multiple quantum well (MQW) region, and the geometry of the scatterers in the PC layer (specifically, their depths and hole profiles).

Presently, PCSELs are typically modelled using effective index approaches, which reduce the three-dimensional (3D) structure to an equivalent two-dimensional (2D) photonic crystal whose performance is analysed using frequency-domain eigen-solvers, most commonly the Plane Wave Expansion (PWE) method [2]. While these semi-analytical techniques are well suited for initial design space exploration, they do not readily allow for the incorporation of realistic laser gain models. Furthermore, from a geometrical perspective, these methods assume no variation in hole cross-sections with depth, rather than the realistic hole profiles that result from fabrication artefacts.

An advancement in the Transmission Line Modelling (TLM) framework is the development of a numerical TLM method based on an unstructured tetrahedral mesh, referred to as the Unstructured TLM (UTLM) method. In UTLM, the computational domain is decomposed into non-overlapping tetrahedral cells forming a Delaunay mesh [3], with the tangential electric and magnetic field components sampled on the faces of each cell and propagated on the transmission line network defined by the corresponding Voronoi mesh [3]. UTLM offers several advantages for PCSEL simulations, including geometric flexibility, unconditional stability, sampling of electric and magnetic field values at the same spatial locations and time instants, and a straightforward ability to incorporate nonlinear laser physics models.

The presentation will expand on the UTLM methodology as applied to PCSELs and discuss the impact of the vertical scatterer shape on PCSEL lasing performance. The results demonstrate the high sensitivity of PCSELs to design parameters, highlighting the need for accurate modelling to achieve optimized laser performance.

[1] M. Yoshida, M. D. Zoysa, K. Ishizaki, Y. Tanaka, M. Kawasaki, R. Hatsuda, B. Song, J. Gelleta, S. Noda, "*Double-lattice photonic-crystal resonators enabling high-brightness semiconductor lasers with symmetric narrow-divergence beams*", Nature Materials, Vol.18. pp.121-128, 2019.

[2] Y. Itoh, N. Kono, D. Inoue, N. Fujiwara, M. Ogasawara, K. Fujii, H. Yoshinaga, T. Inoue, M.D. Zoysa, K. Ishizaki, S. Noda "*High-power CW oscillation of 1.3 mm wavelength InP-based photonic crystal surface emitting lasers*", Optics Express, Vol30. No.16, 2022.

[3] P Sewell., T.M. Benson, C .Christopoulos, D. W. P. T. Thomas, A Vukovic, J. Wykes, "Transmission Line modelling (TLM) based upon unstructured tetrahedral meshes", IEEE Trans on MTT, Vol.53, pp.1919-1928, 2005

Finite element method based frameworks for efficient simulations and optimizations in nano-photonics

Sven Burger,[1,2,*] Fridtjof Betz,[1] Felix Binkowski,[1] Martin Hammerschmidt,[1,2] Klaus Jäger,[1,3] Phillip Manley,[1,2] Matthias Plock,[1,2] Jonas Schaible,[1,3] Philipp-Immanuel Schneider,[1,2] Ivan Sekulic,[1,2] Lin Zschiedrich [1,2]

[1] *Zuse Institute Berlin, Takustraße 7, 14195 Berlin, Germany*
[2] *JCMwave GmbH, Bolivarallee 22, 14050 Berlin, Germany*
[3] *Helmholtz-Zentrum Berlin für Materialien und Energie, Hahn-Meitner-Platz 1, 14109 Berlin, Germany*
[*] *burger@zib.de*

In this contribution we review recent advances in finite element method based implementations for solving the time-harmonic Maxwell's equations. We comment on integration of these into frameworks for complex-analysis based modal analysis tools and machine-learning based optimization frameworks. Various applications for design optimization of nano-photonic setups and comparisons to experimental findings are demonstrated.

The finite element method (FEM) is a popular numerical method for solving differential equations. In nano-photonics it is typically used to solve time-harmonic wave equations in various formulations, derived from the Maxwell's equations. FEM relies on space discretizations with unstructured meshes and on the expansion of the solution to the differential equation with various types of basis functions which are defined locally on the mesh elements. The resulting sparse matrix equations are solved with specialized numerical methods.

The advantages of FEM include its flexibility in the choice of space discretization as well as in the choice of basis functions. We comment on adaptive resolution refinement strategies, automatic differentiation, curvilinear meshing, and convergence properties, as well as on parallel solvers. Some of these features are helpful for optimization frameworks, as well as for efficient and accurate simulations of real-world setups.

Acknowledgements

We acknowledge funding by the Deutsche Forschungsgemeinschaft (DFG, German Research Foundation) under Germany's Excellence Strategy - The Berlin Mathematics Research Center MATH+ (EXC-2046/1, project ID: 390685689) and by the German Federal Ministry of Research, Technology and Space (BMFTR, Forschungscampus MODAL, Project No. 05M20ZBM).

Quantum Dynamics in Nanoplasmonic Cavities

Ortwin Hess[1,*]
[1]*School of Physics and CRANN Institute, Trinity College Dublin, The University of Dublin, Dublin 2, Ireland*
*ortwin.hess@tcd.ie

Nanoplasmonic cavities represent an extreme limit of cavity quantum electrodynamics, compressing optical fields into deeply subwavelength volumes and enabling strong coupling under ambient conditions despite intrinsic Ohmic and radiative losses [1]. Operating at the few-nanometre, few-femtosecond frontier, these systems support ultrafast polariton formation, sub-picosecond Rabi oscillations, enhanced spontaneous emission, and near-field mediated multi-emitter correlations. Yet their inherently open, dispersive and non-Hermitian character demands a rigorous quantum description beyond phenomenological single-mode models.

In this contribution, we present a unified perspective on quantum dynamics in nanoplasmonic cavities that combines device-level architectures [2,3] with a rigorous open-system quantization framework. On the architectural side, waveguide-addressable nanoplasmonic platforms enable efficient in- and out-coupling while maintaining extreme local field confinement. In particular, quantum nanoplasmonic coherent perfect absorption (qnCPA) [2] exploits impedance matching between a plasmonic waveguide and a strongly coupled cavity–emitter system to selectively initialize and stabilize individual dressed states. In this regime, dissipation becomes a control parameter: coherent, unidirectional feeding compensates loss and locks the system into a chosen polariton state.

On the theoretical side, we employ a quantum quasinormal-mode (QNM) framework [4] based on macroscopic QED and complex coordinate transformations. Radiative leakage is regularized via perfectly matched layers, converting open-boundary loss into effective material dissipation and enabling a consistent definition of modal creation and annihilation operators. This yields a modal Fock-space description and a systematically derived Lindblad master equation that captures both coherent and dissipative inter-mode coupling intrinsic to non-Hermitian nanocavities. Benchmark studies demonstrate quantitative agreement with exact macroscopic-QED treatments for spontaneous emission and strong-coupling dynamics.

Together, these results establish a predictive, mode-based quantum-dynamical framework for room-temperature nanoplasmonic cQED. By co-designing ultrafast plasmonic confinement with rigorous open-system quantization, nanoplasmonic cavities emerge not only as platforms for enhanced light–matter interaction, but as controllable, dissipative quantum systems in which loss can be harnessed as a resource for quantum state preparation, stabilization, and on-chip functionality.

References

[1] X. Xiong, N. Kongsuwan, Y. Lai, C. E. Png, L. Su, O. Hess, “Room-temperature plexitonic strong coupling: Ultrafast dynamics for quantum applications, Appl. Phys. Lett. **118**, 130501 (2021).
[2] Y. Lai, D. D. A. Clarke, P. Grimm, A. Devi, D. Wigger, T. Telbig, T. Hofmann, R. Thomale, J.-S. Huang, B. Hecht, O. Hess, “Room-temperature quantum nanoplasmonic coherent perfect absorption”, Nature Commun. **15**, 6324 (2024).
[3] O. Hess, “Nanoplasmonic cavity quantum electrodynamic architectures for room-temperature quantum technologies, Eur. Phys. J. Spec. Top. (2026).
[4] L. Meschede, D. D. A. Clarke, O. Hess, “Quantum Quasinormal Mode Theory for Dissipative Nano-Optics and Magnetodielectric Cavity Quantum Electrodynamics”, APL Quantum **3**, 016103 (2026).

A Theoretical Atomistic Framework for Modeling Nanoplasmonics and Molecular Plasmonics

Chiara Cappelli[1,*]

[1]*Scuola Normale Superiore, Piazza dei Cavalieri, 7, 56126, Pisa, Italy*

*chiara.cappelli@sns.it

The optical response of plasmonic nanostructures can be finely controlled through variations in size, shape, and chemical composition [1], giving rise to a wide range of tunable electromagnetic phenomena. When molecular systems interact with plasmonic substrates, additional effects emerge, spanning from surface-enhanced spectroscopies to plasmon-driven photochemical processes [2]. A reliable theoretical description of plasmonic materials is therefore essential to unravel the mechanisms governing light–matter interactions at the plasmon resonance frequency.

In this contribution, we introduce an atomistic yet classical framework for modeling the plasmonic properties of nanostructures with complex geometries. The approach is broadly applicable to different classes of plasmonic materials, including noble-metal nanoparticles [3] and metal alloys [4], and is designed to scale efficiently to systems comprising more than one million atoms [5]. The model is further integrated with a quantum mechanical description of adsorbed molecular species, yielding a mixed QM/classical scheme suitable for investigating molecular plasmonic effects and surface-enhanced spectroscopic signals, such as Surface-Enhanced Raman Scattering [6-9]. We show that our classical approach for plasmonics can correctly reproduce reference ab initio data [3], and experimental trends [3-4]. By properly accounting for atomistic details, we can accurately describe the nanoplasmonics of systems dominated by quantum effects, such as subnanometer junctions [3,7], geometrical defects [8], and Gold picocavities [9].

This work has received funding from MUR-FARE Ricerca in Italia: Framework per l’attrazione ed il rafforzamento delle eccellenze per la Ricerca in Italia - III edizione. Prot. R20YTA2BKZ.

References

[1] K. L. Kelly, E. Coronado, L. L. Zhao, G. C. Schatz “The Optical Properties of Metal Nanoparticles: The Influence of Size, Shape, and Dielectric Environment” J. Phys. Chem. B, 107, 668 (2003).

[2] J. Langer et al. “Present and Future of Surface-Enhanced Raman Scattering” ACS Nano, 14, 28 (2019).

[3] T. Giovannini, L. Bonatti, P. Lafiosca, L. Nicoli, M. Castagnola, P. Grobas Illobre, S. Corni, C. Cappelli “Do We Really Need Quantum Mechanics to Describe Plasmonic Properties of Metal Nanostructures?” ACS Photonics, 9, 3025 (2022).

[4] L. Nicoli, P. Lafiosca, P. Grobas Illobre, L. Bonatti, T. Giovannini, C. Cappelli “Fully Atomistic Modeling of Plasmonic Bimetallic Nanoparticles: Nanoalloys and Core–Shell Systems” Front. Photon., 1199598 (2023).

[5] T. Giovannini, P. Grobas Illobre, P. Lafiosca, L. Nicoli, L. Bonatti, S. Corni, C. Cappelli “plasmonX: An Open-Source Code for Nanoplasmonics” Comput. Phys. Commun., 291, 110035 (2026).

[6] P. Lafiosca, L. Bonatti, L. Nicoli, T. Giovannini, S. Corni, C. Cappelli “QM/Classical Modeling of Surface-Enhanced Raman Scattering Based on Atomistic Electromagnetic Models” J. Chem. Theory Comput., 19, 3616 (2023).

[7] T. Giovannini, M. Rosa, S. Corni, C. Cappelli “A Classical Picture of Subnanometer Junctions: An Atomistic Drude Approach to Nanoplasmonics” Nanoscale, 11, 6004 (2019).

[8] S. Zanotto, L. Bonatti, M. F. Pantano, V. Miseikis, G. Speranza, T. Giovannini, C. Coletti, C. Cappelli, A. Tredicucci, A. Toncelli “Strain-Induced Plasmon Confinement in Polycrystalline Graphene” ACS Photonics, 10, 394 (2023).

[9] T. Giovannini, L. Nicoli, S. Corni, C. Cappelli “The Electric Field Morphology of Plasmonic Picocavities” Nano Lett., 25, 10802–10808 (2025).

Nonreciprocal plasmons in one-dimensional carbon nanostructures

Álvaro Rodríguez Echarri
Center for Nanophotonics, NWO Institute AMOLF, 1098 XG Amsterdam, The Netherlands
*a.rodriguezecharri@amolf.nl

The ability to direct electromagnetic energy flow in nanoscale plasmonic structures holds promise for developing integrated photonic circuits, optical isolators, and active quantum-optical components. However, light-matter interactions in conventional plasmonic platforms are intrinsically reciprocal and typically require bulky or noise-limited setups based on large applied magnetic fields or nonlinear optical processes to break optical reciprocity. Drift-biased graphene has recently emerged as a promising material platform for nonreciprocal plasmonics, due to the exceptional plasmonic properties of graphene and its ability to sustain ultrahigh carrier drift velocities [1,2]. Thus far, studies have focused almost exclusively on extended graphene sheets, assuming linear electronic dispersion and neglecting quantum finite-size effects. Here, we reveal a large nonlocal and nonreciprocal response in waveguided plasmon polaritons supported by one-dimensional graphene nanoribbons (GNRs, Fig. 1a) and carbon nanotubes (CNTs) under moderate drift bias [3]. Our analysis, based on an atomistic, quantum-mechanical framework that captures finite-size and edge termination effects in the electronic spectrum of these mesoscopic carbon nanostructures, predicts substantial direction-dependent plasmon dispersion in GNRs and CNTs with electronic band gaps. We further discuss how edge termination in GNRs (armchair vs zigzag) and structural chirality in CNTs critically shape the nonreciprocal response, which can mediate directionally biased dipole-dipole interactions over hundreds of nanometers. Such control could be leveraged for directional quantum emission (Fig. 1c), and nonreciprocal photonic functionalities in ultrathin platforms. These findings open new opportunities for realizing nanoscale isolators, directional plasmonic waveguides, and nonreciprocal quantum-optical devices without relying on magnetic fields or high-power nonlinearities.

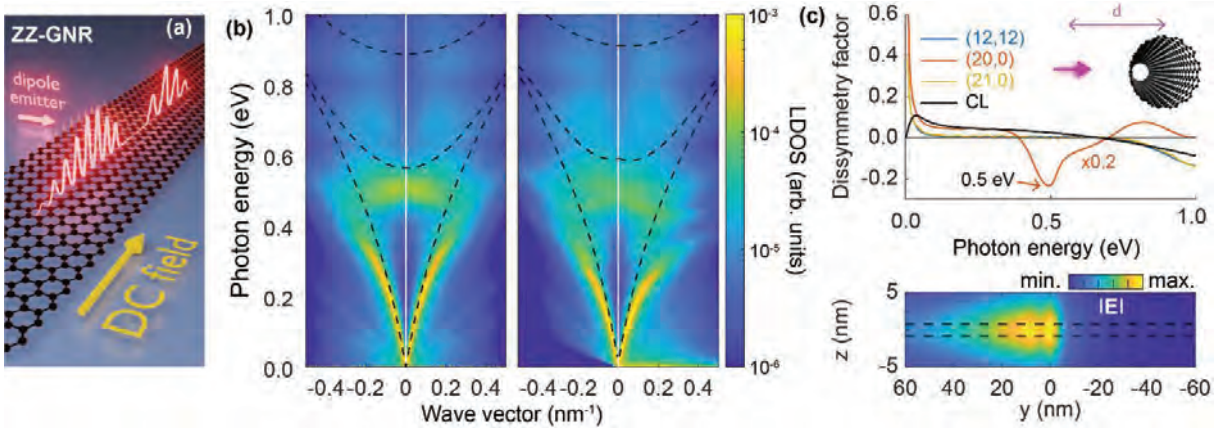

Fig. 1. (a) Schematics of surface plasmons in a biased zigzag graphene nanoribbon (ZZ-GNR) excited by a dipole. (b) LDOS of unbiased (left) and biased (right) 10 nm wide ZZ-GNR subjected to a DC field of 5.2 MV/m (with EF= 0.5 eV doping). (c) Top: Dissymmetry factor (relative difference between left and right LDOS), in carbon nanotubes (CNT) with different chiralities (m,n). (c) Bottom: (20,0)-CNT electric field at photon energy of 0.5 eV under the bias field.

References

[1] Y. Dong et al., "Fizeau drag in graphene plasmonics", Nature **594**, 513 (2021).
[2] W. Zhao et al., "Efficient Fizeau drag from Dirac electrons in monolayer graphene", Nature **594**, 517 (2021).
[3] A. Rodríguez Echarri, F. J. García de Abajo, and J. D. Cox, "Nonreciprocal plasmons in one-dimensional carbon nanostructures", Nat. Commun. **17**, 1114 (2025).

The flow of Fisher information in electromagnetism

Stefan Rotter, TU Wien, Institute for Theoretical Physics

In my talk, I will discuss how the concept of Fisher information provides a unifying framework for understanding the fundamental limits of optical measurements. When we infer properties of an object from scattered light, Fisher information quantifies how much can, in principle, be learned from the measurement, independently of any specific reconstruction algorithm. I will show how this viewpoint leads to practical strategies for improving optical experiments, including the use of wavefront shaping to actively maximise the information carried by scattered light [1].

A particularly striking recent result is that Fisher information can be treated as a physical quantity that flows through space: its density and flux obey a continuity equation that closely mirrors the Poynting theorem for electromagnetic energy [2, 3]. This analogy provides new physical intuition for how information is redistributed in optical systems. In the final part of the talk, I will briefly outline how these ideas extend beyond wave physics and how analogous notions of Fisher-information flow can be defined in artificial neural networks, offering a bridge between optical measurement theory and modern machine-learning methods [4, 5].

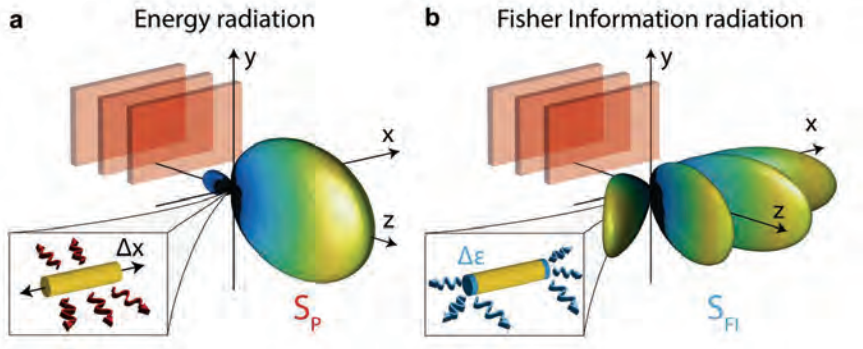

Figure 1: (a,b) An incoming plane wave impinges on a nanorod, leading to a scattered wave. (a) The energy radiated into the far-field is described by the Poynting vector $\mathbf{S}_P$. (b) The radiation pattern of the Fisher information flux vector $\mathbf{S}_{FI}$ is very different. For the measurements of the x-position of the target this is due to interference between Fisher information sources located at the opposite ends of the target (blue regions shown in the inset).

References

[1] D. Bouchet, S. Rotter, and A. P. Mosk, "Maximum information states for coherent scattering measurements," *Nature Physics* **17**, 564 (2021).

[2] J. Hüpfl *et al.*, "Continuity equation for the flow of Fisher information in wave scattering," *Nature Physics* **20**, 1294 (2024).

[3] M. Weimar *et al.*, "Controlling the flow of information in optical metrology," arXiv:2508.13640

[4] I. Starshynov *et al.*, "Model-free estimation of the Cramér–Rao bound for deep learning microscopy in complex media," *Nature Photonics* **19**, 593 (2025).

[5] M. Weimar *et al.*, "Fisher information flow in artificial neural networks," *Physical Review X* **15**, 031072 (2025).

Multipole analysis of the resonant electromagnetic response of particle clusters and metasurfaces

A. B. Evlyukhin

Institute of Quantum Optics, Leibniz University Hannover, Hannover 30167, Germany
Cluster of Excellence PhoenixD, Leibniz University Hannover, Hannover 30167, Germany
evlyukhin@iqo.uni-hannover.de

The use of multipole analysis to elucidate the mechanisms of resonant scattering in nanostructures is widespread and highly effective. Here, we present several important examples of modeling and multipole analysis of a range of resonant effects in nanoparticle structures, including conventional particle and membrane metasurfaces. Our examples cover both plasmonic and all-dielectric systems. We first demonstrate the application of direct and secondary multipole analysis to studying anapole effects in finite-size composite dielectric structures [1] and plasmonic particles [2]. The properties of metasurfaces composed of such structures are also discussed. We then present several analytical and semi-analytical multipole models for analyzing the physical mechanisms of collective resonances excited in conventional particle metasurfaces and membrane metasurfaces composed of holes in thin films. The universality of the multipole approach for understanding the resonance properties of various types of metasurfaces is demonstrated using the example of Fano resonances associated with accidental bound states in the continuum excited in symmetric metasurfaces composed of particles [3], as well as a discussion of the resonant response of membrane metasurfaces. In the latter case, a dipole-quadrupole model is presented for oblique irradiation, allowing the study of complex phenomena in membrane metasurfaces arising from multipole interference, including anapole lattice effects, generalized Kerker effects, Fano resonances, and quasi-bound states in the continuum. A number of other characteristic examples of the effective application of multipole methods are also presented [4].

References

[1] A. A. Basharin, E. Zanganeh, A. K. Ospanova, P. Kapitanova, A. B. Evlyukhin. ”Selective superinvisibility effect via compound anapole”, Phys. Rev. B 107, 155104 (2023).

[2] E. Hassan, A. B. Evlyukhin, A. Calà Lesina, ”Anapole plasmonic meta-atoms for nearly transparent metamaterials”, Laser Photonics Rev. 19, 2400118 (2025).

[3] I. Allayarov, A. Calà Lesina, A. B. Evlyukhin, ”Anapole mechanism of bound states in the continuum in symmetric dielectric metasurfaces”, Phys. Rev. B 109, L241405 (2024).

[4] I. Allayarov, V. Aita, D. Roth, B. van Casteren, A. Yu. Bykov, A. B. Evlyukhin, A. V. Zayats, A. Calà Lesina, ”Strong coupling of collective optical resonances in dielectric metasurfaces”, Light: Science & Applications 14, 387 (2025).

Bias-free optical nonreciprocity and directional dichroism

L.M. Manez-Espina[1], B. Amrahi[2], I. Faniayeu[3], R. Cichelero[3], A. Dmitriev[3], A. Diaz-Rubio[1], and V.S. Asadchy[2]

[1] *Nanophotonics Technology Center, Universitat Politecnica de Valencia, Valencia 46022, Spain*

[2] *Department of Electronics and Nanoengineering, Aalto University, Espoo, 02150, Finland*

[3] *Department of Physics, University of Gothenburg, Gothenburg, 41296, Sweden*

*viktar.asadchy@aalto.fi

Reciprocity is a cornerstone of wave physics, but many optical functions require nonreciprocal response. At optical frequencies, nonreciprocity is usually achieved using external magnets, active time modulation, or strong nonlinearities, which complicate integration and often work only for a single polarisation. This limits practical deployment in systems that operate with unpolarised light and demand compact, passive components.

In this invited presentation, we introduce a bias-free metasurface that produces pronounced optical isolation in an ultrathin, subwavelength platform. The concept combines self-magnetised ferrite nanodisks in a stable vortex state with a resonance mechanism that strongly enhances light–matter interaction, enabling a "one-way transparency" regime without any external magnetic field. The physical picture is intuitive: the metasurface behaves as a synthetically moving medium, so forward and backward propagation experience measurably different absorption and transmission. Figure 1 illustrates the key ingredients and the resulting spectral response: the vortex meta-atoms (Fig. 1a) and the sharp separation of forward/backward transmittance that yields a clear isolation window (Fig. 1b). Beyond isolation, the same mechanism supports near-unity directional dichroism that links scattering and thermal behaviour, offering opportunities for compact nonreciprocal photonics, wavefront control, and energy-management concepts where direction matters.

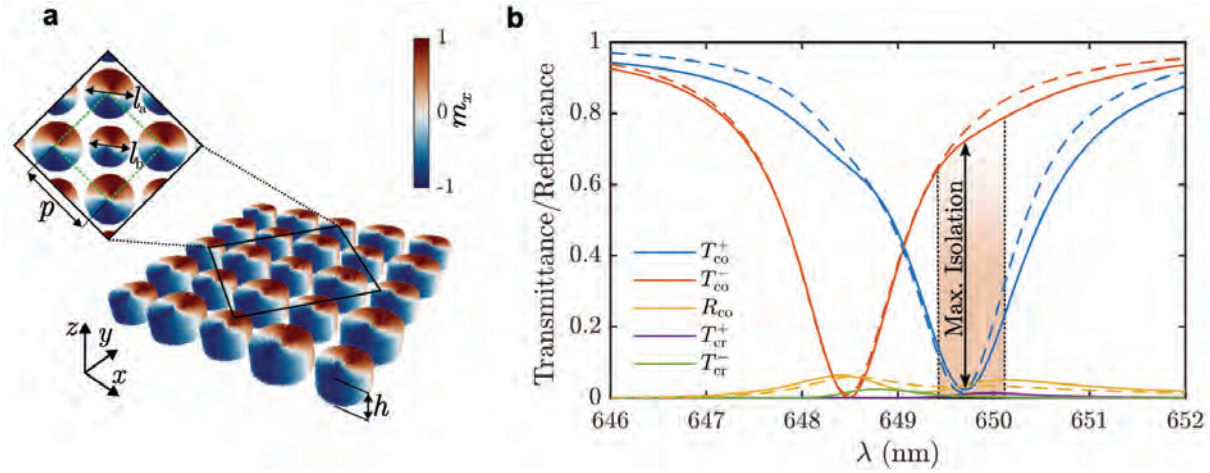

Fig. 1. Bias-free optical nonreciprocity in a vortex metasurface. (a) Array of self-magnetised ferrite nanodisks in a uniform vortex state. (b) Forward/backward transmission spectra showing an isolation window (maximum marked).

References

[1] Máñez-Espina, L. M., et al. "Giant bias-free nonreciprocity for unpolarized light via synthetic motion." arXiv:2510.14069 (2025).

Inverse design of free-form metadevices

M. Nyman[1], T. J. Sturges[1], O. Kuster[2], Y. Augenstein[3], M. L. Schubert[1], J. D. Fischbach[1], and C. Rockstuhl[1,2]

[1] *Institute of Nanotechnology, Karlsruhe Institute of Technology, Karlsruhe, 76131, Germany*

[2] *Institute of Theoretical Solid State Physics, Karlsruhe Institute of Technology, Karlsruhe, 76131, Germany*

[3] *Flexcompute Inc., Boston, Massachusetts, United States*

*carsten.rockstuhl@kit.edu

Modern fabrication techniques like 3D nanoprinting allow precise placement of material in subwavelength voxels as small as 100nm or less, covering length scales up to millimeters in both two and three dimensions. This ability to structure materials with such accuracy opens up new opportunities for creating photonic devices with custom properties. However, to fully harness this potential, we need effective methods to generate digital blueprints that can be reliably converted into physical hardware. This requires efficient inverse-design techniques that (a) navigate the large design space with many degrees of freedom, (b) incorporate constraints from the specific fabrication process, and (c) consider manufacturing imperfections to ensure feasible experimental realization. In this contribution, we highlight our latest progress in this area, focusing on two complementary development paths.

First, we investigate continuous surface profiles designed to shape electromagnetic field distributions in two, three, and even four dimensions, the latter involving spatiotemporal field structuring. Our approach leverages automatic differentiation of forward solvers to enable gradient-based inverse design. Key challenges include the parametrization of complex surfaces and the formulation of objective functions that capture the desired field transformations given the constraints of only a two-dimensional surface that is structured in a continuous fashion [1,2].

Second, we explore free-form bulk material architectures for steering light in selected applications. Here, we employ topology optimization using gradients computed via the adjoint method to efficiently optimize millions of degrees of freedom. A significant challenge is ensuring fabricability, which requires maintaining structural connectivity of both the material and the void regions, respectively, and incorporating process-specific constraints so that optimized structures can be directly realized [3,4].

For both research directions, we demonstrate the effectiveness of our design pipelines through selected examples developed in close collaboration with experimental partners.

References

[1] T. J. Sturges, M. Nyman, S. Kalt, K. Pälsi, P. Hilden, M. Wegener, C. Rockstuhl, and A. Shevchenko, „Inverse-designed 3D laser nanoprinted phase masks to extend the depth of field of imaging systems“ ACS Photonics **Vol. 11** 3765, (2024)

[2] M. L. Schubert, J. D. Fischbach, M. Nyman, L. Lüer, C. J. Brabec, C. Rockstuhl, and T. J. Sturges, „Wide angle tolerant solar spectral splitter for lateral tandem solar cells“ APL Photonics **Vol. 10**, 066105 (2025)

[3] O. Kuster, Y. Augenstein, C. Rockstuhl, and T. J. Sturges, “A three-dimensional polarization-insensitive grating coupler tailored for 3D nanoprinting” arXiv:2508.20894 (2025)

[4] O. Kuster, Y. Augenstein, R. N. Hernández, C. Rockstuhl, and T. J. Sturges, „Inverse Design of 3D Nanophotonic Devices with Structural Integrity Using Auxiliary Thermal Solvers“ Nanophotonics **Vol. 14**, 1415 (2025)

Simulation and Optimization of Large-Scale Metasurfaces

J. Niegemann[1,*], D. Huynh[2], Han-Hsiang (Michael) Cheng[3], Thibault Leportier[1], Dylan McGuire[1], Adam Reid[1]

[1]*Ansys, part of Synopsys, Canada*

[2]*Ansys, part of Synopsys, Germany*

[3]*Ansys, part of Synopsys, Japan*

*jens.niegemann@synopsys.com

Metasurfaces consist of precisely engineered meta-atoms with sub-wavelength dimensions. Through careful optimization of the geometry and spatial arrangement of these elements, one can achieve precise control over the phase, amplitude, and polarization of transmitted or reflected light. Recent progress in metasurface simulation and fabrication has attracted considerable attention from both academia and industry. Nevertheless, designing and optimizing large-scale metasurfaces remains a formidable challenge, requiring advances in simulation methodologies and effective utilization of modern high-performance computing (HPC) infrastructure.

The initial stage of metasurface design typically involves constructing a comprehensive meta-atom database. In this presentation, we examine and compare different numerical methods for simulating individual meta-atoms, specifically highlighting the respective advantages and limitations of the finite-difference time-domain (FDTD) method and rigorous coupled-wave analysis (RCWA). With a suitable database established, the subsequent step involves optimizing the meta-atom arrangement to achieve the desired optical response. We compare several optimization strategies, with particular emphasis on adjoint methods, which have proven especially effective for large-scale metasurface optimization.

Optimization procedures typically rely on approximations such as the local periodic approximation (LPA), making rigorous verification of the final design essential prior to fabrication. To address this need, we demonstrate the use of multi-GPU systems to perform full-scale FDTD simulations of optical metasurfaces with diameters exceeding 1 mm. Once the metasurface design has been finalized and validated, engineers frequently need to simulate the complete optical system, which may incorporate both conventional optical elements and metasurfaces. Raytracing is generally the preferred approach for such system-level simulations; however, incorporating metasurfaces into raytracing workflows without compromising computational efficiency or accuracy remains challenging. We demonstrate that the recently developed Windowed Fourier Transform (WFT) method [2] preserves the computational efficiency of raytracing while providing more accurate treatment of metasurfaces compared to previous approaches.

References

[1] Han-Hsiang (Michael) Cheng, et al., "Ray-tracing method for large-scale metalenses in multiwavelength imaging system," Proc. SPIE 13378, High Contrast Metastructures XIV, 1337809 (2025)

Modelling high-NA EUV lithography

Peter Evanschitzky* and Andreas Erdmann

Fraunhofer Institute for Integrated Systems and Device Technology IISB, Schottkystrasse 10, 91058 Erlangen, Germany

*peter.evanschitzky@iisb.fraunhofer.de

The latest generation of computer chips employs extreme ultraviolet (EUV) lithography with a wavelength of 13.5 nm. Although the small wavelength promises a much better resolution compared to DUV lithography at 193 nm wavelength, the used reflective projection optics and reflective masks introduce several imaging artifacts like non-telecentricities, various contrast-loss mechanisms and feature dependent shifts of the best focus position. After a brief introduction to the basic modelling of EUV lithography, dedicated modeling techniques will be employed to understand and optimize the image formation in high-NA EUV lithography with a NA of 0.55. Examples of important imaging challenges and potential solutions will be shown. In the figure left an example is given.

Another increasingly important aspect of EUV lithography modelling is the fully rigorous and sufficiently fast simulation of light diffraction from larger mask areas with more complex structures. Curvilinear mask layouts and structures derived from SEM inspection are two examples that are getting more and more important. In both cases the typically used Manhattan-like structure types are replaced by free form shapes described with polygons. Furthermore, mask area sizes such as 100 x 100 wavelength and more often need to be considered in the simulations. Such use cases require highly accurate fully rigorous mask simulations that solve the Maxwell equations very precisely and are therefore very challenging with respect to simulation times. The full parallelization and an optimized GPU implementation of our RCWA (Rigorous Coupled-Wave Analysis) based mask solver addresses this problem and will be presented. The right part in the figure illustrates the situation. EUV-specific optimizations of the algorithm and of the implementation will be shown. Finally, simulation examples demonstrate accuracy and superior speed that can be reached with the approach.

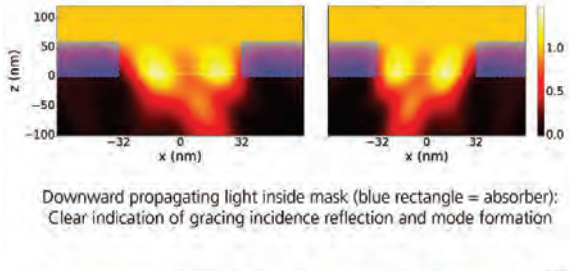

Downward propagating light inside mask (blue rectangle = absorber): Clear indication of gracing incidence reflection and mode formation

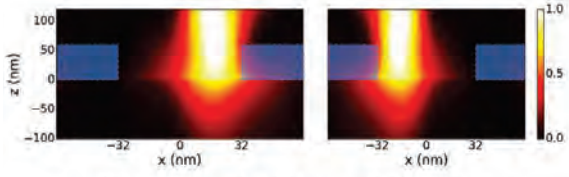

Upward propagating light inside mask (blue rectangle = absorber): Missing mode, important for image formation

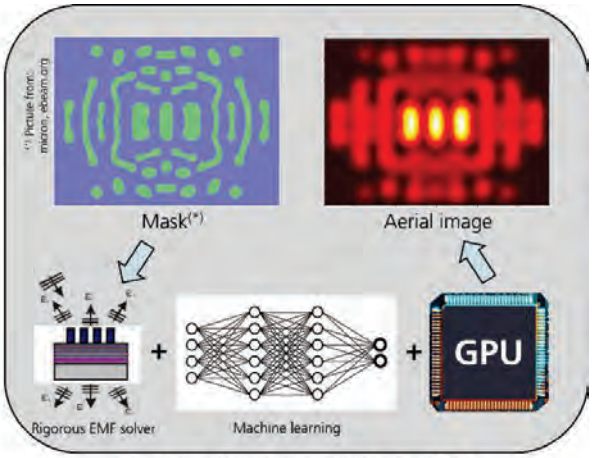

Simulation of curvilinear mask cutout with fully rigorous RCWA solver with GPU support

Cavity-resonator-integrated grating filters for second harmonic generation

A .-L. Fehrembach [1,*], E. Popov [1], A. Monmayrant [2] O. Gauthier-Lafaye [2] S. Calvez [2]

[1] *Aix Marseille Univ, CNRS, Centrale Marseille, Institut Fresnel, Marseille, France*
[2] *LAAS-CNRS, Université de Toulouse, CNRS, Toulouse, France*
[*] *mailto:anne-laure.fehrembach@fresnel.fr*

Cavity resonator integrated grating filters (CRIGF) [1] consist of a sub-wavelength coupling grating with a few tens of periods (GC), surrounded by two distributed Bragg reflectors (DBR), etched onto a multilayer stack of lossless dielectric materials (see figure). When illuminated by an incident beam covering the GC, CRIGF exhibit resonances characterized by a strong electromagnetic field. Our work exploits this property to enhance second harmonic generation (SHG) [2].

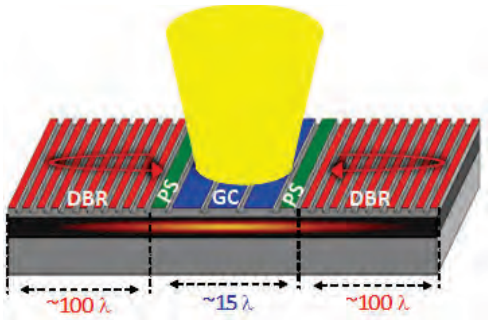

In our first study [2], we numerically and experimentally achieved a conversion efficiency $\eta = P_{2\omega}/[P_\omega]^2$ on the order of $8\text{x}10^{-6}\text{W}^{-1}$ (where P_ω is the incident power and $P_{2\omega}$ is the power generated by SHG). This conversion efficiency is one order of magnitude higher than that achievable with infinite resonant gratings but two orders of magnitude lower than that of much longer ribbon waveguide components. In this presentation, we will review the approaches we have explored to improve the SHG conversion efficiency of the CRIGF.

The first part will focus on the mode matching between a mode at the pump frequency and one at the harmonic frequency. We will discuss the complexity of the stack design required and its sensitivity to fabrication errors. The second part will adress increasing the quality factor Q (the ratio of the resonance wavelength to its spectral width) of the resonance at ω. We will describe two methods to achieve this: using a quasi-dark mode [3] or a GC with a bi-atom based pattern [4]. The high quality factors achieved (above 10^5) highlight the existence of a critical coupling regime [5,6], for which the SHG conversion rate is maximized. Our results are supported by experimental measurments [7].

Acknowledgements: this work was supported by the AID (ANR-ASTRID RESON project).

References

[1] K. Kintaka et al. *Cavity-resonator-integrated grating input/output coupler for high-efficiency vertical coupling with a small aperture* Opt. Lett. 35, pp. 1989-1991, 2010.
[2] F. Renaud et al. *Second-harmonic-generation enhancement in cavity resonator integrated grating filters* Opt. Lett. 44, pp. 5198-5201, 2019.
[3] A.-L. Fehrembach et al. *Dark mode-in-the-box for enhanced second-harmonic generation in corrugated waveguides* Opt. Expr. 29 (25), pp 40981 (2021).
[4] A.-L. Fehrembach et al. *Cavity-resonator integrated bi-atom grating coupler for enhanced second-harmonic generation* Opt. Expr. 30 (21), pp 38789 (2022).
[5] A. Yariv *Universal relations for coupling of optical power between microresonators and dielectric waveguides* Electron. Lett. 36 (4), pp321-322 (2000).
[6] E. Popov et al. *Extreme enhancement of the quality (Q)-factor and mode field intensity in cavity-resonator gratings* Opt. Expr. 30 (14), pp25390 (2022).
[7] E. Hemsley et al. *Critical coupling in cavity-resonant integrated-grating filters (CRIGFs)* Opt. Expr. 31 (17), pp27274 (2023).

Nanoparticles Identification from Scattering Data

Alexander A. Iskandar
[1]*Physics of Magnetism and Photonics Research Division, Faculty of Mathematics and Natural Sciences, Institut Teknologi Bandung, Bandung, 40132, Indonesia*
*a.a.iskandar@itb.ac.id

In modern nanoparticle (NP) identification methods, challenges such as limited access to spectroscopy and microscopy techniques, and difficulties in interpreting spectral data, have created a critical gap in the efficient and accessible analysis of NPs. Nanoparticles, whether dielectric, metallic, hybrid, or composite, have been used in diverse applications due to their unique optical properties. Metallic-based and hybrid metallic-based NPs are particularly notable for supporting plasmonic resonances. These phenomena have been crucial in applications such as biosensing, imaging, and solar energy harvesting. In contrast, dielectric nanoparticles are valued for their ability to support electric and magnetic Mie resonances, enabling a range of unique applications.

Nanoparticle synthesis can proceed via bottom-up approaches, where NPs are assembled from atomic building blocks through methods such as chemical reduction, sol-gel processing, or self-assembly, or via top-down approaches, where NPs are derived from bulk materials using techniques such as laser ablation, etching, or ball milling. These processes may result in unintended outcomes, including particle-size deviations, impurity contamination, or aggregation. Traditionally, the composition, size, distribution, and aggregation state of NPs are determined using spectroscopy methods, such as Energy-Dispersive X-ray Spectroscopy and Dark-Field Scattering Spectroscopy, and microscopy methods, such as Transmission Electron Microscopy. However, these techniques are not always accessible. UV–Vis Absorption Spectroscopy offers a more affordable and rapid alternative for NP identification, but interpreting the resulting spectra is complicated by similarities across different configurations. Recent advancements in machine learning (ML) have enabled the development of approaches that address this inverse identification problem.

Results, from ongoing work, on the identification of NP composition, size, distribution, and aggregation state using ML-assisted decision-making from scattering spectra will be presented. The training data set of scattering and extinction cross sections is generated from Mie theory and the T-matrix method. Sets of spectral characteristics are extracted and used as the descriptor in the machine learning algorithm. Two sets of descriptors have been chosen: the first set consists of spectral primary and secondary peaks and dip parameters (wavelengths, heights, and linewidths), and the second set consists of parameters from a multi-Lorentzian fit to the spectra. A specific ML algorithm is used depending on the case being considered, i.e., size and composition determination or aggregation-state determination. Supervised StratifiedKfold training and validation using these generated datasets yielded good results for composition analysis with Random Forest algorithms and for aggregation-state classification with Support Vector Machine. Key performance metrics for composition analysis included an accuracy of 78%, with a minimum precision of 54% and a recall larger than 56%. For aggregation-state classification, the Support Vector Machine achieved an accuracy of 90% and larger, with minimum precision of 76%, and a recall larger than 73%. The ML model was also tested with experimental scattering spectra and yielded good decision results.

References

[1] D. Ramdani, N. Innayah, A. Qoddri, A. Soehianie, S. Viridi and A.A. Iskandar, “Identifying Nanoparticles Aggregates from Its Scattering Spectra with Machine Learning”, Proceeding of the 15th International Symposium on Modern Optics and Its Applications (ISMOA) 2025, Bali, Indonesia – to be published in Journal of Physics Conference Series (2026).

Numerical modelling of fiber lasers based on active fibers with structured cores

P. Peterka*, M. Grabner
Institute of Photonics and Electronics of the Czech Academy of Sciences, Prague, CZ 182000, Czechia
*peterka@uf.cz

Fiber lasers, although conceived nearly simultaneously with the groundbreaking inventions of the laser and the single-mode optical fiber in the 1960s, had to wait several decades for their golden era. Today, they outperform other laser sources in terms of high brightness and beam quality, efficient pumping, improved thermal management, and compactness. Despite rapid progress in fiber laser technology, particularly since the beginning of the new millennium, many challenges remain unresolved, motivating the exploration of novel fiber designs. Among these, the structured-core (or pixelated-core) fiber design represents a promising approach toward a universal solution for large-mode-area active fibers in high-power fiber lasers. In this conference presentation, we review three examples of nanostructured and structured-core fibers:

- Pedestal-free Tm-doped fiber concept enabling efficient cooling and reliable fiber splicing [1]
- A multi-rod core, thulium-doped fiber designed for enhanced cooling and mitigation of diffusion-related issues, including numerical modeling of fiber heating effects and the associated increase in amplified spontaneous emission power [2]
- Dual-wavelength operation of structured-core fibers featuring spatial separation of core regions doped with different rare-earth elements, e.g., Yb and Er, allowing a single active fiber to operate at multiple wavelengths within a single laser cavity. A numerical model for the optimization of Er/Yb-doped fibers will be presented [3]

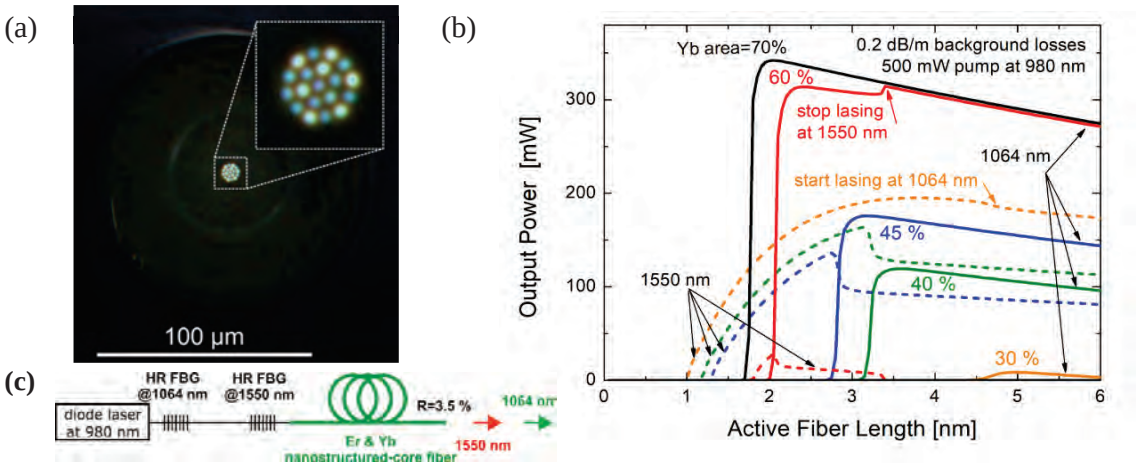

Fig. 1. (a) Structured-core cross section, its core contains 7 ytterbium rods (brighter spots) and 12 erbium rods. (b) Modeling of laser output power at 1550 nm and 1064 nm, (c) fiber laser setup.

References

[1] P. Peterka, J. Aubrecht, D. Pysz, M. Franczyk, O. Schreiber, M. Kamrádek, I. Kasik, R. Buczyński, "Development of pedestal-free large mode area fibers with Tm doped silica nanostructured core," Opt. Express 31 (2023) 43004–43016. https://doi.org/10.1364/OE.503047

[2] M. Grábner, B. Švejkarová, J. Aubrecht, J. Pokorný, P. Honzátko, P. Peterka, "Rise of amplified spontaneous emission in high-power thulium-doped fiber lasers and amplifiers due to selfheating," Optics & Laser Technology 180 (2025) 111428. https://doi.org/10.1016/j.optlastec.2024.111428

[3] I. Barton, P. Peterka, M. Grabner, J. Aubrecht, M. Kamradek, O. Podrazky, P. Varak, D. Pysz, M. Franczyk, R. Kasztelanic, R. Buczynski, and I. Kasik, "Structured Ytterbium and Erbium-doped silica fiber for dual wavelength laser operation," submitted to IEEE J. Lightwave Technol.

Semi-analytical modeling of feedback trapping in optical nanocavities

B.F. Gøtzsche [1,2], P.T. Kristensen [1,2], M. Wubs [1,2,*]

[1] *Department of Electrical and Photonics Engineering, Technical University of Denmark, Ørsteds Plads 343, 2800 Kgs. Lyngby, Denmark*

[2] *NanoPhoton—Center for Nanophotonics, Technical University of Denmark, Ørsteds Plads 345A, 2800 Kgs. Lyngby, Denmark*

[*] *mwubs@dtu.dk*

Nanoparticles can be trapped by optical forces, not only in optical tweezers but also in optical nanocavities. Plasmonic nanocavities can have modes with strongly subwavelength mode volumes but their quality factors are modest because of material loss. Recently it was shown that also dielectric cavities do not need to satisfy any diffraction limit for their mode volumes. Dielectric nanocavities with extreme dielectric confinement exist that have negligible loss, with quality factors that are orders of magnitude larger than with metals (see Figure).

Due to the narrower cavity linewidth, dielectric cavity resonances can be shifted by a trapped particle itself, resulting in a steeper optical potential. Such feedback trapping – also known as "self-induced back-action" - affects the optical forces. A spatial mapping of these forces in a cavity usually requires redoing a full solution of Maxwell's equation for the cavity-with-particle for every position of the particle. Here instead we present a semi-analytical model that only requires a single calculation of the dominant quasinormal mode of the cavity without the particle, in order to calculate the optical force, including effects of feedback trapping, for any position in the nanocavity.

We show the high accuracy of the method and its efficiency when compared to full numerical approaches. Furthermore, we discuss the new insights obtained by our method and possible further extensions.

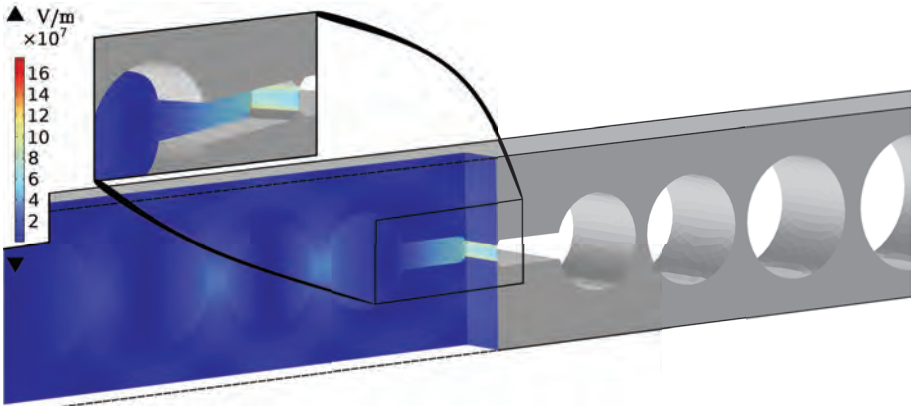

Figure: Sketch of a tapered nanobeam waveguide with dents in the central waveguide region, as an example of a dielectric nanostructure that supports a highly localized cavity mode that can be used to optically trap nanoparticles, and better so because of self-induced back-action effects.

Optimized Principal Volume in the Green Dyadic Method

Alain Dereux
ICB UMR 6303 CNRS, Université Bourgogne Europe, 9 Avenue A. Savary, Dijon, France
alain.dereux@ube.fr

Accurate computation of electromagnetic fields is essential across fundamental and applied optics, yet many realistic scattering problems resist closed-form solutions and require robust numerical methods. Simplified approaches are never satisfactory to address the regime featuring the same order of magnitude of both the typical size (*s)* of the scatterers and the incident wavelength (λ). The realistic values of the optical properties are important in this regime because they are related to resonance phenomena.

Differential solvers (FEM, FDTD) are efficient but must discretize the surrounding domain and impose absorbing boundary treatments that can introduce spurious modes. Integral-equation approaches based on Green dyadics avoid discretizing the environment and hence handle radiation conditions exactly. Surface integral methods further reduce unknowns by discretizing only boundaries, thus reducing significantly the computing time. However, they require to choose between rather subtle approximations modeling effective surface currents (not to be confused with external or induced currents in the volume of the scatterer). This can be viewed as a dependence on the treatment of boundary conditions. Volume integral formulations discretize only the scatterer. The first method of this kind was the discrete dipole approximation (DDA) [2] in which the volume of the scatterer is represented by an array of cubes described by their electric polarizability as given the Clausius-Mossotti formula. This method is effective if $s << \lambda$ but is greedy for the regimes $s \sim \lambda$ and $s >> \lambda$.

The Green dyadic method [3] generalizes the DDA because it is expressed in terms of the bulk optical properties of the scatterer (dielectric function and magnetic permeability), making more straightforward to cope with magnetic or anisotropy effects. It allows for a more flexible approach of the discretization volumes that are not limited to cubes. In this context, the discretization volume are called *principal volumes* because they are not only accounting for a weighting factor but also for a depolarization effect that is specific to their shapes. Although the physics of principal volumes is established [4], most reported applications of the volume Green dyadic method used cubic voxels featuring a same size, thereby not differing of the DDA. We show that standard Gaussian quadrature can produce a broad dispersion of principal-volume magnitudes. Such dispersion degrades the conditioning of the resulting linear system (Lippmann–Schwinger type), impairing solver robustness and accuracy.

To remedy this, we propose an optimization strategy for principal-volume discretization illustrated on a spherical scatterer. Starting from a chosen number of radial nodes n_r, we select polar and azimuthal node counts so that integration weights remain nearly homogeneous around their mean. This compromise preserves the accuracy benefits of angular quadrature while avoiding extreme weight dispersion. For given s/λ, the spherical discretization yields far fewer principal volumes than an equivalent cubic padding featuring n_r nodes on the equatorial radius. This procedure allows matching the canonical data of Mie scattering [5] over a wide range of ratios s/λ without changing the total number of voxels.

We conclude that, for integral-equation discretizations, prioritizing weight homogeneity (reciprocal condition-number improvement) over strict Gaussian weight optimality produces more reliable linear systems and more robust scattering solutions while significantly reducing the number of voxels relatively to raw padding with cubes.

References

[1] P. S. Mavrikakis and O. J. F. Martin, ACES Journal 40, 269 (2025).
[2] E. M. Purcell and C. R. Pennypacker, Astrophys. Journal 186, 705 (1973).
[3] J. P. Kottmann and O. J. F. Martin, IEEE Trans. Antennas Propag. 48, 719 (2000).
[4] A. D. Yaghjian, Proceedings of the IEEE 68, 248-263 (1980).
[5] H. Blumer, Zeitschrift Phys. 32, 119 (1925) and Zeitschrift Phys. 38, 304 (1926).

Computing resonance modes and resonance expansions using AAA rational approximation

F. Betz [1], M. Hammerschmidt [2], L. Zschiedrich [2], S. Burger [1,2], F. Binkowski [1,*]

[1] *Zuse Institute Berlin, Berlin, 14195, Germany*
[2] *JCMwave GmbH, Berlin, 14050, Germany*
[*] *binkowski@zib.de*

We review numerical methods based on AAA rational approximation for photonic applications.

Theoretical Background

A resonance occurs when a system responds very strongly to certain frequencies of light, producing highly localized electromagnetic fields [1, 2]. These resonances are fundamental properties of photonic systems and can be described mathematically by the poles of the system's electromagnetic response [3]. Although photonic systems can have many resonances, often only a few are needed to accurately describe how the systems behave in the frequency range of interest [4]. The AAA algorithm [5] provides a rational approximation that yields low-dimensional models when few poles dominate, and has recently gained significant attention in numerical mathematics and applications [6].

Application

We demonstrate the use of AAA rational approximation on several photonic systems: (i) a chiral metasurface, where we compute resonance modes, perform modal expansions, and incorporate sensitivity information into the AAA framework [7]; (ii) a photonic crystal fiber, where the method gives only the relevant resonance modes while directly filtering out cladding and higher-order modes [8]; and (iii) systems with scattering thresholds, in which hidden resonances can be revealed through AAA rational approximation [9].

Acknowledgements

We acknowledge funding by the Deutsche Forschungsgemeinschaft (DFG, German Research Foundation) under Germany's Excellence Strategy - The Berlin Mathematics Research Center MATH+ (EXC-2046/1, project ID: 390685689) and by the German Federal Ministry of Research, Technology and Space (BMFTR, Forschungscampus MODAL, project 05M20ZBM).

References

[1] M. Zworski, Notices Amer. Math. Soc. **46**, 319 (1999).
[2] P. Lalanne, W. Yan, K. Vynck, C. Sauvan, J. P. Hugonin, Laser Photonics Rev. **12**, 1700113 (2018).
[3] F. Binkowski, F. Betz, R. Colom, P. Genevet, S. Burger, Phys. Rev. B. **109**, 045414 (2024).
[4] A. Nicolet, G. Demésy, F. Zolla, C. Campos, J. E. Roman, C. Geuzaine, Eur. J. Mech. A Solids **100**, 104809 (2023).
[5] Y. Nakatsukasa, O. Sète, L. N. Trefethen, SIAM J. Sci. Comput. **40**, A1494 (2018).
[6] Y. Nakatsukasa, L. N. Trefethen, arXiv:2510.16237 (2025).
[7] F. Betz, M. Hammerschmidt, L. Zschiedrich, S. Burger, F. Binkowski, Laser Photonics Rev. **18**, 2400584 (2024).
[8] F. Binkowski, F. Betz, M. Hammerschmidt, L. Zschiedrich, S. Burger, Nanophotonics **14**, 1665 (2025).
[9] F. Betz, F. Binkowski, J. D. Fischbach, N. Feldman, L. Zschiedrich, C. Rockstuhl, A. F. Koenderink, S. Burger, Laser Photonics Rev. **19**, e00811 (2025).

Numerical modeling and shaping of nanoscale light-matter interactions with Discontinuous Galerkin methods and Machine Learning algorithms

A. Gobé, M. Elsawy, S. Lanteri* and C. Scheid
*Stephane.Lanteri@inria.fr

Modeling and simulation of nanoscale light-matter interactions is an important part of photonic device design. Harvesting and tailoring these interactions with the help of inverse design approaches is an increasingly considered objective of computational nanophotonics. An inverse design methodology is generally based on two ingredients: on the one hand, a numerical method for characterizing the optical performance of a given design of the photonic device at hand, which will be referred in the sequel as the *numerical characterization* method; on the other hand, a *numerical optimization* algorithm, which has to be compatible with the required number of design parameters and the computational cost of the evaluation of a single design with the numerical characterization method. In this contribution, we address this objective with an advanced computational framework that combines two main numerical ingredients: (1) high order Discontinuous Galerkin (DG) methods for solving the system of time-domain [1] or frequency-domain [2] Maxwell equations in 3D coupled to appropriate differential models of physical dispersion in photonic materials and, (2) one of the most efficient global optimization techniques that belongs to the class of Bayesian optimization and known as the Efficient Global Optimization (EGO) method [3]. The resulting numerical methodology is exploited for the inverse design of various photonics devices including metamaterial-based absorbers, plasmonics nanostructures for sensing and optical metasurfaces.

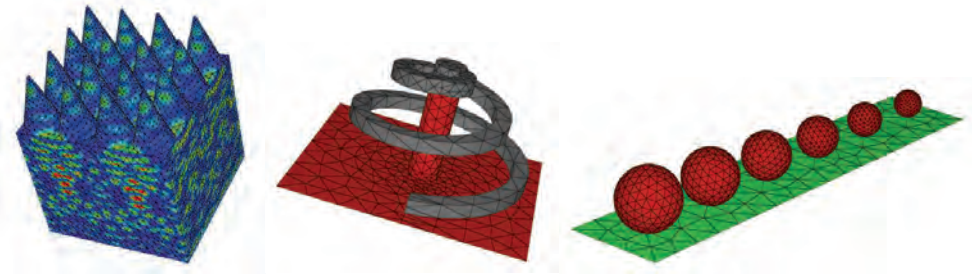

Fig. 1. Sample of photonic devices that are studied with the ML-based inverse design methodology combining the DGTD fullwave solver and the EGO optimization algorithm. From left to right: a nanostructured photovoltaic cell, a metamaterial-based absorber and a metasurface.

References

[1] S. Lanteri, C. Scheid and J. Viquerat. *Analysis of a generalized dispersive model coupled to a DGTD method with application to nanophotonics*. SIAM J. Sci. Comp., Vol. 39, No. 3, pp. A831–A859 (2017)
[2] E. Agullo, L. Giraud, A. Gobé, M. Kuhn, S. Lanteri and L. Moya. *High order HDG method and domain decomposition solvers for frequency-domain electromagnetics.* Int. J. Numer. Model. Electr. Netw. Dev. Fields, Vol. 33, No. 2 (2019)
[3] D. Jones. *Efficient global optimization of expensive black-box functions*. J. Glob. Optim., Vol. 13, No. 4, pp. 415-447 (1998)

Photonic reservoir computing on a system with hysteresis

S.Phang

George Green Institute for Electromagnetics Research, University of Nottingham, Nottingham, NG7 2RD, UK
**sendy.phang@nottingham.ac.uk*

Neuromorphic photonics aims to harness light-matter interaction to replicate neural computation architectures, enabling ultrafast, energy-efficient processing for machine learning tasks. Among various approaches, photonic reservoir computing (PhRC) has emerged as a particularly promising framework due to its architectural simplicity and compatibility with passive, high-bandwidth optical components. In PhRC, only the Read-Out layer is trained, while the core transformation, performed by the reservoir, remains fixed. This makes the PhRC highly suitable for hardware-level implementations of optical computing systems. Existing PhRC implementations include electro-optical delay systems[1, 2, 3], and on-chip passive photonic structures[4]. While strong nonlinear dynamics are readily achieved in fibre and electro-optical platforms, on-chip PhRC systems often rely on weak intrinsic nonlinearities, with nonlinearity introduced at the detection via photodetector saturation. This limits control over internal reservoir dynamics and restricts design flexibility.

In this contribution, we present a passive, on-chip PhRC architecture in which the reservoir nonlinearity originated from the Kerr nonlinearity of a Bragg grating operated near its photonic band edge. Operation close to the bandgap enhances the nonlinear response and provides access to distinct dynamical regimes, ranging from weak to strong hysteresis depending on the operating frequency. Tuning the carrier frequency simultaneously controls both the strength of the nonlinearity and the on–off contrast of the photonic neuron. Short-term memory is introduced by embedding the nonlinear Bragg grating in a resonant feedback loop, where the round-trip time defines the temporal memory scale. The resulting architecture couples resonant dynamics with band-edge-enhanced nonlinearity, enabling a compact and fully passive on-chip reservoir. However, reservoir performance depends critically on the co-design of the resonator parameters and the nonlinear band-edge dynamics. Full-wave electromagnetic method is used to model the system as a whole. Learning is performed in silico using linear regression at the read-out stage, enabling systematic hyperparameter optimisation over operating frequency, carrier power, and resonator round-trip time. Performance is evaluated using the NARMA-10 benchmark task. The results reveal pronounced sub-wavelength sensitivity of the optimal hyperparameters, with task error exhibiting periodic dependence on the resonator round-trip time at a scale comparable to the optical carrier period. These effects cannot be captured by simplified models and demonstrate the necessity of full-wave modelling for accurate prediction.

References

[1] Lennert Appeltant, Miguel Cornelles Soriano, Guy Van der Sande, Jan Danckaert, Serge Massar, Joni Dambre, Benjamin Schrauwen, Claudio R Mirasso, and Ingo Fischer. Information processing using a single dynamical node as complex system. *Nature communications*, 2(1):468, 2011.

[2] Gleb Anufriev, David Furniss, Mark Farries, and Sendy Phang. Non-spectroscopic sensing enabled by an electro-optical reservoir computer. *Optical Materials Express*, 12(5):1767–1783, 2022.

[3] Gleb Anufriev, David Furniss, Mark C Farries, Angela B Seddon, and Sendy Phang. An experimental demonstration of neuromorphic sensing of chemical species using electro-optical reservoir computing. *Scientific Reports*, 14(1):27915, 2024.

[4] Sendy Phang, David Furniss, Christopher Mellor, Günther Roelkens, Angela B Seddon, Peter Bienstman, and Trevor M Benson. Neuromorphic sensing via temporal signal signature processed by photonic reservoir computer. In *Optical Biopsy XIX: Toward Real-Time Spectroscopic Imaging and Diagnosis*, volume 11636, page 116360H. SPIE, 2021.

Poster abstracts

Compact angular filtering with metagratings

Mahmoud A. A. Abouelatta[1,*], Karim Achouri[1]
[1]*Laboratory, Laboratory for Advanced Electromagnetics and Photonics, École Polytechnique Fédérale de Lausanne (EPFL), 1015 Lausanne, Switzerland*
*mahmoud.abouelatta@epfl.ch

Although the 4f lens system serves as a foundational Fourier-optics architecture for angular filtering in spatial modulators, imaging devices, and data storage, its physical bulk presents a significant limitation for integrated photonics. In this study, we introduce a nanostructured system that replicates these filtering functions, as shown in Fig.1, within a device footprint five orders of magnitude thinner than a standard free-space 4f setup[1]. This dramatic reduction in scale is achieved by engineering the angular scattering response of metagratings. Specifically, we utilize the complex interplay between angle-sensitive two-dimensional dipolar resonances, the Kerker-like cancellation of dipoles, and intrinsic diffraction propagation conditions to produce sharp-edge angular filtering. This metagrating platform demonstrates high-efficiency performance as either a low-pass filter or a tunable high-pass filter within the transmission regime. Furthermore, the system exhibits robust angular invariance across the complete spatial Fourier domain and allows for the implementation of a reflection-domain bandpass filter that can be controlled via diffraction cutoff parameters.

The fabrication process involves the use of KOH etching on a silicon wafer with a nitride mask to produce an array of periodic triangular ridges. These silicon structures are then transformed into silica through a process of thermal oxidation. Two stages of oblique gold evaporation are then employed, resulting in the formation of gold hat structures positioned atop the ridges. Experimental characterization in the near-infrared regime, conducted through angular dispersion and full spatial Fourier space measurements, reveals high-pass and low-pass filters with power suppression levels exceeding 30 dB and 10 dB, respectively, beyond their intended cutoff angles. These empirical findings show exceptional agreement with both theoretical frameworks and full-wave electromagnetic simulations. By providing a high-performance, compact alternative to bulky optical components, this proposed system suggests a viable route toward lens-free spatial filtering in electromagnetic regimes such as the ultraviolet, terahertz, or X-ray ranges, where the precise fabrication and alignment of traditional lenses or pinholes are notoriously difficult to achieve.

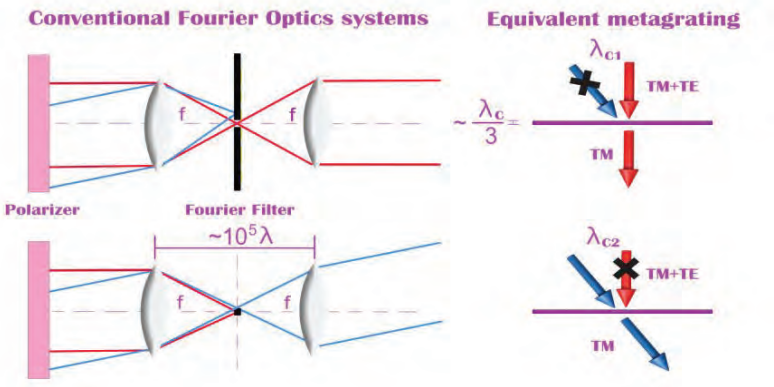

Fig. 1. Schematic of the proposed nanosystem, functionally equivalent to a standard 4f optical system[1].

References

[1] Abouelatta, Mahmoud AA, and Karim Achouri. "Metapinhole: Planar Fourier Optics Without Lenses." arXiv preprint arXiv:2509.05555 (2025).

Efficient Metasurface Modeling via Optimal Multipolar Decomposition of Bianisotropic Metasurfaces

Hossein Allahverdizadeh [1,*], Karim Achouri [1]

[1] *Laboratory for Advanced Electromagnetics and Photonics, Institute of Electrical and Microengineering, École Polytechnique Fédérale de Lausanne (EPFL),Lausanne, Switzerland*
[*] *hossein.allahverdizadeh@epfl.ch*

Multipolar decomposition is a powerful method for analyzing and designing interesting properties in metasurfaces, such as the Kerker effect, symmetry protected or accidental bound states in the continuum, and beam steering. To use the full benefits of this moment based method as efficiently as possible, we must ensure that no extra or redundant multipolar orders are included. This is an important step in the analysis or synthesis of metasurfaces based on multipolar moments; otherwise, dealing with a large number of multipole moments increases the model complexity and becomes computationally expensive.
The major factors that determine the number of multipolar moments required to describe the full properties of a metasurface can be categorized as follows: the electrical size of the object, lattice coupling effects, symmetry origin (Wyckoff position), and the choice of coordinate origin used for the multipolar decomposition [1].
In this work, we aim to reduce higher order multipole contributions by identifying the optimal coordinate position for multipolar decomposition, corresponding to an equilibrium position for the moments. To increase the degrees of freedom in choosing the decomposition origin for moments that may have different equilibrium positions, we separate the response into even and odd parity components [2]. This separation ensures that an origin shift applied to one parity set behaves orthogonally with respect to the other and does not disturb the overall response, which is formed by the superposition of these moments. In the next step, assigning effective electric and magnetic boundary conditions at these positions allows reproducing the full scattering behavior of the metasurface using fewer multipole moments, ultimately enabling a dipolar level modeling.

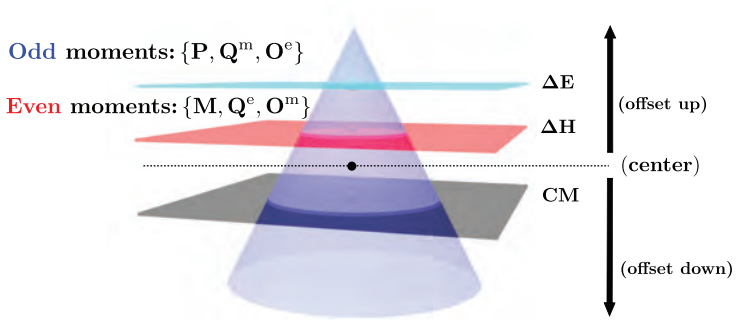

Fig. 1. Choice of the multipolar origin for different parities, modeled through electric and magnetic boundary conditions.

References

[1] A. V. Kildishev, K. Achouri, and D. Smirnova, "The art of finding the optimal scattering center(s)", Adv. Opt. Mater. **13**(4), 2402787 (2025).
[2] H. Allahverdizadeh and K. Achouri, "Multipolar angular scattering of substrated metasurfaces", Phys. Rev. B **112**(24), 245420 (2025).

Machine learning-driven inverse design of plasmonic metasurfaces

Amirmostafa Amirjani[1,*], Sweta Saha[1], and Ewald Janssens[1]
[1]*Quantum Solid-State Physics, Department of Physics and Astronomy, KU Leuven, 3001 Leuven, Belgium*
*amirmostafa.amirjani@kuleuven.be

The design of nanophotonic metasurfaces presents a fundamental challenge due to the vast number of possible geometries and the complex relationship between structure and optical response. Conventional design methods rely heavily on forward simulations and iterative trial-and-error optimization, which are computationally expensive and often fail to capture the full diversity of feasible solutions.
This research addresses these limitations by developing an inverse design framework that can automatically generate metasurface patterns tailored to specific optical properties in the range of visible and near-IR, with a focus on absorption and resonance control. The proposed approach integrates three key components: a bidirectional autoencoder that establishes a smooth latent space learning of the images and spectra with reduced dimensionality, a generative adversarial model that introduces valid design generation with respect to desired spectra performing inverse design, and a physics-informed neural network that enforces physical consistency in the generated solutions. Together, these elements form a unified pipeline that begins with a desired target spectrum and outputs candidate metasurface designs that are both realistic and physically viable.
Obtained results from simulations demonstrate that the framework can accurately reproduce geometrical solution for a respective target spectrum. This work establishes an innovative paradigm for the inverse design of metasurfaces, combining data-driven generative modeling with physics-based validation. Beyond the proof-of-concept demonstrated here, the approach provides a scalable and efficient route to designing next-generation optical devices for applications in sensing, energy harvesting, communications, and quantum technologies.

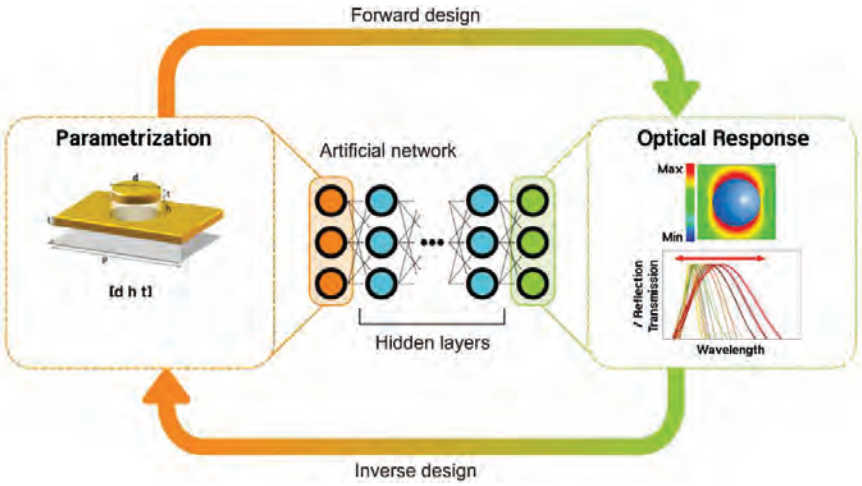

Fig. 1. Schematic representation of the NN approach for the inverse design of the metasurface parameters.

Modulational instability recurrence in second-harmonic generation

Andrea Armaroli [1,*], Stefania Malaguti,[1], Simone Ferraresi [1],
Gaetano Bellanca [1], and Stefano Trillo [1]

[1] *Department of Engineering, University of Ferrara, Ferrara, 44122 Italy*
[*] *andrea.armaroli@unife.it*

Modulational instability (MI) is pervasive in nonlinear optics: it manifests itself as the exponential growth of sideband pairs at the expense of a continuous wave pump. Beyond the initial growth stage, the MI dynamics turns out to be recurrent with the power flowing back and forth from the carrier to a sideband comb. The case of cubic nonlinearity gives rise to a non-trivial phase-space dynamics [1]. In the last few years, quadratic nonlinear effects have seen a resurgent interest, particularly because of the development of thin-film lithium niobate platforms. The dynamics of second-harmonic generation (SHG) is thus more and more accessible. Apart from the energy exchange between fundamental (FF) and second harmonic (SH), the propagation in a dispersive medium yields the appearance of MI sidebands around both components. Here, we show that a regular and recursive behavior must be expected also in a completely different regime which involves normal dispersion and high SHG-MI gain with no analogy whatsoever with the cubic case [2].

In order to model the SHG process in an optical waveguide, we use the following model

$$i\frac{\partial u_1}{\partial z} - \frac{\beta_1}{2}\frac{\partial^2 u_1}{\partial t^2} + u_2 u_1^* e^{i\delta k z} = 0;\; i\frac{\partial u_2}{\partial z} - \frac{\beta_2}{2}\frac{\partial^2 u_2}{\partial t^2} + \frac{u_1^2}{2}e^{-i\delta k z} = 0, \tag{1}$$

where u_j are FF ($j = 1$) and SH ($j = 2$) are the envelopes with spectra around frequencies $j\omega$, δk denotes the SHG phase-mismatch and $\beta_{1,2} = \pm 1$ the normalized group-velocity dispersion (GVD) coefficients. Stationary ($\partial/\partial t = 0$) solutions of Eqs. (1) exhibit MI: in the normal GVD regime, the pure SH pump mode ($u_1 = 0$) is MI unstable, for $\delta k > 0$, mainly via a three-wave mixing (3WM) process $2\omega \to (\omega - \Omega) + (\omega + \Omega)$, where Ω is the peak gain detuning. At $\delta k = 2$, this mode undergoes a bifurcation with a mixed FF-SH mode which has similar MI features. We assess whether and how these processes reverse at some distance giving rise to spatial recurrence.

A truncation of Eqs. (1) limited to the CW components at FF and SH along with a single pair of sidebands around the FF allows us to reduce the evolution to an integrable one degree of freedom Hamiltonian system. This method was extensively applied to MI in cubic media and gives an excellent qualitative agreement between the 3WM process and numerical solutions of Eqs. (1): the pure SH mode exhibits nonlinear recurrence and its period is predicted with excellent accuracy. When the mixed FF-SH mode is considered, a regular behavior is still observed close to the bifurcation point. Its description requires, though, an averaging procedure based on Hori-Lie transforms that allows us to explain the regular behavior and satisfactorily predict the recurrence period.

The advantages and limitations of this approach will be discussed. Our results will be of interest for an improved understanding of nonlinear conversion and photon pair generation in quadratic nonlinear waveguides.

References

[1] A. Mussot, C. Naveau, M. Conforti, A. Kudlinski, F. Copie, P. Szriftgiser, and S. Trillo, "Fibre multi-wave mixing combs reveal the broken symmetry of Fermi-Pasta-Ulam recurrence," Nature Photonics **12**, 303–308 (2018).

[2] A. Armaroli, S. Ferraresi, G. Bellanca, S. Malaguti, F. Baronio, and S. Trillo, "Recurrent nonlinear modulational instability via down-conversion in quadratic media," Phys. Rev. A **112**, 053525 (2025).

Environmental Effects on Emitter–Plasmon Strong Coupling

Stavros Athanasiou [1,*], Oliver J.F. Martin [1],

[1] *Nanophotonics and Metrology Laboratory (NAM), Swiss Federal Institute of Technology Lausanne (EPFL), 1015 Lausanne, Switzerland*

[*] *stavros.athanasiou@epfl.ch*

The interaction of quantum emitters with plasmonic cavities has been extensively studied over the past decade. Early theoretical works demonstrated that strong coupling can, in principle, be achieved despite the intrinsically large dissipation rates and broadband nature of plasmonic modes, a prediction later confirmed by numerous experiments. While initial theoretical studies primarily considered isolated nanostructures, experimental realizations increasingly involve plasmonic resonators supported on substrates or embedded in layered electromagnetic environments.

In this work, we provide new theoretical insights into the emitter-plasmon strong coupling (Figure 1(a)). We analyze and compare isolated and layered configurations, highlighting how environmental modifications and mode hybridization influence the coupling strength and spectral response. We employ the macroscopic quantum electrodynamics framework and perform electromagnetic calculations to obtain the spectral density.

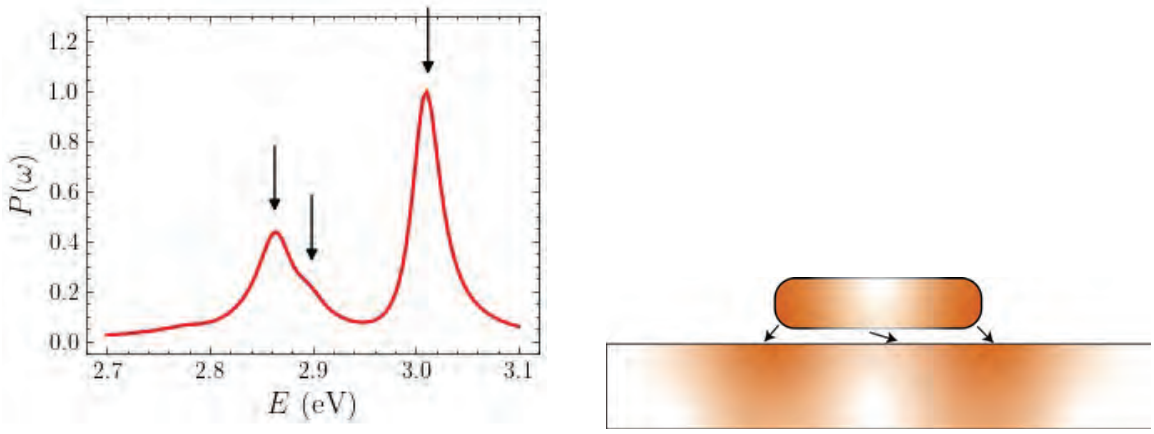

Fig. 1.: Strong coupling in plasmonic systems. (a) Emitter polarization spectrum exhibiting vacuum Rabi splitting in the strong coupling regime. (b) Schematic of the layered plasmonic system, illustrating the layered electromagnetic environment and the inhomogeneous emitter-plasmon coupling.

We further investigate the inhomogeneous coupling experienced by ensembles of emitters in plasmonic cavities, as in Figure 1(b). We quantitatively distinguish between strongly and weakly coupled emitters within the same system and assess how each contributes to the observed spectral features, including mode splitting, linewidth broadening, and background response. These results clarify how spatial and environmental inhomogeneities shape the signatures of strong coupling in realistic plasmonic platforms.

A detailed understanding of emitter-plasmon strong coupling is a key ingredient for the design of nanoscale systems supporting coherent light–matter interactions at room temperature and for controlling chemical and photochemical processes through tailored electromagnetic environments.

Fabrication tolerance analysis of modal phase matching for second-harmonic generation in MgO-doped LNOI waveguides

S. Ferraresi [1], A. Alaeddini [2], D. Fu [3], T. Li [3], G. Bellanca [1,*], K. Gallo [3]

[1] *Department of Engineering, University of Ferrara, Ferrara, 44122, Italy*
[2] *DIET, Sapienza University of Rome, Rome, 00184, Italy*
[3] *Nonlinear and Quantum Photonics Group, KTH Royal Institute of Technology, Stockholm, 10691, Sweden*
[*] *gaetano.bellanca@unife.it*

Lithium Niobate on Insulator (LNOI) has emerged as the leading platform for highly efficient nonlinear optical frequency conversion. However, achieving Modal Phase Matching (MPM) between the fundamental and higher-order second-harmonic modes requires precise dispersion engineering, making the device performance and functionality strictly dependent on the fabrication process yield. In this work, we perform a comprehensive numerical investigation into the phase matching tolerances of etched MgO-doped $LiNbO_3$ ridge waveguides.

Finite-element mode solvers have been employed to create multi-parameter heatmaps to visualize the phase-matching conditions across the whole design space. We performed a parametric sweep of waveguide geometry and temperature to map the sensitivity of the propagation constant mismatch ($\Delta\beta$), revealing the critical influence of sidewall verticality ($\partial\Delta\beta/\partial\vartheta$) on the MPM.

While the simulations predict a theoretical conversion efficiency slightly below the $100\,\%\,\mathrm{W}^{-1}\,\mathrm{cm}^{-2}$ mark for the optimized geometry (i.e., $884\,\mathrm{nm}$-wide, fully etched $600\,\mathrm{nm}$-thick ridge waveguide), the heatmaps demonstrate that slight geometrical deviations can significantly detune the device (see Fig. 1). To address these fabrication constraints, we further evaluated the thermo-optic tuning capabilities of the platform. By modeling the temperature-dependent refractive indices of the materials, we show that thermal tuning can effectively compensate for nm-scale geometrical imperfections, shifting the phase-matching condition back to the target wavelength. These results provide a much needed tolerance map for the fabrication of robust, high-efficiency LNOI nonlinear devices.

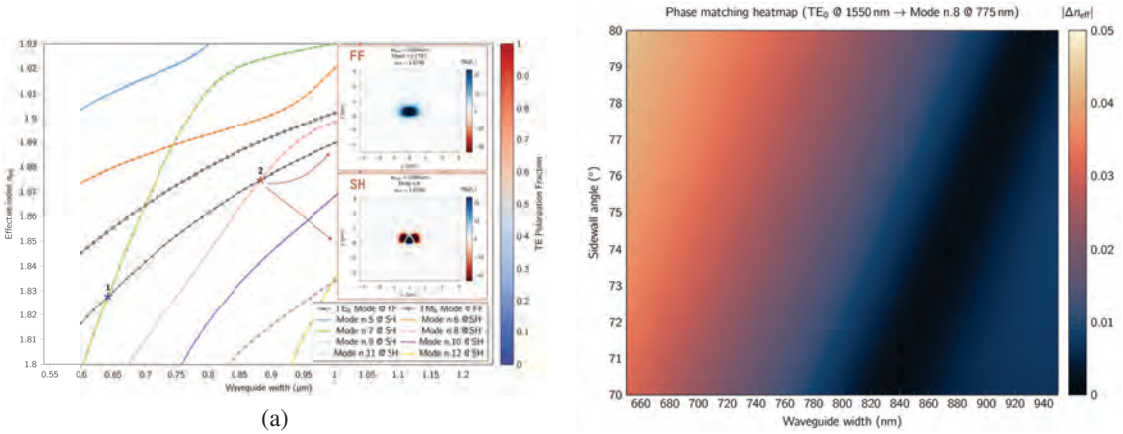

(a) (b)

Fig. 1.: **Modal Phase Matching (MPM) analysis**: (a) Dispersion curves for fundamental and higher-order SH modes; inset shows field profiles for the optimized geometry. (b) Sensitivity of the phase mismatch (Δn_{eff}) to variations in waveguide width and sidewall angle.

Inverse Design of InP Nanocavities for Photonic-Crystal-Based Random Lasing Networks

E. Bianco [1,2*], S. Iadanza [1,2], K. Moselund [1,2]

[1] *Paul Scherrer Institut (PSI), Laboratory of Nano and Quantum Technologies, 5232 Villigen PSI, Switzerland*
[2] *École Polytechnique Fédérale de Lausanne (EPFL), Integrated Photonics and Optoelectronics Laboratory, 1015 Lausanne, Switzerland*
[*] *enrico.bianco@epfl.ch*

Indium Phosphide (InP) is a well-established semiconductor for on-chip lasing, and the growing interest in random lasing systems stems from their ability to minimize the impact of fabrication errors on lasing modes. A pioneering implementation of a random lasing network using InP waveguides arranged in a Voronoi topology has shown remarkable results, particularly in machine learning applications [1]. However, the challenge of controlling losses at each Y-branch and modes non-linear interaction remains a limitation. In this context, photonic crystal (PhC) cavities present a promising platform for highly integrated random lasing systems [2], as they enhance nonlinear interactions through stronger light-matter coupling [3] and allow for better control of bending losses [4], due to their ability to accurately manipulate light propagation and dispersion.

To incorporate these PhC cavities into a random lasing network, the initial step is to simulate and optimize the properties of elementary PhC cavities. For this, we utilize the `Legume` Python library [5], which allows to perform a guided mode expansion analysis of PhC slabs. This approach enables an in-depth investigation of the band structure and mode profiles within the nanocavities. Additionally, an optimization procedure is applied to each cavity to enhance its resonance quality factor by minimizing an associated cost function using the `Adam` optimization algorithm [6]. By focusing on an uncladded dispersion-adapted (DA) cavity with air holes arranged in a hexagonal lattice (see Fig. 1), we demonstrate that a resonant mode with a quality factor of Q = 10^9 can be achieved.

Parameter	Value
Lattice constant	1.000
Hole radius	0.313
Slab thickness	0.927
Slab refractive index	3.17
Upper cladding refractive index	1.00
Lower cladding refractive index	1.00

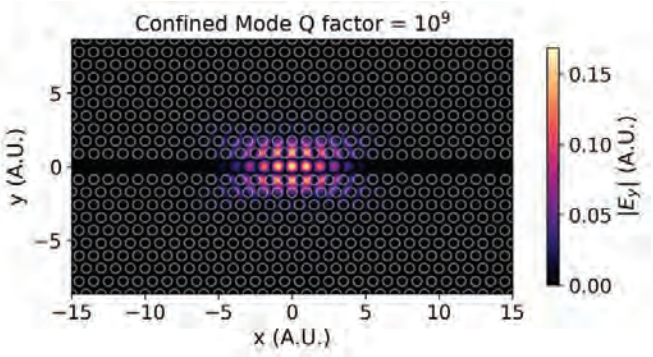

Fig. 1. $|E_y|$ distribution of the resonant mode inside the uncladded InP-based DA simulated supercell, composed of 30×20 periodic air holes (circles in the structure). The main geometrical and physical parameter are reported in the left table; all the spatial quantitites are adimensional.

References

[1] W. K. Ng, J. Dranczewski, A. Fischer, T. V. Raziman, D. Saxena, T. Farchy, K. Stenning, J. Peters, H. Schmid, W. R. Branford, M. Barahona, K. Moselund, R. Sapienza, J. C. Gartside, "Few-Shot Retinomorphic Vision in a Nonlinear Photonic Network Laser", arXiv (2025).

Electro-optical simulation of an integrated Ge-Si photodetector

M. Bonàs Vera [1,2*], B. Ding [1], S. Iadanza [1,2], A. Fontcuberta i Morral [3], K. E. Moselund [1,2]

[1] *Laboratory for Nano and Quantum Technologies, PSI, Villigen, 5232, Switzerland*
[2] *Integrated Nanoscale Photonics and Optoelectronics Laboratory, EPFL, Lausanne, 1015, Switzerland*
[3] *Laboratory of Semiconductor Materials, EPFL, Lausanne, 1015, Switzerland*
[*] *mariona.bonasvera@epfl.ch, mariona.bonas-vera@psi.ch*

In this work, we present a multiphysics simulation framework for an in-plane Ge-Si photodetector, based on the Template-Assisted Selective Epitaxy (TASE) technique [1]. TASE is an epitaxial growth fabrication method that allows to selectively replace patterned silicon structures with crystalline germanium (see Fig 1A), allowing to monolithically integrate active regions directly within the passive silicon photonic circuit. By using this approach, integrated photodetectors can be fabricated with geometries that are naturally in-plane and self-aligned with the passive circuit; which enables efficient waveguide coupling. Figure 1B depicts a photodetector scheme with the aforementioned properties.

The presented work focuses on the simulation of the Ge-Si heterojunction (see Fig 1C) as a first and essential step towards a full electro-optical model of the integrated photodetector. We intentionally constrain the device geometries and doping profiles to realistic fabrication limits, to ensure that the optimized structures are manufacturable. We use Ansys Lumerical FDTD solver to compute the wavelength-dependent carrier generation in the germanium region (as seen in the cross section of Fig 1C); these generation profiles are then imported into Ansys Lumerical CHARGE solver to evaluate dark and photo-current characteristics under applied bias.

The preliminary results demonstrate that the simulation framework is capable of estimating key device parameters, such as current-voltage characteristics (see Fig 1D), responsivity and spectral response. While the current study is limited to the heterojunction region, the simulation framework can be extended to full device simulations, including waveguide coupling, bandwidth estimation and eye-diagram analysis. These simulations establish a foundation to further optimize the device geometries, and will guide the fabrication and experimental validation of real devices.

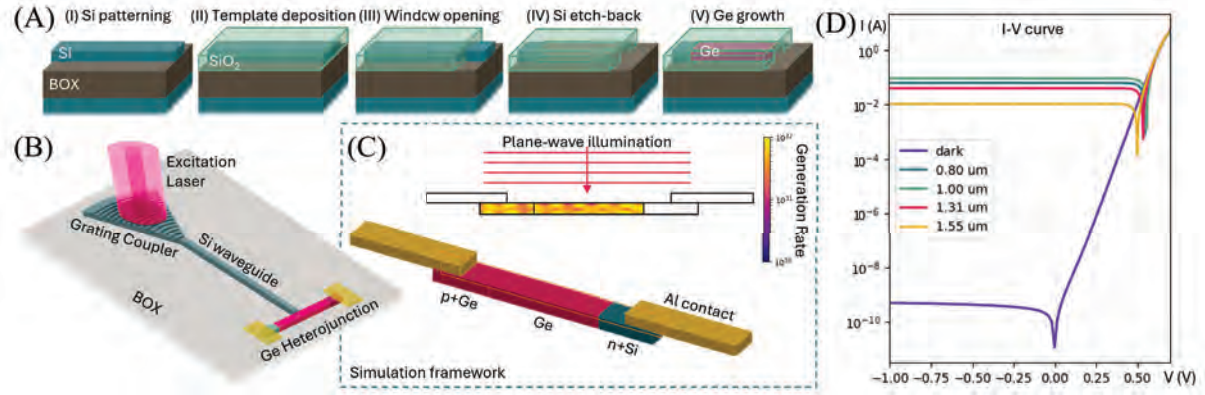

Fig. 1. (A) TASE fabrication process and (B) resulting in-plane Ge-Si photodetector concept. (C) Multiphysics simulation domain showing carrier generation profiles mapped from FDTD to the CHARGE solver. (D) Extracted I-V characteristics.

References

[1] H. Schmid, et al., "Template-assisted selective epitaxy of III–V nanoscale devices for co-planar heterogeneous integration with Si", Appl. Phys. Lett. **106**, 233101 (2015).

Traps and tricks in the eigenmode analysis of periodic metallic nanostructures

Sergejs Boroviks [1,*], Ilia Lykov [1], Olivier J.F. Martin [1]

[1] *Nanophotonics and Metrology Laboratory, Swiss Federal Institute of Technology Lausanne (EPFL), 1015 Lausanne, Switzerland*

[*] *sergejs.boroviks@epfl.ch*

Although light diffraction from plasmonic gratings and metasrufaces was rigorously investigated since the beginning of 20th century [1], and the physical understanding of *scattering anomalies* and *collective resonances*is well-established [2, 3], a inconsistency of terminology and interpretations of the underlying electromagnetic modes persist within the community. Furthermore, with the development of numerical simulation methods Finite-element-method-based numerical solvers like Comsol Multiphysics, electromagnetic simulations became widely available, however remain sometimes misused or incorrectly set up.

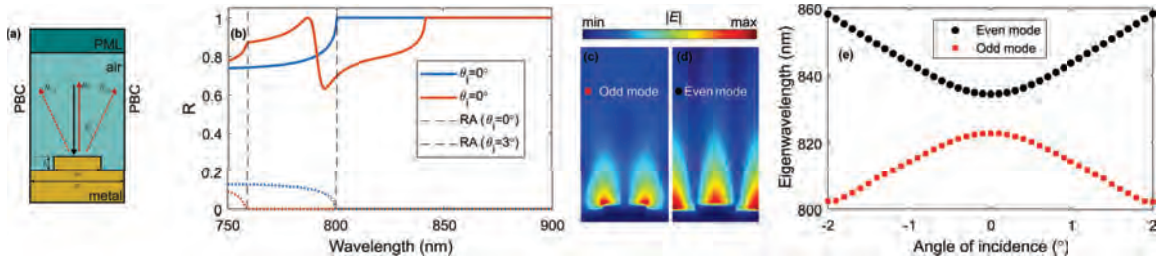

Fig. 1. (a) Simulation domain and imposed boundary conditions. (b) Reflection spectra at normal and 3° angles of incidence. (c) and (d) Field distributions of the odd and even eigenmodes supported by the grating. (e) Eigenmode dispersion.

In this presentation, we will some common traps and practical tricks to correctly set-up simulation model and resolve issues with convergence and reliability. We will discuss how to interpret numerical results and sort out so-called *spurious modes*, which inevitably appear among the found eigenmodes due to finite simulation domain geometry, periodic boundary conditions (PBC) and perfectly matched layers (PML), as shown in Fig. 1a. We will analyze dispersion of the eigenmodes of the system (Fig. 1e) and relate it to the spectral features (Fig. 1b) and examine associated near-field patterns (Fig. 1c and d) [4]. Furthermore, in the view of recent interest in *the bound state in the continuum* (BIC) [5], we will analyze their appearance within the eigenmodes of the system as well as their signatures in the scattering spectrum.

References

[1] R.W. Wood, "XLII. On a remarkable case of uneven distribution of light in a diffraction grating spectrum", The London, Edinburgh, and Dublin Philosophical Magazine and Journal of Science **4**, 396 (1902).

[2] U. Fano, "The Theory of Anomalous Diffraction Gratings and of Quasi-Stationary Waves on Metallic Surfaces (Sommerfeld's Waves)", J. Opt. Soc. Am. **31**, 213 (1941).

[3] A. A. Maradudin, I. Simonsen, J. Polanco, R. M. Fitzgerald, "Rayleigh and Wood anomalies in the diffraction of light from a perfectly conducting reflection grating", J. Opt. **18**, 024004 (2016).

[4] S. Boroviks, I. Lykov, O. J. F. Martin, "Interplay between Bound State in the Continuum and the Generalized Kerker Effect in Plasmonic Metasurfaces", *Manuscript in preparation* (2026).

[5] K. L. Koshelev, *et al.*,, "Interplay between Bound State in the Continuum and the Generalized Kerker Effect in Plasmonic Metasurfaces", Physics Uspekhi **66**, 494 (2023)

Multiscale computation of optical properties of soot nanoparticles: Coupling between atomistic DADI model and SIE method

N. Brosseau-Habert[1,2], P. Mavrikakis[3], G. Le Breton[1], S. Picaud[2], O. Martin[3], M. Devel[1]
[1]: *Institut FEMTO-ST, UMLP, Besançon, 25000, France*
[2]: *Institut UTINAM, UMLP, Besançon, 25000, France*
[3] : *NAM, EPFL, Lausanne, 1015, Suisse*
*nicolas.brosseau-habert@umlp.fr

We present a multiscale framework to compute the UV-visible optical properties of soot nanoparticles by bridging an atomistic model (Dynamic Atomic Dipole Interactions, DADI) with a continuum Surface Integral Equations (SIE) solver (T-PMCHWT formulation).

DADI uses atomic positions and frequency-dependent atomic polarizabilities to compute absorption cross sections and can also provide frequency-dependent effective complex refractive indices by Rayleigh-Debye-Gans inversion. These indices, combined with an outer surface description of a nanoparticle, are supplied to SIE to treat large geometries beyond the atomistic scale. We benchmark the approach on isolated primary soot spherules, represented by spheres in SIE, and on a two-spherule system (separated, in contact, or interpenetrated), and then apply it to a realistic aggregate.

For isolated spherules, DADI and SIE agree across the UV-visible and both match T-matrix. For two separated spherules, the mass absorption cross section (MAC) present small localized near-UV deviations when approaching contact (~2% at 225 nm when they are close, ~2.5% at contact). The visible remains consistent and within literature ranges (at 550 nm in contact: 6.62 $m^2 g^{-1}$ with DADI vs 6.90 $m^2 g^{-1}$ with SIE). For interpenetrated spherules, both methods predict a ~5 nm red shift and ~7% reduction of the main UV peak. Finally, absorption cross sections of a real soot nanoparticles, whose surface was modeled with 3D-tomography, are calculated with SIE using either refractive indices calculated by DADI for two separated spherules or refractive indices calculated for interpenetrated spherules. Corresponding results are given Fig.1. These calculations highlight the power of the coupling between DADI and SIE for computing optical properties of realistic soot nanoparticles and take into account at the same time the geometric and some chemical effects induced by interpenetration of spherules forming a nanoparticle, on its absorption spectrum.

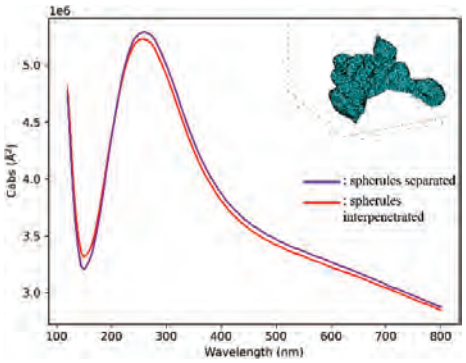

Fig. 1. Absorption cross sections (in Å²) of a real soot nanoparticle calculated with SIE.

References

[1] A. M. Kern and O. J. F. Martin, "Surface integral formulation for 3D simulations of plasmonic and high permittivity nanostructures", J. Opt. Soc. Am. A, **Vol. 26**, No.4, 732 (2009).

[2] N. Brosseau-Habert et al., "Changes of optical properties of two carbonaceous nanoparticles upon their coalescence: Computations at the atomistic level", JQSRT, **Vol. 346**, 109592 (2024).

Far-Field Patterns of Different Second-Harmonic Sources in Plasmonic Nanostructures

E. Buhara[1,*], S. Broviks[1], O.J.F. Martin[1]
[1]*Nanophotonics and Metrology Laboratory, Swiss Federal Technology Institute of Lausanne (EPFL), Lausanne, 1015, Switzerland*
*ebru.buhara@epfl.ch

Under the electric dipole approximation, inversion symmetry prevents second order nonlinear effects in centrosymmetric materials due to vanishing second order susceptibility. However, SHG occurs in plasmonic nanostructures and originates from both surface and bulk contributions. While SH measurement can provide general information about total SHG, far-field radiation patterns offer a method for distinguishing between these sources. Recent studies have indicated that surface SHG typically exhibits a dipolar emission pattern, whereas bulk SHG leads to higher-order multipolar radiation. However, these patterns also evolve with nanostructure size, making it critical to establish systematic criteria for their differentiation.

$$P_{surf}(r,2\omega) = \chi_{\perp\perp\perp}\mathrm{E}_{\perp}(r,\omega)\mathrm{E}_{\perp}(r,\omega) + \chi_{\parallel\parallel\perp}\mathrm{E}_{\parallel}(r,\omega)\mathrm{E}_{\perp}(r,\omega)$$

$$P_{bulk}(r,2\omega) = \gamma_{bulk}\nabla[\mathrm{E}(r,\omega)\mathrm{E}(r,\omega)] + \gamma_{bulk}[\mathrm{E}(r,\omega)\,\nabla\,]\mathrm{E}(r,\omega).$$

To systematically examine the behaviors of each SHG emission from gold nanostructures, numerical simulations were performed using the finite-element method (COMSOL Multiphysics). Each SHG signal was computed using different current densities related to the polarization's components in the above equations. While overall trend in SHG intensities is very similar for all different sources, the far field patterns exhibit differences which can be used for identification. For small structures (r < 120 nm), the SHG far-field responses are simpler with predominantly dipolar contributions. As the structure size increases (r > 120 nm), additional higher-order multipolar modes appear, leading to more complex far-field distributions. In particular, for radii exceeding 150 nm, quadrupolar contributions become non-negligible, leading to increased asymmetry in the emission pattern.

Far-field SHG analysis provides a robust method for distinguishing between surface and bulk nonlinear sources. Our findings suggest that small nanostructures primarily exhibit SHG with dipolar emission, while larger structures transition toward more complex responses, manifesting in more intricate angular patterns. These insights can guide the design of experimental work that can be used as distinguishing bulk and surface SHG in plasmonic material.

References

[1] Sipe, J. E., So, V. C. Y., Fukui, M., & Stegeman, G. I., "Analysis of second-harmonic generation at metal surfaces." Physical Review B Vol. 21, No. 10, 4389, 1980.
[2] Wang, F. X., Rodríguez, F. J., Albers, W. M., Ahorinta, R., Sipe, J. E., & Kauranen, M., "Surface and bulk contributions to the second-order nonlinear optical response of a gold film." Physical Review B-Condensed Matter and Materials Physics Vol. 80, No. 23, 233402, 2009.
[3] Benedetti, A., Centini, M., Bertolotti, M., & Sibilia, C., "Second harmonic generation from 3D nanoantennas: on the surface and bulk contributions by far-field pattern analysis." Optics express Vol. 19, No. 27, 26752-26767, 2011

Transfer Matrix Modeling of Strong Light-Matter Coupling in the THz Range

N. Charrouj[1,*], Y. Ivonyak[1,2], D. Yavorskiy[1,2], V. Umansky[3], W. Knap[1,2], M. Białek[1]

[1]*Centera, Institute of High Pressure Physics, Polish Academy of Sciences, Warszawa, Poland*

[2]*Centera, Cezamat, Technical University of Warsaw, Poland*

[3]*Weitzman Institute of Science, Rehovot, Israel*

*ncharrouj@unipress.waw.pl

Strong light-matter coupling between cavity photons and matter excitations gives rise to polaritons-hybrid quasiparticles exhibiting coherent and periodic energy exchange between light and matter. In the terahertz regime, this coupling can involve the cyclotron resonance of a two-dimensional electron gas (2DEG), resulting in so-called Landau polaritons [1].

Using time-domain terahertz (THz) magneto-spectroscopy, we directly measure phase-resolved Rabi oscillations in the time domain, related to periodic energy exchange between Fabry-Perot cavity modes and cyclotron modes in a high-mobility 2DEG based on GaAs/$Al_{0.36}Ga_{0.64}$As quantum well. The phase-resolved measurements reveal oscillatory energy exchange consistent with coherent polaritonic dynamics, going beyond the conventional frequency-domain observation of Rabi splitting. The strength of the coupling and the oscillation frequency are controlled by the electron density and cavity geometry. These results provide a direct view of the coherent light–matter interaction underlying the formation of Landau polaritons.

To provide a complete theoretical description that accounts for the presence of the 2DEG, the underlying semiconductor layers, and the metallic holder, we employ a semi-classical modeling approach based on the transfer matrix method, which is widely used in optics and radio-frequency electromagnetism [2]. We consider an electromagnetic wave incident normally from vacuum onto the layered structure. Since the quantum-well barrier thickness is on the order of 50 nm, we can assume the 2DEG is located at the surface of a GaAs semiconductor layer of thickness *d* and dielectric permittivity ε, which is backed by a metallic copper substrate. Given the incident electric field E_{int} and magnetic field H_{int}, the reflected field amplitudes can be determined by applying appropriate boundary conditions and assembling the total system transfer matrix. This semi-classical framework successfully reproduces the main experimental features. Our results demonstrate that the coupling of linearly polarized photons with a chiral matter mode, such as the cyclotron resonance, leads to the formation of a middle polariton, which is caused by the optical activation of a normally inactive chiral mode.

References:

[1] X. Li et al., “Vacuum Bloch–Siegert shift in Landau polaritons with ultra-high cooperativity, Nature Photonics, vol. 12, pp. 324–329, 2018.

[2] M. Born and E. Wolf, Principles of Optics, 7th ed.,Cambridge University Press, Cambridge, 1999.

High Quality factor Whispering Gallery Mode Microsphere Resonator Coupled to an On-Chip Waveguide

Naresh Choudhary[1,2,*], Manjunath Somarapalli[2], Shankar Kumar Selvaraja[2]

[1] *Indian Institute of Technology Madras*
[2] *Centre for Nano Science and Engineering (CeNSE), Indian Institute of Science*
*ee25d038@smail.iitm.ac.in

Whispering gallery mode (WGM) microsphere resonators deliver ultra-high quality (Q) factors surpassing other light confinement methods. Additionally, WGM microsphere offers straight forward fabrication without needing high-end lithography equipment or cleanroom facilities.

This work presents a comprehensive analytical-simulation-experimental study of silica microsphere resonators coupled to on-chip silicon nitride (SiN) waveguide, targeting optimized evanescent coupling between the microsphere and waveguide to achieve ultra-high Q-factor. For intrinsic Q-factor evaluation, a COMSOL-based model was developed and validated against analytical results across various modes and sphere diameters. Extrinsic Q-factors were obtained through analytical calculations involving mode field overlap integrals, using field distributions extracted from COMSOL for specific waveguide and microsphere dimensions. Experimentally, microspheres of varying diameters were fabricated by melting the tips of cleaved optical fibers.

These spheres were evanescently coupled to the SiN waveguide, and transmission spectra were recorded. The results revealed resonance dips with a free spectral range (FSR) of ~2.5 nm and Q-factors around 10^5 .This work lays the groundwork for subsequent application-driven research in ultra-sensitive sensing and integrated photonic systems.

References

1. Vahala, K. Optical microcavities. Nature 424, 839–846 (2003).
2. Chiasera, A., Dumeige, Y., Féron, P., Ferrari, M., Jestin, Y., Nunzi Conti, G., Pelli, S., Soria, S. and Righini, G.C. (2010), Spherical whispering-gallery-mode microresonators. Laser & Photon. Rev., 4: 457-482.

GPU accelerated tool for analysis of large scale diffractive optical elements

Adria Cobos Concha[1,2,*], Rafal Kukolowicz[1], Guillem de la Torre[1], Fernando Díaz-Doutón[2]
[1]*Inmersia Computers S.L., Barcelona, 08908, Spain*

[2]*Centre for Sensors, Instruments and Systems Development (CD6), Universitat Politècnica de Catalunya, Terrassa, 08222, Spain*

*adria.cobos@upc.edu

Diffractive optical elements (DOEs) are widely used in numerous photonic applications. Passive DOEs comprise a broad class of devices such as metasurfaces, surface relief gratings (SRGs) and holographic optical elements (HOEs). Although based on nano- and microstructured modulation, many advanced applications use large-scale DOEs spanning millimeter to centimeter scales. Mentioned DOEs are often characterized using numerical methods to accurately predict light propagation and diffraction efficiency, such as FDTD, FEM, and RCWA. However, in the context of large-scale DOEs both FDTD and FEM require discretizing the entire computational volume with fine meshes to resolve nanoscale features. As a result, computational time and memory scale rapidly with domain size, making optimization and iterative design impractical [1]. In contrast, RCWA [2] exploits the periodic nature of DOEs, offering faster simulations and making it more suitable for large-area design and optimization. Furthermore, commercial software with many solver capabilities, such as COMSOL (*Comsol AB*) and Lumerical (*Ansys Inc.*), are often cumbersome to use and suboptimal for conditions involving large-scale DOEs.

Given this context, we developed an in-house software analysis tool optimized and focused on solving arbitrarily large-scale DOE structures. Naturally, this tool employs a custom-developed RCWA solver that supports full anisotropy and layered materials. Moreover, it can launch thousands of RCWA solvers through GPU parallelization, achieving a time reduction of >10–50× compared to commercial software. Consequently, it enables optimization routines to run on a reasonable timescale.

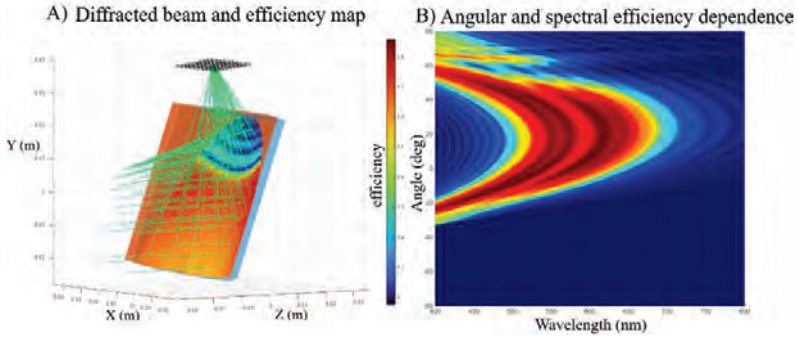

Fig. 1. Examples of the developed software utilities: (A) Large-scale DOE showing ray tracing and the diffraction efficiency map of the diffracted light. (B) Angular and spectral dependence of the first diffracted order of a DOE.

Acknowledgements: With the support of the Industrial Doctorate Plan of the Department of Research and Universities of the Government of Catalonia.

References

[1] C. Kang, et al., "Large-scale photonic inverse design: computational challenges and breakthroughs", *Nanophotonics* **13**, 3765 (2024).

[2] M. G. Moharam, et al., "Stable implementation of the rigorous coupled-wave analysis for surface-relief gratings: enhanced transmittance matrix approach", *J. Opt. Soc. Am. A* **12**, 1077 (1995)

Resonance prediction for plasmonic metal-insulator-metal waveguide filters

Shafaq Ejaz*, Manfred Hammer, Jens Förstner

Theoretical Electrical Engineering, Paderborn University, Paderborn, Germany
*shafaq@mail.uni-paderborn.de

Metal-insulator-metal waveguide filters of variable cavity width are considered in 2-D. Using the modes of the cavity segment and reflectance matrices of the coupling regions, our semi-analytical transfer matrix model allows to predict the transmission resonances. Numerical finite-element simulations confirm the results.

Plasmonic MIM filters

Segments of metal-insulator-metal (MIM) waveguides can be combined in manifold ways to enable optical filter functions [1]. We consider a configuration where two narrower, single-mode channels access a central wider, multimode cavity segment. Fig. 1(a) shows a schematic of our 2-D model. Finite-element simulations (COMSOL) lead to the transmittance pattern of Fig. 1(c), with a regular series of resonances beyond a cavity width of about $W = 750\,\mathrm{nm}$, at a distance of $\Delta W \approx 202\,\mathrm{nm}$.

Prediction of resonant configurations

The modes of the central cavity segment, with complex effective indices n_{eff} as shown in Fig. 1(b), establish a transfer matrix T for the guided wave propagation along the cavity. Next we compute numerically a reflectance matrix R for the coupling regions at both ends of the cavity. We then assume that a transmission resonance requires an initial field that is reproduced as good as possible after one cavity roundtrip. Resonances can thus be identified as minima in the level μ of the smallest (absolute) eigenvalue of $\mathsf{RTRT} - 1$. Fig. 1(c) shows an excellent agreement with the direct simulations.

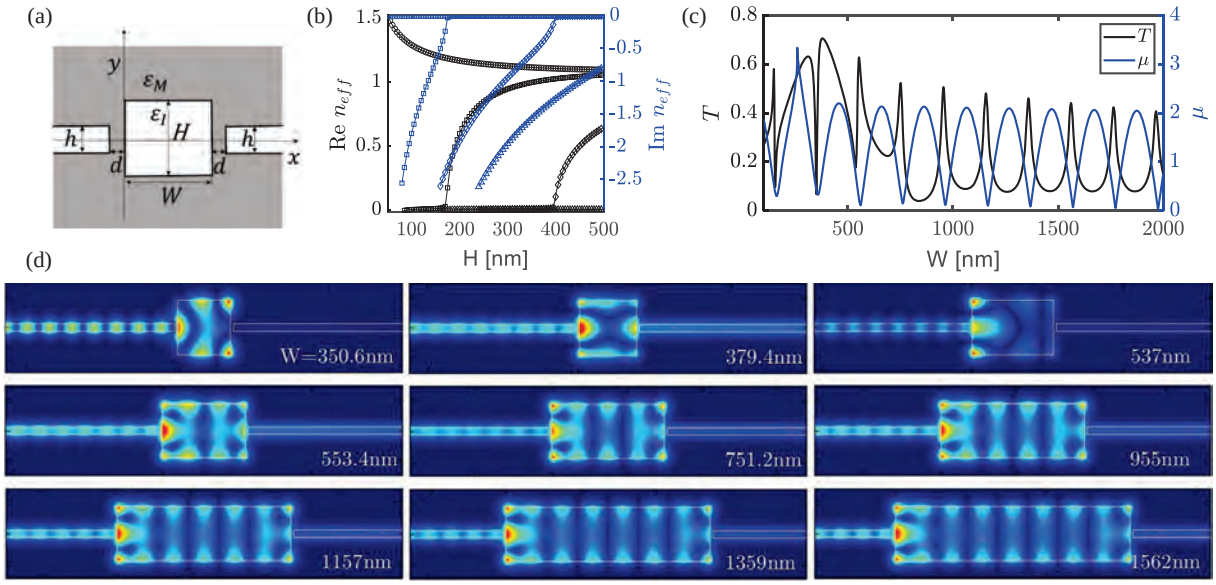

MIM filter, schematic (a); effective mode indices n_{eff} vs. height H (b), transmittance T and roundtrip-matrix eigenvalue μ vs. cavity width W (c); absolute magnetic field pattern for different cavity widths (d). Parameters: $\varepsilon_{\mathrm{M}} = -7.014 - \mathrm{i}0.212$ (Ag), $\varepsilon_{\mathrm{I}} = 1$, $\lambda = 450$ nm, gaps $h = 50$ nm, $H = 360$ nm, $d = 20$ nm.

References

[1] G. Veronis, Z. Yu, S.E. Kocabas, D.A.B. Miller, M.L. Brongersma, S. Fan, *Metal-dielectric-metal plasmonic waveguide devices for manipulating light at the nanoscale*, Chinese Opt. Lett. **7**, 302–308 (2009).

Mittag-Leffler expansion of the scattering matrix for spherical particles via rescaled scattering channels

E. Fösleitner[1,*], A. C. Valero[1], Z. Sztranyovszky[2], E. A. Muljarov[3], K. Koshelev[4], T. Weiss[1]
[1]*Institute of Physics, University of Graz, and NAWI Graz, Universitätsplatz 5, 8010 Graz, Austria*
[2]*School of Physics and Astronomy, University of Birmingham, Birmingham B15 2TT, United Kingdom*
[3]*School of Physics and Astronomy, Cardiff University, Cardiff CF24 3AA, UK*
[4]*Department of Electronic Materials Engineering, Research School of Physics, Australian National University, Canberra, ACT, Australia*

*elias.foesleitner@uni-graz.at

The scattering matrix, which connects the incoming and outgoing waves of a scatterer, plays a central role in describing light-matter interaction and its pole expansion provides a powerful framework for replacing full-wave simulations with resonance-based models. In this work, we investigate the analytic continuation of the optical scattering matrix and its pole expansion in terms of optical resonances for spherical particles [1,2]. While it is well established that resonance frequencies appear as poles of the scattering matrix in the complex frequency plane, obtaining a pole expansion using the Mittag-Leffler theorem remains challenging for the commonly used scattering channels from Mie theory, due to their exponential divergence in the complex frequency plane.

We demonstrate that a Mittag-Leffler expansion of the scattering matrix becomes possible through an appropriate rescaling of the basis, i.e., the incoming and outgoing waves, and provide a rigorous framework on how this rescaling of the basis affects the scattering matrix. We show that certain rescalings remove exponential divergences in the scattering matrix, which we refer to as regularization. Moreover, we demonstrate that the choice of rescaling is not unique and that certain choices can fundamentally alter the analytic continuation of the scattering matrix. We identify the emergence of additional, non-physical poles (see, e.g., the poles with positive imaginary part in Fig. 1), referred to as channel poles, that do not originate from the optical resonances of the system.

These results suggest that regularizations of the scattering matrix could enable efficient pole expansion schemes for more complex three-dimensional scatterers, thereby broadening the range of systems accessible to modal analysis in photonics.

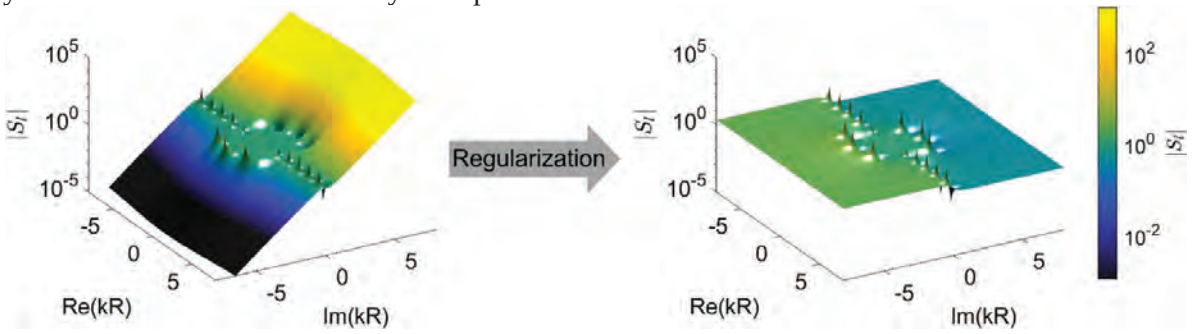

Figure 1: Magnitude of the scattering matrix element S_l for a sphere with refractive index n = 2.5, radius R = 100 nm, and multipole order l = 3 in the complex wavenumber plane. Left: The scattering matrix using conventional Mie basis diverges exponentially in the complex kR plane. Right: Using rescaled basis functions removes this divergence, enabling a Mittag-Leffler expansion.

References

[1] T. Weiss and E. A. Muljarov, "How to calculate the pole expansion of the optical scattering matrix from the resonant states", Phys. Rev. B **98**, 085433 (2018).

[2] S. V. Lobanov, W. Langbein, and E. A. Muljarov, "Resonant-state expansion applied to three-dimensional open optical systems: Complete set of static modes", Phys. Rev. A **100**, 063811 (2019).

Mie Void Resonators for Programmable Quantum Emission Control

Yuchao Fu[1,*], Sergejs Boroviks[1], Olivier J. F. Martin[1]
[1] *Nanophotonics and Metrology Laboratory, Swiss Federal Institute of Technology Lausanne (EPFL); 1015 Lausanne, Switzerland.*
*yuchao.fu@epfl.ch

Controlling light emission at the nanoscale is central to many nanophotonic technologies, including quantum light sources, fluorescence imaging, and optical information encoding. While plasmonic nanostructures can strongly enhance emission, their performance is often limited by intrinsic ohmic losses. Dielectric resonators provide a low-loss alternative, yet their optical modes are typically confined inside high-index materials, which restricts efficient coupling with emitters located in the surrounding environment. Here we introduce silicon Mie void resonators, nanoscale air cavities etched into a dielectric substrate that represent the complementary geometry of conventional Mie particles. By relocating resonant electromagnetic modes into the low-index void region, this architecture enables emitters to interact directly with confined fields while minimizing material absorption. This configuration provides a flexible platform for tuning optical excitation and radiative emission within a single subwavelength cavity. We establish a quantitative framework that connects the geometry of the void resonator with two key mechanisms governing emission modulation: excitation enhancement resulting from local field concentration and radiative-rate modification associated with the Purcell effect. Full-wave electromagnetic simulations are used to analyze multipolar resonances, field confinement, and emitter–resonator coupling across a broad parameter space. The theoretical predictions are validated experimentally using gradient and uniform arrays of silicon Mie voids fabricated by focused ion beam milling. Fluorescence measurements reveal geometry-dependent emission modulation together with resonance-assisted shortening of the emission lifetime. A strong correlation between calculated emission tuning factors and measured fluorescence intensities confirms the predictive capability of the proposed model. Leveraging this mechanism, we further demonstrate a bimodal nanophotonic pattern with near-diffraction-limited pixel resolution, enabling distinct optical responses in bright-field, dark-field, and quantum-emission channels. These results establish Mie void resonators as a versatile platform for programmable nanoscale light–matter interaction, with promising applications in quantum photonics, optical encryption, high-resolution fluorescence imaging, and nanoscale sensing.

Physics-Informed Neural Networks for Confocal Fluorescence Imaging Under Wave-Optics Constraints

F.Z. Goffi[1,*], M. Soltaninezhad[1,2], E. Corbetta[1,2], T. Bocklitz[1,2]
Photonic Data Science Department, Leibniz Institute of Photonic Technology (IPHT), Jena, Germany
[2]*Institute of Physical Chemistry (IPC) and Abbe Center of Photonics (ACP),*
Friedrich Schiller University (FSU), Jena, Germany
*fatima.goffi@leibniz-ipht.de

Incorporating wave-optics equations within learning enables accurate confocal image reconstruction and supports model-based inverse problems in fluorescence microscopy. Here, we develop a physics-informed neural network (PINN) [1]. A framework for confocal microscopy in which reconstruction is constrained by wave-propagation PDEs and confocal detection physics, aiming to improve physical fidelity and generalization across imaging conditions.

The forward operator is formulated through the microscope system response, modeling illumination and detection PSFs together with a pinhole to link a parametric specimen representation to the recorded intensity [2]. Key experimental and simulation settings, including wavelength, numerical aperture (NA), excitation conditions, and fluorophore emission intensity, are treated as explicit parameters, making it straightforward to adapt the reconstruction to different optical configurations and environmental conditions. The training objective combines measurement/data-consistency terms with PDE-residual losses that penalize deviations from the wave-optical model, improving robustness under noise and limited supervision.

We validate the PINN outputs by benchmarking against real confocal images. These experimental confocal data serve as the ground-truth reference for quantitative and qualitative comparison. Beyond image recovery, the same framework can be used as an inverse model to estimate specimen characteristics encoded in the parametric representation (e.g., fluorophore brightness/concentration and structural descriptors) by optimizing them under the wave-optical forward model. This unifies reconstruction and parameter inference within a single physics-constrained learning pipeline for confocal fluorescence microscopy [3].

References

[1] M. Raissi, P. Perdikaris, and G.E. Karniadakis. “Physics-informed neural networks: A deep learning framework for solving forward and inverse problems involving nonlinear partial differential equations”, Journal of Computational physics 378, 686-707 (2019).
[2] J. Mertz, “Introduction to optical microscopy”, Cambridge University Press (2019).
[3] Z. Burns, and L. Zhaowei. “Untrained, physics-informed neural networks for structured illumination microscopy”, Optics Express 31.5, 8714-8724 (2023).

Momentum-related orthogonality of modes in dielectric optical waveguides

Denis A. Kopylov, Manfred Hammer*

Institute for Photonic Quantum Systems (PhoQS), Paderborn University, Paderborn, Germany
* *manfred.hammer@uni-paderborn.de*

Beyond power orthogonality, the guided modes of dielectric channels satisfy orthogonality conditions related to the momentum of the optical electromagnetic field. The modes thus act as individual carriers of momentum.

Guided optical waves

Consider a straight lossless dielectric channel waveguide along the z-axis, specified through the tensorial Hermitian relative permittivity $\hat{\epsilon}(x,y)$ that is a function of the transverse x-y-coordinates only. Guided electromagnetic fields in the frequency domain are superpositions of guided modes

$$(\boldsymbol{E},\boldsymbol{H})(x,y,z)=\sum_m c_m\,(\boldsymbol{E}_m,\boldsymbol{H}_m)(x,y)\,\exp(-\mathrm{i}kN_mz)$$

for vacuum wavenumber k, assuming a time dependence $\sim\exp(\mathrm{i}\omega t)$ with frequency $\omega=k\mathrm{c}$, for vacuum speed of light c. Individual modes with electromagnetic profile $(\boldsymbol{E}_m,\boldsymbol{H}_m)$ and effective index N_m contribute with amplitudes c_m.

Momentum-related orthogonality

For the above guided field, the momentum flux M, the momentum (Minkowski, time-averaged, z-component, [1]) transferred per time unit through a cross-section plane, can be written

$$M=\langle\boldsymbol{E},\boldsymbol{H};\boldsymbol{E},\boldsymbol{H}\rangle\,,$$

where, for two integrable electromagnetic fields $\boldsymbol{E}_\mathrm{a}$, $\boldsymbol{H}_\mathrm{a}$ and $\boldsymbol{E}_\mathrm{b}$, $\boldsymbol{H}_\mathrm{b}$, the product $\langle\,.\,;\,.\,\rangle$ is

$$\langle\boldsymbol{E}_\mathrm{a},\boldsymbol{H}_\mathrm{a};\boldsymbol{E}_\mathrm{b},\boldsymbol{H}_\mathrm{b}\rangle=\frac{1}{4}\iint\left[\epsilon_0\,(\boldsymbol{E}_\mathrm{a}\odot(\hat{\epsilon}\boldsymbol{E}_\mathrm{b})^*+\boldsymbol{E}_\mathrm{b}^*\odot\hat{\epsilon}\boldsymbol{E}_\mathrm{a})+\mu_0\,(\boldsymbol{H}_\mathrm{a}\odot\boldsymbol{H}_\mathrm{b}^*+\boldsymbol{H}_\mathrm{b}^*\odot\boldsymbol{H}_\mathrm{a})\right]\mathrm{d}x\,\mathrm{d}y,$$

with

$$\boldsymbol{A}\odot\boldsymbol{B}=\frac{1}{2}\,(A_xB_x+A_yB_y-A_zB_z)\,.$$

Using the former definitions, we show [2] that nondegenerate modes m, n of the same channel, normalized to power P_m, are orthogonal as

$$\langle\boldsymbol{E}_m,\boldsymbol{H}_m;\boldsymbol{E}_n,\boldsymbol{H}_n\rangle=\delta_{mn}\,M_m,\quad\text{with}\quad P_m/M_m=\omega/(kN_m)=\mathrm{c}/N_m.$$

The momentum transferred per time unit along the channel, $M=\sum_m|c_m|^2M_m$, thus separates into contributions of individual modes.

We shall outline the derivation of these relations, report on a numerical check for the vectorial hybrid modes of realistic thin-film lithium niobate channels, and discuss implications. In particular, the momentum-related modal orthogonality paves the way towards a rigorous, self-consistent procedure for the quantization of guided electromagnetic fields in the typical channels found in integrated photonic circuits [2].

References

[1] D. J. Griffiths. Resource letter EM-1: Electromagnetic momentum. *American J. Physics*, 80(1):7–18, 2012.
[2] D. A. Kopylov and M. Hammer. Classical and quantum electromagnetic momentum in anisotropic optical waveguides, 2025. arXiv:2512.16495 [quant-ph].

Multi-Photon Dynamics without Mode Decomposition

B. L. Inci [1,*], D. Schulz [1],

[1] Chair for Micro- and Nanoelectronics, TU Dortmund, 44227, Germany
*berndlevent.inci@tu-dortmund.de

Numerical simulations of quantum optical processes in integrated and nanophotonic structures are increasingly challenged by strong material inhomogeneities, complex geometries, and nontrivial boundary conditions. While classical real-space methods such as finite-difference or finite-integration techniques efficiently capture these features, many quantum-optical approaches still rely on mode decompositions [1] numerically [2] or analytically [3] accessible eigenfunctions, which become impractical for realistic structures.

In this contribution, we present a real-space formulation of quantum electrodynamics that directly builds on structure-preserving discretizations of Maxwell's equations. Starting from the source-free Maxwell dynamics, the corresponding operator is identified as the single-particle generator of photon propagation and discretized using the Finite Integration Technique (FIT) [4]. This leads to a selfadjoint discrete operator that fully encodes material inhomogeneities, geometry, and boundary conditions.

Based on this operator, a consistent bosonic lattice Hamiltonian of the form $\hat{H} = \hat{\psi}^\dagger D \hat{\psi}$ is constructed, enabling the direct simulation of single- and multi-photon states in real space without mode decomposition. The resulting equations of motion describe a unitary single-particle dynamics, from which multi-photon interference effects emerge solely due to bosonic symmetry and coherent scattering, without introducing explicit photon–photon interaction terms.

We demonstrate the approach for the propagation of a single-photon wave packet in an inhomogeneous waveguide and verify photon-number conservation in the discrete setting. To illustrate the capability of the framework to capture genuine multi-photon effects, we simulate the spatial probability distribution of two-photon interference at a 50/50 beam splitter. The numerical results are compared to the ideal unitary beam-splitter model of the Hong–Ou–Mandel effect, showing good agreement and quantifying deviations caused by numerical dispersion and finite spatial resolution.

The presented framework establishes a direct connection between classical real-space electromagnetics and quantum-optical many-body dynamics. It provides a scalable and flexible tool for studying quantum interference and multi-photon propagation in complex photonic structures, with potential applications in integrated quantum photonics, on-chip interferometry, and the design of quantum optical devices in realistic geometries.

References

[1] W. C. Chew, A. Y. Liu, C. Salazar-Lazaro, W. E. I. Sha, "Quantum Electromagnetics: A New Look—Part II", IEEE J. Multiscale Multiphysics Comput. Tech. 1, 85 (2016).
[2] D.-Y. Na, J. Zhu, W. C. Chew, F. L. Teixeira, "Quantum information preserving computational electromagnetics", Phys. Rev. A 102, 013711 (2020).
[3] S. Scheel, S. Y. Buhmann, "Macroscopic quantum electrodynamics—concepts and applications", Acta Phys. Slovaca 58, 675 (2008).
[4] M. Clemens, T. Weiland, "Discrete electromagnetism with the finite integration technique", Prog. Electromagn. Res. 32, 65 (2001).

A generalized perturbative approach for the computation of nonlinear scattering problems

Jérémy ITIER [1,*], Gilles RENVERSEZ [1], Frédéric ZOLLA [1],

[1] *Aix Marseille Univ, CNRS, Centrale Med, Institut Fresnel, Marseille, France*
jeremy.itier@fresnel.fr

We developed a perturbative technique for modeling the scattering of light by a nonlinear material. This approach eliminates the need for an iterative algorithm to solve the fully coupled nonlinear problem. We demonstrate its effectiveness in the case of a nonlinear anisotropic cylinder.

The modeling of the scattering of light by nonlinear materials leads, even for a monochromatic source, to a system of coupled nonlinear partial differential equations. Two main approaches are commonly employed to solve these equations. The first consists in directly solving the coupled nonlinear system through iterative methods; however this approach is very time-consuming. The second approach relies on perturbation theory. Assuming that the field amplitudes are sufficiently small, the coupled nonlinear system can be decoupled into a set of linear equations that are solved sequentially. In this work, we generalize this approach to the n-th order for the full system of nonlinear equations describing light scattering in the harmonic domain, and compare it with the solution obtained using a previously reported direct iterative approach [1].

A plot of the second-harmonic electric field is shown in Fig. 1 for a nonlinear two-dimensional LiNbO3 cylinder illuminated by a TM-polarized incident wave. The rigorous solution, computed using an iterative scheme [1], is shown alongside the solutions obtained with the perturbative approach at orders 2 and 4. We observe that the second-order perturbative approach, commonly referred to as the undepleted-pump approximation, deviates significantly from the rigorous solution, whereas the fourth-order result matches it very well. Furthermore, we observe that the computation time required by the perturbative approach is drastically reduced compared to the iterative approach. Consequently, the generalized perturbative approach developed in this work should be useful for the design and optimization of photonic devices requiring accurate control of nonlinear processes.

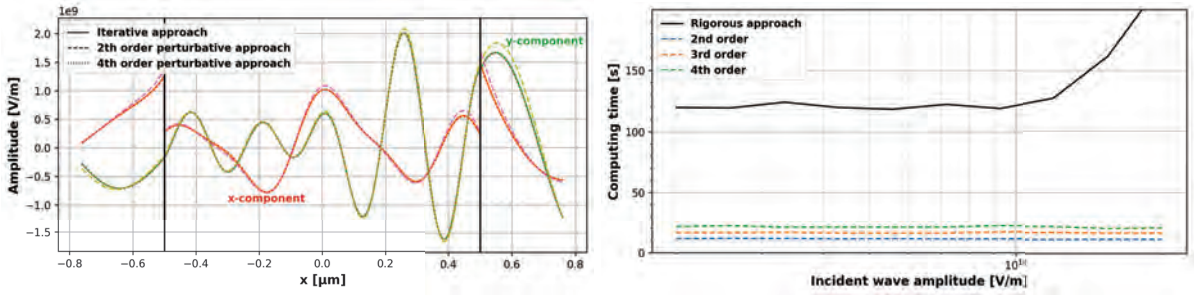

Fig. 1. Nonlinear scattering by a LiNbO3 2D cylinder. On the left, the real amplitude of the second harmonic $\mathbf{E}(2\omega)$ is shown along the x axis, for a TM incident plane wave with an amplitude of $E_0 = 2.10^{10} V/m$. The two solid black vertical bars represent the cylinder interface. On the right the computation time is shown as a function of the incident-wave amplitude, for both approaches and at different orders.

References

[1] Jérémy Itier, Gilles Renversez, and Frédéric Zolla. Scattering modeling by a nonlinear slab: Exact solution of the full vector problem. *Physical Review A*, 112(6):063506, December 2025.

Preprint: **arXiv:2512.17608**

PyMieDiff: Enabling differentiable Mie scattering through PyTorch

Oscar K. C. Jackson [1,*], Peter R. Wiecha [2] Simone De Liberato[1,3] Otto L. Muskens[1]

[1] *School of Physics and Astronomy, Faculty of Engineering and Physical Sciences, University of Southampton, SO17 1BJ Southampton, UK*

[2] *LAAS-CNRS, Université de Toulouse, UPS, Toulouse, France*

[3] *Istituto di Fotonica e Nanotecnologie – Consiglio Nazionale delle Ricerche (CNR), Piazza Leonardo da Vinci 32, Milano, Italy*

[*] *o.k.jackson@soton.ac.uk*

Understanding light-matter interactions, especially for sub-wavelength spherical particles, is foundational to many scientific fields. Recent advancements in machine learning have generated significant interest in end-to-end differentiable frameworks. We present our work on PyMieDiff [1], a PyTorch-based toolkit for modelling core–shell spherical particles with native support for automatic differentiation, as illustrated in Figure 1. By implementing standard Mie recurrence relations, including spherical Bessel/Hankel functions, angular functions, and vector spherical harmonics, within PyTorch's autograd backend, we enable a fully differentiable workflow for computational nanophotonics. It's architecture ensures seamless integration with the broader PyTorch ecosystem, which we demonstrate by coupling PyMieDiff with TorchGDM [2], a differentiable Green's Dyadic Method package, for multi-particle simulations and embedding it as a native layer in physics-informed "tandem" neural networks to eliminate the need for surrogate training.

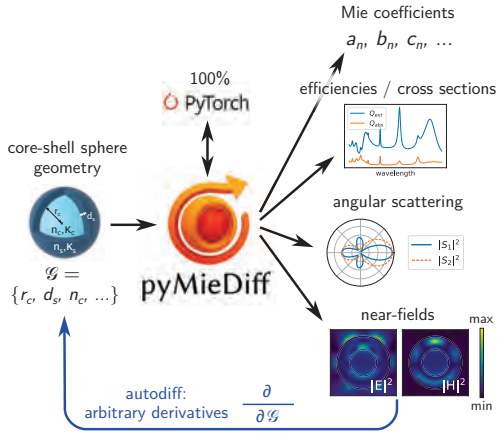

Fig. 1. The API exposes a class for defining core-shell spheres, with optional tabulated materials. It computes extinction, absorption and scattering efficiencies, far-fields and S-matrix elements, as well as near-fields, all with autograd, large-scale parallel processing and GPU support. The results shown are from a gold-silicon core-shell particle with core radius $r_c = 100\,\text{nm}$ and shell radius $r_s = 200\,\text{nm}$, placed in vacuum and illuminated by a linearly polarized plane wave. Image reproduced from our work [1].

References

[1] O. K. C. Jackson, S. De Liberato, O. L. Muskens, P. R. Wiecha, PyMieDiff: A differentiable Mie scattering library, arXiv preprint arXiv:2512.08614 (2025).

[2] S. Ponomareva, A. Patoux, C. Majorel, A. Az´ema, A. Cuche, C. Girard, A. Arbouet, and P. Wiecha, TorchGDM, SciPost Phys. Codebases 60 (2025).

2D/3D FDTD Modeling of Coaxial Waveguide with Magnetized Nonlinear Ferrite and Slow-Wave Structure.

S. Karelin*, I. Onishchenko
National Science Center «Kharkiv Institute of Physics and Technology», Ukraine
*sergeykarelin1976@gmail.com

A coaxial waveguide partially filled with magnetized ferrite and insulating dielectric enables pulse-front compression and oscillation packet generation at 0.3–10 GHz [1]. Its numerical modeling uses a 2D axially symmetric FDTD scheme coupled with parallel solution of nonlinearized Landau-Lifshitz equations via Runge-Kutta methods [2]. Using this approach, in [3] it was shown that an insulating dielectric with permittivity $\varepsilon > 60$ enables long-lasting oscillations via a Cherenkov-like effect, but its practical potential is limited due to high-frequency dielectric losses in materials with extremely high permittivity, such as water. To enhance performance, we propose a spiral central conductor design, mimicking high-permittivity dielectrics, with ferrite placed inside. Due to the loss of axial symmetry in the spiral design, the FDTD model [2] was extended to 3D coordinates. Simulations show that the waveguide with ferrite and spiral conductor generates a long-lasting oscillation packet similar to that of a high-permittivity dielectric-filled waveguide (Fig. 1). The prolonged oscillation train with the slow-wave structure is likely related to changes in the transverse electromagnetic field distribution, enhancing energy transfer efficiency and reducing losses. Further studies are needed to clarify this mechanism.

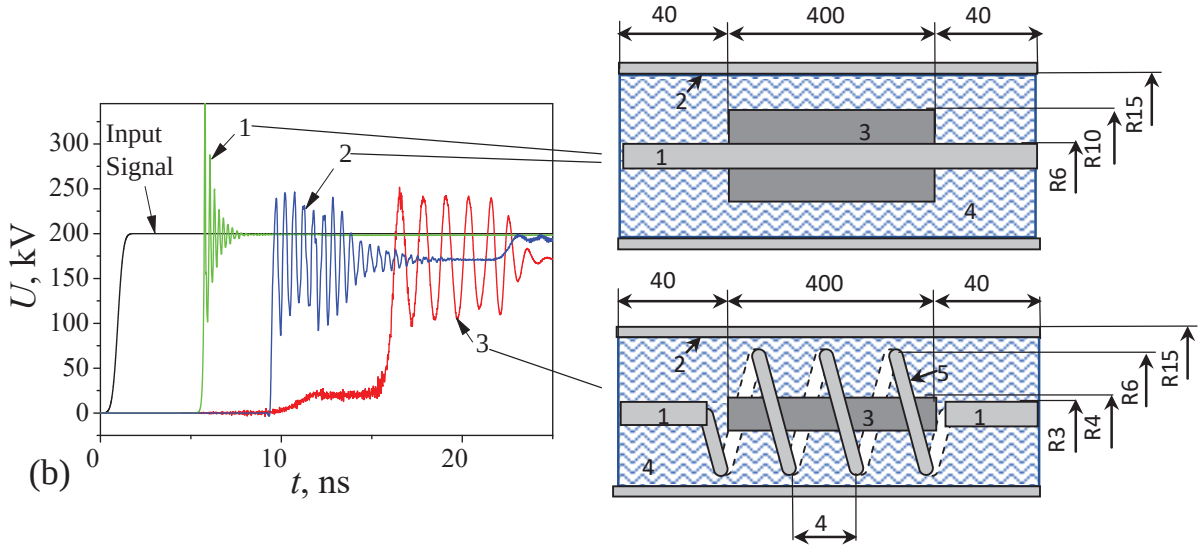

Fig. 1. Coaxial waveguide filled with dielectric $\varepsilon = 2.25$ (curve 1) and $\varepsilon = 80$ (curve 2) and coaxial waveguide with spiral conductor with dielectric $\varepsilon = 2.25$ (curve 3). Ferrite (all cases): $M_S = 300$ kA/m, $H_0 = 30$ kA/m, $\alpha = 0.1$, $\varepsilon = 12$. 1 – inner conductor, 2 – outer conductor, 3 – ferrite, 4 – insulating dielectric, 5 – spiral conductor

References

[1] J.E. Dolan, "Simulation of shock waves in ferrite-loaded coaxial transmission lines with axial bias", J. Phys. D: Appl. Phys. **32**, 1826 (1999).
[2] S.Y. Karelin, "FDTD analysis of nonlinear magnetized ferrites: simulation of oscillation forming in coaxial line with ferrite", Telecomm. Radio Eng. **76**, 873 (2017).
[3] S.Y. Karelin, V.B. Krasovitsky et al., "Quasi-harmonic oscillations in a nonlinear transmission line, resulting from Cherenkov synchronism", Probl. At. Sci. Technol. 122, **65** (2019)

Inverse-designed Si-Sb2S3 tunable multi-mode interference coupler

P. Kepič[1,*], C. Li[2], H. Yu[2], S. Maier[2], T. Šikola[1,3], H. Ren[2] and F. Ligmajer[1,3]

[1] *Central European Institute of Technology, Brno University of Technology, Purkyňova 123, Brno, 612 00, Czech Republic*

[2] *School of Physics and Astronomy, Monash University, Melbourne, VIC, 3800, Australia*

[3] *Institute of Physical Engineering, Faculty of Mechanical Engineering, Brno University of Technology, Technická 2, Brno, 616 69, Czech Republic*

* peter.kepic@ceitec.vutbr.cz

While GST-based phase-change materials dominate tunable photonic integrated circuits (PICs), their performance is limited by large absorption in the crystalline state. Here we present an inverse-designed, tunable multi-mode interference (MMI) coupler based on a hybrid Si–Sb_2S_3 structure, exploiting the large refractive-index contrast ($\Delta n > 1$) and nearly zero losses in both phases of Sb_2S_3 (Fig. 1a). Amorphous Sb_2S_3 was deposited at room temperature by pulsed laser deposition (10 Hz, 0.5 J/cm², Ar 100 mTorr) onto 300 nm Si on r-cut sapphire, targeting 30 nm but yielding 37 nm thickness (Fig. 1b), followed by a 256 nm SiO_2 protective cap. Optical constants of amorphous and crystalline Sb_2S_3 in Fig. 1a were obtained by spectroscopic ellipsometry, giving n = 2.38 (amorphous) and n = 2.85 (crystalline) at 1550 nm. The MMI coupler geometry was optimized using an inverse-design workflow based on the open-source script spins-B [2] to maximize routing to output 1 in the amorphous state and to reverse the functionality after crystallization. The device, which consists of an input coupler, two output couplers, and the optimized Si–Sb_2S_3 MMI patch (Fig. 1c), was fabricated by electron-beam lithography and characterized at 1550 nm by mapping the output intensities relative to a reference waveguide. Compared to pixel-based laser-written devices [3], this approach offers a faster (potentially switchable via single-shot), more compact, and more energy-efficient alternative to prior designs and establishes a promising direction for tunable PIC platforms.

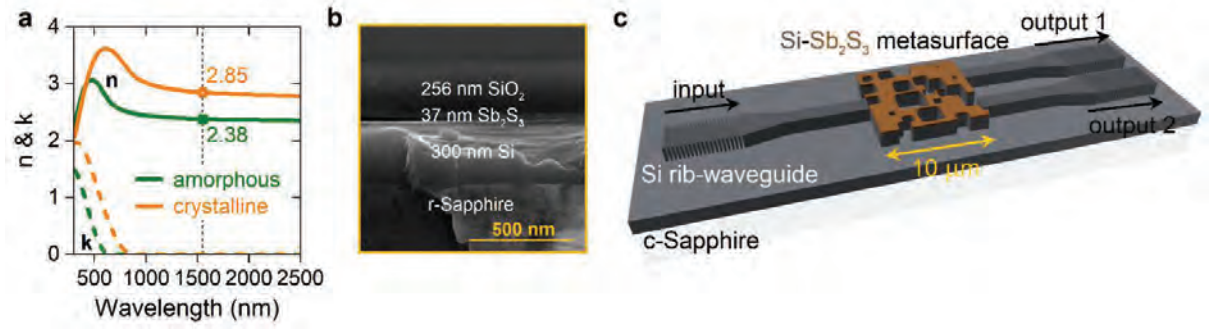

Fig. 1. a) Measured refractive index and extinction coefficient of 37 nm Sb_2S_3 film from (b) in amorphous (green) and crystalline (orange) phases. The dashed line highlights the 1550 nm wavelength of interest. b) SEM micrograph of r-Sapphire-Si- Sb_2S_3-SiO_2 multilayer cross-section with listed thicknesses c) Scheme of the inverse-designed Si-Sb_2S_3 tunable integrated meta-switch.

References

[1] Y. Yang, et al., “Integrated metasurfaces for re-envisioning a near-future disruptive optical platform”, Light: Science & Applications, 12, 152 (2023).

[2] S. Molesky, et al., “Inverse design in nanophotonics”, Nature Photonics, 12, 659–670 (2018).

[3] M. Delaney, et al., “Nonvolatile programmable silicon photonics using an ultralow-loss Sb2Se3 phase change material”, Sci. Adv., 7, 25 (2021).

Photonic structures in transition metal dichalcogenides for integrated quantum photonics

A. Kohlwes [1,*], Z. Li [2], T. Shegai [2], D.E. Reiter [1]

[1] TU Dortmund University, Otto-Hahn-Str. 4, 44227 Dortmund, Germany
[2] Chalmers University of Technology, Gothenburg, SE-412 96 Göteborg, Sweden
*Anita.Kohlwes@tu-dortmund.de

Integrated photonics relies on nanostructured materials, including single-photon emitters, waveguides, or photonic cavities. While most existing approaches use different materials for active and passive components, we aim to realize a single-material, all-in-one photonic platform based on transition-metal dichalcogenides (TMDCs). With this goal in mind, we simulate passive photonic TMDC structures using Maxwell solvers such as FDTD or FEM and optimize their performance. A special focus lies on finding the optimal height of the waveguide, as the realistically thickness that can be fabricated is often limited. In the figure below, we show an overview (top-left figure) how much power can be guided by a $MoTe_2$ waveguide for different width and height. Around the overview-plot different mode-profiles are shown for selected width-height combinations. Our numerical results help to derive clear design rules toward experiments that maximize performance while remaining compatible with planar processing.

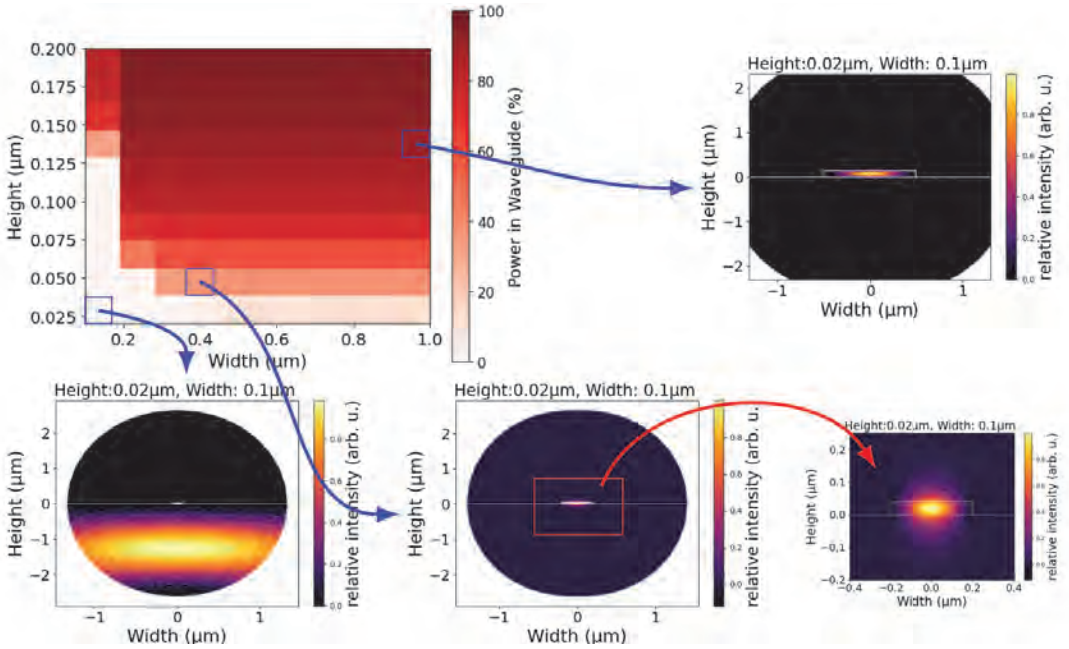

Fig. 1. Top-left: Overview how much power is guided by a rectangular waveguide for different height and width. All other plots: Mode profiles for selected width-height combinations.

Following the optimization of simple wave guides, we introduce a periodic array of holes in the waveguide to create a photonic bandgap. By tuning the period and hole diameter, we design efficient mirrors and a stopband at the target wavelength for TMDC single-photon emitters Our results represent a first step towards a single-material TMDC photonic platform.

Decoupling nonlinear excitation and emission using dual bound states in the continuum

Changliang Li[1,2*], Sergejs Boroviks[1], Luo Feng[2], Olivier Martin[1]

[1]*Nanophotonics and Metrology Laboratory, Swiss Federal Institute of Technology Lausanne (EPFL); 1015 Lausanne, Switzerland*

[2]*School of Materials Science and Engineering, Nankai University, Tianjin 300350, China*

*changliang.li@epfl.ch

Lanthanide-doped upconversion nanoparticles (UCNPs) convert near-infrared photons into visible emission with negligible autofluorescence and are widely explored for bioimaging, optical security and nonlinear photonics. However, their intrinsically small absorption cross-sections and multiphoton excitation pathways require high pump intensities, limiting efficiency and integration in compact photonic systems. Here we demonstrate a photonic strategy that decouples nonlinear excitation and radiative emission channels using dielectric metasurfaces supporting dual bound states in the continuum (BICs). The metasurfaces host two spectrally separated high-Q resonances: a strongly localized quasi-BIC near 980 nm that amplifies the pump field driving nonlinear excitation, and a radiative quasi-BIC in the visible spectrum that governs directional emission. This separation enables independent engineering of excitation and radiation processes through lattice periodicity and symmetry breaking, without spectral interference between the two channels. Integrating $NaYF_4$: Yb^{3+}/Er^{3+} nanoparticles onto the metasurfaces yields upconversion enhancements exceeding 3.7×10^3 at 650 nm and 9.2×10^2 at 540 nm under low pump powers, outperforming previously reported plasmonic and dielectric single-resonance platforms. The large enhancement originates from a multiplicative mechanism that combines nonlinear pump-field amplification with controlled photon extraction. These results establish dual-BIC channel engineering as a general paradigm for manipulating nonlinear light–matter interactions, providing a route toward energy-efficient nonlinear emitters and integrated photonic systems.

Self-Consistent Optical-Thermal Modeling of VO_2 Nanoparticles for Tunable Photonic Applications

J. Kabát[1,2], P. Kepič[1], T. Bačová[2], F. Ligmajer[1,2,*]

[1]*Brno University of Technology, Central European Institute of Technology, Brno, Czech Republic*

[2] *Brno University of Technology, Faculty of Mechanical Engineering, Brno, Czech Republic*

*filip.ligmajer@vutbr.cz

Vanadium dioxide (VO_2) is a phase-change material exhibiting an insulator-to-metal transition near 68 °C, accompanied by pronounced changes in refractive index and absorption. These properties make VO_2 attractive for tunable and nonlinear photonic devices. In this work, we present results of numerical simulations of the optical properties of VO_2 nanoparticles, specifically accounting for the coupled dynamics of heat propagation and temperature-induced electromagnetic effects. We utilize an iterative convergence algorithm to solve for the steady-state temperature of VO_2 nanospheres and nanodiscs. Our results reveal a phenomenon termed "nonlinear ignition": the onset of a localized surface plasmon resonance in the metallic phase creates a positive feedback loop between absorption and photothermal heating. This leads to an abrupt, step-like jump in temperature and optical state once a critical threshold intensity is reached. We demonstrate that this threshold is highly sensitive to the thermal bias and refractive index of the substrate. Furthermore, we analyze the integration of VO_2 into hybrid silicon nitride (SiN) waveguides for on-chip amplitude modulation. Contrary to intuition, we find that a direct-contact configuration can be superior to designs utilizing low-index buffer layers. By optimizing the VO_2 patch thickness, high extinction ratios can be achieved with manageable loss. This work establishes a robust framework for designing scalable, energy-efficient photonic devices based on the intrinsic thermodynamics of VO_2.

Intelligent Multimodal Meta-lens Imaging and Perception

X. Liu[1,*], O. J. F. Martin[1]

[1]*Nanophotonics and Metrology Laboratory, Swiss Federal Institute of Technology Lausanne (EPFL), EPFL-STI-NAM, Station 11, CH- 1015 Lausanne, Switzerland*

*xiaoyuan.liu@epfl.ch

Meta-lenses built from engineered nanoantenna arrays enable compact imaging with reduced spherical aberrations [1-3]. However, broadband operation remains challenging due to chromatic aberrations from wavelength-dependent phase, material dispersion, and resonances, leading to a trade-off among efficiency, aperture, and bandwidth. Traditional solutions such as multilayer stacking or sophisticated dispersion engineering often increase fabrication complexity and limit scalability. To address these issues, we propose a deep learning-based computational achromatic meta-lens that enables full-color imaging without complex physical dispersion engineering. We develop MetaScope, an optics-driven neural network for chromatic correction and segmentation in miniaturized endoscopy. Gradient-guided distillation improves joint optimization, yielding better color fidelity, sharper reconstructions, and higher segmentation accuracy than state-of-the-art methods on clinical imaging tasks. We further introduce binocular meta-lenses by integrating two meta-lenses on a single substrate to realize an ultracompact stereo vision system with depth perception, replacing conventional dual-camera setups. We demonstrate applications in digital image correlation (DIC), particle image velocimetry (PIV), and assisted driving perception. For digital image correlation, the binocular meta-lens achieves below 2 μm precision in in-plane translation and accurately reconstructs 3D deformation fields in bending tests. For particle image velocimetry, it recovers 3D velocity fields using binocular disparity and particle displacement, reaching a vortex-ring diameter error of about 1.25%. The stereo vision system further integrates imaging, object detection, instance segmentation, and depth estimation into a unified stereo meta-lens pipeline for driving assistance. Overall, this work highlights the potential of meta-lenses combined with computation to deliver ultracompact, high-performance imaging systems across biomedical, mechanics, fluid, and driving vision applications.

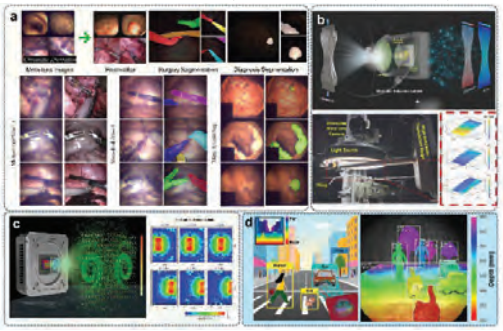

Fig. 1. AI-enabled meta-lens vision. **a** Meta-lens endoscopy. **b** DIC for surface deformation measurement. **c** PIV for fluid flow diagnosis. **d** Multimodal intelligent driving vision.

References

[1] W. Li, W. Pan, X. Liu, et al., "MetaScope: Optics-Driven Neural Network for Ultra-Micro Metalens Endoscopy," ICCV2025, 25938 (2025).

[2] X. Liu, Z. Zhao, S. Xu, et al., "Meta-lens Particle Image Velocimetry," Adv. Mater. **36**(17), 2310134 (2024).

[3] Z. Zhao, X. Liu, Y. Ji, et al., "Meta-lens digital image correlation," Opto-Electron. Adv. **8**, 250014 (2025).

[4] X. Liu, W. Li, T. Yamaguchi, et al., "Stereo Vision Meta-lens Assisted Driving Vision," ACS Photonics **11** (7), 2546 (2024).

A framework for modelling scattering of polarization-entangled photons

I. Lopushenko

Faculty of Information Technology and Electrical Engineering, University of Oulu, Oulu, FI-90014, Finland
ivan.lopushenko@oulu.fi

Applications involving light scattering mechanisms rapidly progress from utilizing traditional polarized light beams towards more complex sources, such as topological beams carrying orbital angular momentum, photon sources with quantum entanglement, and advanced light sources which combine these features [1]. In this regard, the ways to tailor non-classical light to improve sensing and imaging techniques have yet to be explored: both empirically and from the perspective of fundamental light-matter interaction [2]. Current work aims to contribute to this rapidly developing field by building upon recent findings that enabled tracking of the scattering of polarization-entangled photon states in turbid media. In particular, it has been demonstrated that radiative transfer models, which resolve polarized light tracing via iterative solution to the Bethe-Salpeter equation (BSE) [3], can be generalized to track the evolution of the quantum state of polarization-entangled photon pair when one of the partner photons is scattered inside the specimen which resembles biological tissue, while another photon propagates through a reference channel [4].

The proposed approach is based on the known concept of multiple beam Stokes parameters [5], which is rooted in the relationship between Wolf's coherency matrix and quantum state density matrix, and which in turn can be interpreted in terms of the relationship between scattering and probability amplitudes for the pure states, including entangled ones. Although such field-to-probability inference must be treated with great caution, this method allows one to evaluate the probability amplitudes of the polarization-entangled photon pairs which undergo scattering, provided that the corresponding scattering phase function is known. Currently, it remains to be seen whether the proposed method is mainly applicable in the case when partner photons are spatially or temporally detuned or it allows further generalizations, which is one of the central topics of ongoing studies. It is already clear that, at the very least, the proposed concept allows to move beyond the scattering of the single partner photon to the scattering of both partner photons. Additionally, it is stressed that the indicated approach is in fact independent of the specific BSE-based polarization tracking and therefore can potentially act as a framework to generalize many of the existing well-developed light scattering techniques which operate with scattering diagrams, from Lorentz-Mie theory to the vector radiative transfer equation, enabling further research into scattering dynamics of quantum-entangled photonic states.

References

[1] R. Fickler, R. Lapkiewicz, W. N. Plick, M. Krenn, C. Schaeff, S. Ramelow, A. Zeilinger, "Quantum entanglement of high angular momenta," Science **338**, 6107 (2012).

[2] I. Meglinski, I. Lopushenko, A. Sdobnov, A. Bykov, "Phase preservation of orbital angular momentum of light in multiple scattering environment," Light Sci. Appl. **13**, 214 (2024).

[3] E. Akkermans, P. E. Wolf, R. Maynard, G. Maret, "Theoretical study of the coherent backscattering of light by disordered media," J. Phys. France **49**, 77 (1988).

[4] V. R. Besaga, I. V. Lopushenko, O. Sieryi, A. Bykov, F. Setzpfandt, I. Meglinski, "Bridging classical and quantum approaches for quantitative sensing of turbid media with polarization-entangled photons," Laser Photonics Rev., e01172 (2026).

[5] D. F. V. James, P. G. Kwiat, W. J. Munro, A. G. White, "Measurement of qubits," Phys. Rev. A **64**, 052312 (2001).

Structural perturbation theory for bound states in the continuum

Lijun Yuan [1], Ya Yan Lu [2,*]

[1] *School of Mathematics and Statistics, Chongqing Technology and Business University, Chongqing, China*
[2] *Department of Mathematics, City University of Hong Kong, Kowloon, Hong Kong*
[*] *mayylu@cityu.edu.hk*

In open lossless dielectric structures with 1D periodicity, resonant modes depend on a real Bloch wavenumber β and form bands with a complex dispersion relation $\omega = \omega(\beta)$, where ω is complex. A bound state in the continuum (BIC) is a special resonant mode with a real ω. Given a BIC (with Bloch wavenumber β_* and frequency ω_*) in a structure with dielectric function $\varepsilon_*(\mathbf{r})$, it is important to study the resonant modes with β near β_* (for the fixed structure) [1, 2, 3] , and it is also important to consider the effect of structural perturbations, since in practice, perturbations are always present.

For a 2D structure $\varepsilon_*(\mathbf{r})$ that is periodic in y and finite in z, we consider perturbed structures with a dielectric function $\varepsilon(\mathbf{r}) = \varepsilon_*(\mathbf{r}) + \delta F(\mathbf{r})$, where $\mathbf{r} = (y, z)$, $F(\mathbf{r})$ is the perturbation profile that preserves the periodicity in y, both ε_* and F are even functions of z, and $\delta \geq 0$ is the amplitude of the perturbation. We study five cases: (1) F real and symmetric (i.e. even) in y, (2) F is real and asymmetric in y, (3) F is purely imaginary with $\mathrm{Im}(F) \geq 0$, (4) F is purely imaginary with $\mathrm{Im}(F) \leq 0$, and (5) F is complex and $\mathcal{PT}$-symmetric in y, i.e., $\overline{F}(-y, z) = F(\mathbf{r})$.

Case (1) has previously been analyzed for different types of BICs [4, 5]. In general, BICs may exist in the perturbed structure. Case (2) for symmetry-protected BICs has been studied in [2, 6]. In general, BICs do not exist in the perturbed structure. We analyze different types of BICs and determine the β at which the resonant mode has the largest Q factor. Case (3) corresponds to structures with a small material loss. Again, we determine the β at which the Q factor is maximized. Case (4) is for structures involving gain media. The eigenmodes satisfying the outgoing radiation condition (as $z \to \pm\infty$) can have positive, zero or negative $\mathrm{Im}(\omega)$. We determine the β at which $\mathrm{Im}(\omega)$ is a local maximum. Those modes with $\mathrm{Im}(\omega) = 0$ are the lasing threshold modes (LTMs). They are not BICs, sine they have non-zero outgoing waves. Again, we determine the values of β for the LTMs. It is well known that each LTM corresponds to a coherent perfect absorption (CPA) solution in the complex-conjugated structure. For case (5), gain and loss are balanced as far as $\varepsilon(\mathbf{r})$ is concerned, but outgoing eigenmodes can have positive, zero and negative $\mathrm{Im}(\omega)$. Interestingly, the real frequency modes are either BICs or LTMs, and in fact, they appear in pairs. Again, we determine the β for which $\mathrm{Im}(\omega)$ is a local maximum or equals 0. Our results for cases (4) and (5) are completely new.

References

[1] L. Yuan, Y. Y. Lu, "Strong resonances on periodic arrays of cylinders and optical bistability with weak incident waves," Phys. Rev. A **95**, 023834 (2017).
[2] L. Yuan and Y. Y. Lu, "Perturbation theories for symmetry-protected bound states in the continuum on two-dimensional periodic structures," Phys. Rev. A **101**, 043827 (2020).
[3] N. Zhang, Y. Y. Lu, "Perturbation theory for resonant states near a bound state in the continuum," Phys. Rev. Lett. **134**, 013803 (2025).
[4] L. Yuan, Y. Y. Lu, "Bound states in the continuum on periodic structures: perturbation theory and robustness," Opt. Lett. **42**, 4490 (2017).
[5] N. Zhang, Y. Y. Lu, "Bifurcation of bound states in the continuum in periodic structures," Opt. Lett. **49**, 1461 (2024).
[6] K. Koshelev, S. Lepeshov, M. Liu, A. Bogdanov, Y. Kivshar, "Asymmetric metasurfaces with high-Q resonances governed by bound states in the contonuum," Phys. Rev. Lett. **121**, 193903 (2018).

Numerical Analysis of Finite-Difference PML Modes in Free-Space Problems

H. Lüder*, I. Koltchanov, A. Richter

VPIphotonics GmbH, Hallerstr. 6, 10587 Berlin, Germany
**hannes.lueder@vpiphotonics.com*

Perfectly matched layers (PMLs) are layers of artificial materials that provide strong attenuation for incident waves without introducing reflections. They are the most widely used method to emulate free-space conditions in numerical simulations of scattering problems. When PMLs are introduced into eigenvalue problems, so-called PML modes appear. These modes can be interpreted as a discrete approximation of the continuous radiation-mode spectrum of the corresponding open-boundary problem. The PML modes can be used to incorporate radiating solutions into eigenmode-based methods such as mode matching and coupled-mode theory [1, 2].

While some classes of eigenmode problems (e.g. bend-mode radiation or power leakage into a high-index substrate) require PMLs merely to allow the (quasi-)guided mode to become leaky, the accurate representation of scattered or free-space propagating fields (e.g. for waveguide discontinuities or waveguide facet emission into free space) crucially depends on the availability of correct PML modes.

In this study, we analyze the influence of finite-difference discretization on PML modes by comparing exact analytical and numerical solutions. We verify the (non-conjugated [2]) mode orthogonality for numerical PML modes and discuss practical limitations in representing free-space propagation using PML modes. Figs. 1 (a) and (b) compare exact and numerical solutions for an analytically solvable problem. While excellent agreement is observed for many modes, a clear deviation becomes apparent around mode 42. Beyond this point, the numerically calculated modes are influenced by the discretization. Fig. 1 (d) shows that numerical mode orthogonality still holds beyond this point, although it degrades. An additional branch of modes (42/43, 50/51) appears; these modes are highly localized in the PMLs (Fig. 1 (c)) and exhibit numerical degeneracy (highlighted with circles in Fig. 1 (d)).

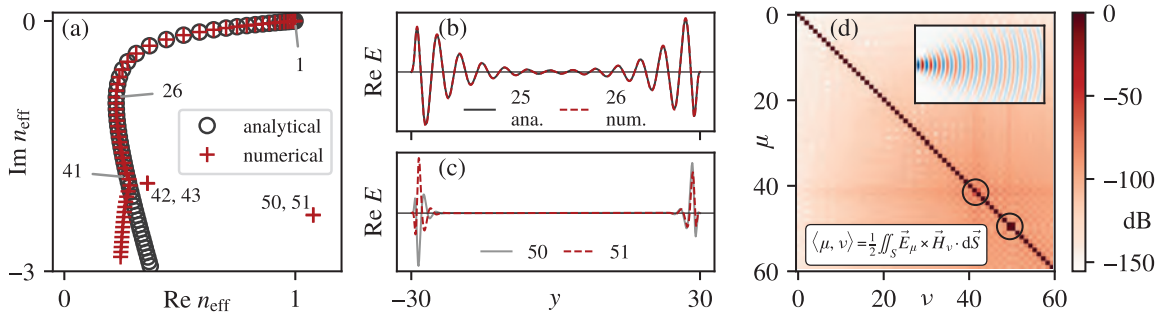

Figure 1: ***(a)*** *Effective mode indices (exact analytical and numerical finite-difference solutions) for a pure PML eigenmode problem (vacuum bounded by PML and PEC boundaries; here calculated in 1D for simplicity).* ***(b)****,* ***(c)*** *Mode field profiles of selected modes.* ***(d)*** *Numerical evaluation of the given non-conjugated orthogonality relation (log scale). Inset: Reconstruction of a Gaussian beam using the calculated set of PML modes.*

References

[1] H. Derudder, D. De Zutter, F. Olyslager, "Analysis of waveguide discontinuities using perfectly matched layers", Electron. Lett. **34** (22), 19134 (1998).

[2] W.-P. Huang, J. Mu, "Complex Coupled-Mode Theory for Optical Waveguides", Opt. Express. **17** (21), 19134 (2009).

Insights into the fluorescence and energy transfer simulations of periodic structures

I. Lykov [1,*], S. Boroviks [1], O. J. F. Martin [1]

[1] *Nanophotonics and Metrology Laborotory, Swiss Federal Technology Institute of Lausanne (EPFL), Lausanne, 1015, Switzerland*

[*] *ilia.lykov@epfl.ch*

In this work, we discuss the limitations of simulations employing periodic boundary conditions (PBCs) for modeling fluorescence enhancement and energy transfer (ET). We find that the use of PBCs along with the dipole radiation sources may lead to incorrect predictions, unless carefully configured. Through a comparative analysis, we show potential pitfalls of applying PBCs in nanophotonic simulations involving localized emitters and suggest recipes for accurate modelling.

The resonant waveguide grating, illustrated in the Fig. 1(a), is particularly suitable for demonstrating the limitations of PBC-based simulations. First, it is a two-dimensional system, which significantly reduces computational cost and enables simulations of finite gratings with a large number of periods within reasonable calculation times. Second, as reported in Ref. [1], this structure supports bound states in the continuum (BICs), which are delocalized modes of the system.

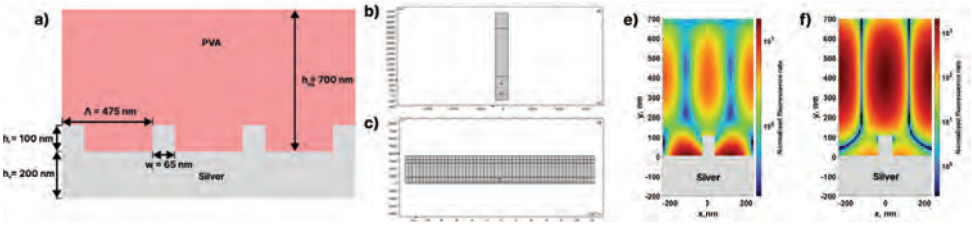

Fig. 1. (a) Considered resonant waveguide grating. (b) Simulation domain of an infinite grating (single unit cell with periodic boundary conditions). (c) Simulation domain of a finite grating (N periods with perfectly matched layers). e) The fluorescencene enhancement calculated for different positions of the emitter in cases of f) finite grating with PMLs and g) elementary cell with PBCs.

Two COMSOL models were developed: an elementary unit cell with periodic boundary conditions applied at the lateral boundaries (Fig. 1(b)), and a finite grating model terminated by perfectly matched layers (PMLs) (Fig. 1(c)). Fluorescence enhancement of an emitter was calculated for different positions within the unit cell for both configurations at the BIC wavelength. The results obtained for the finite grating (Fig. 1(e)) and the PBC model (Fig. 1(f)) differ in absolute magnitude (maximum value), which can be partly attributed to the increased quality factor in the PBC case. However, this does not explain the difference in their spatial dependence (i.e. the distribution of the enhancement within the unit cell). This qualitative discrepancy highlights fundamental limitations of PBC-based simulations for describing emitter–structure interactions in such systems.

References

[1] S. Azzam, V. Shalaev, A. Boltasseva, A. Kildishev ”Formation of Bound States in the Continuum in Hybrid Plasmonic-Photonic Systems”, Phys. Rev. Lett. **121**, 253901 (2018).

Simulation of InP electro-optic modulator based on Pockels and Kerr effects

C. Garcia Marcilla [1,*], S. Iadanza [1], E. Cha [1], K. Moselund [2]

[1] *Paul Scherrer Institut (PSI), Laboratory of Nano and Quantum Technologies, 5232 Villigen PSI, Switzerland*
[2] *École Polytechnique Federale de Lausanne (EPFL), Integrated Photonics and Optoelectronics Laboratory, 1015 Lausanne, Switzerland*
[*] *cristina.garciamarcilla@epfl.ch*

Electro-optic (EO) modulators are essential to optical communication systems because they enable electrical signals to impart information onto an optical signal. They are based on a modulation of the refractive index, which can be achieved efficiently via the linear EO or Pockels effect. The sign and magnitude of the resulting change in refractive index depend on the crystal orientation, the applied electric field, and the light polarization [1]. For the standard (110) InP wafer and an electric field applied parallel to the [001], the linear EO effect becomes maximum for light polarization parallel to [110], modulating only the TM-polarized light (see Fig. 1(b-c)). In particular, the change in the refractive index is given by $\Delta n = 1/2\, r_{41}\, n_o^3$ [2], E, where n_0 is the ordinary refractive index, r_{41} the EO tensor component, and E the applied field. Notably, the EO coefficient of InP r_{41} ∼1.68 pm/V [3] is considerably weaker compared to the EO coefficient in $LiNbO_3$. Nevertheless, the higher refractive index of III–V semiconductors can partially compensate for the weaker EO coefficient, while their lower dielectric constant also allows for easier phase-matching in traveling designs [1]. Additionally, the quadratic EO or Kerr coefficient is ∼5x larger in InP compared to $LiNbO_3$ [3], which becomes relevant in resonant structures like photonic crystal cavities (see Fig. 1(a)).
This work presents simulations of the Pockels and Kerr effects in a coplanar InP EO modulator as a first step towards developing a comprehensive electro-optic model for an integrated modulator. The simulations are conducted using the finite difference eigenmode (FDE) module and the CHARGE module within the Ansys Optics Lumerical software package. Preliminary results (see Fig. 1(d)) demonstrate that the framework can effectively quantify the individual contributions of the Pockels and Kerr effects, paving the way towards a fully optimized InP-based EO device design.

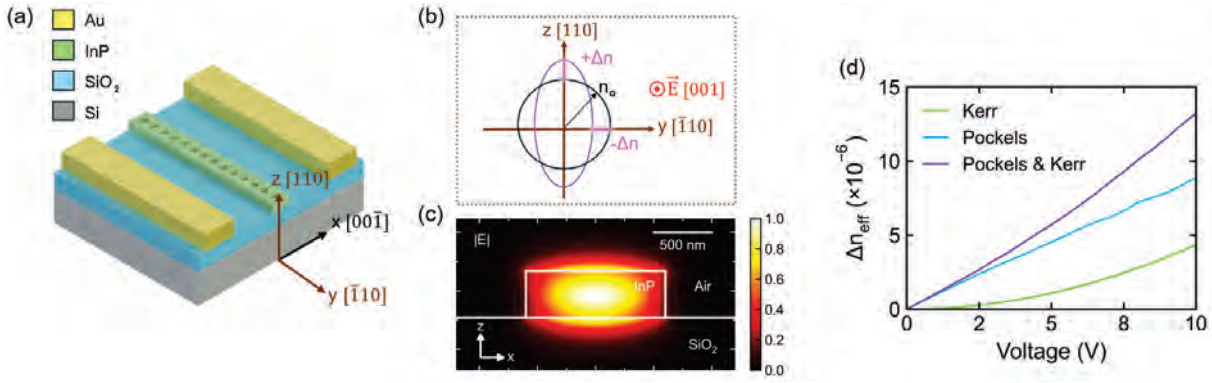

Fig. 1. (a) Resonant InP EO modulator based on a photonic crystal cavity. (b) Planar projection of the InP index ellipsoid. Without an applied electric field along the [001] axis, InP is optically isotropic in-plane (black circle). When an external electric field is applied along the [001] axis, the ellipsoid deforms (purple ellipse) with major and minor axes along the [110] or [$\bar{1}$10] directions. (c) Optical electric field profile of the simulated TM-polarized mode. (d) Simulated refractive index change of the TM mode as a function of applied voltage.

A surface integral equation framework for light scattering in layered media

P. S. Mavrikakis [1,*], O. J. F. Martin [1]

[1] *Nanophotonics and Metrology Laboratory, EPFL, Lausanne, CH-1015, Switzerland*
[*] *parmenion.mavrikakis@epfl.ch*

The rigorous modeling of light scattering within stratified backgrounds is critical for modern optics. The surface integral equation (SIE) method offers a powerful framework for analyzing scattering phenomena [1]. However, its application to layered environments is often hindered by the complexity of the associated Green's functions. In this work, we introduce HELIOS, a C++ SIE solver that overcomes such limitations. It integrates a robust singularity extraction technique [2] that handles singularities, ensuring numerical stability and allowing for the arbitrary placement of scatterers within a stratified medium. Furthermore, the code implements a tabulation-interpolation scheme [3] to accelerate the matrix-filling process [4]. By circumventing repeating integral evaluations, computational overhead is significantly reduced. This approach is particularly advantageous for modeling stratified systems – such as biosensors, nanophotonic devices, and optical coatings – since high accuracy and efficiency are retained without increasing the degrees of freedom. The versatility and accuracy of HELIOS are presented through numerical examples, highlighting its potential to advance research in nanophotonics.

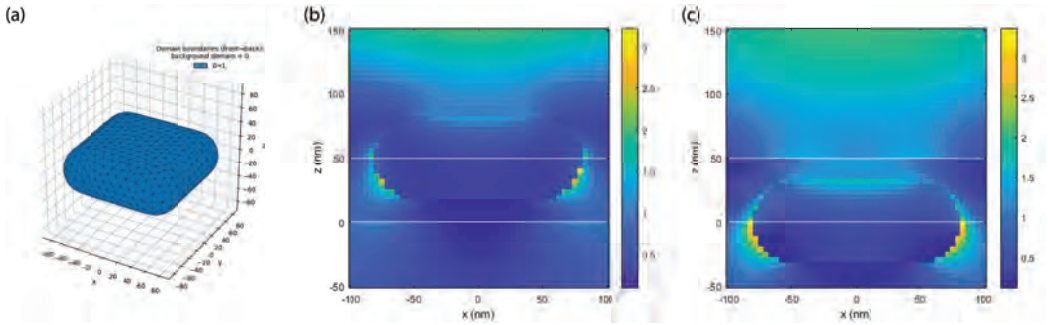

Fig. 1. Au nanoscatterer embedded in a stratified medium. (a) Discretized surface mesh of the scatterer's geometry, and (b)-(c) total electric near-field distributions in the $y = 0$ plane at an excitation wavelength of $\lambda = 500$ nm. The system is illuminated by a plane wave propagating in the $-z$ direction and polarized along the x-axis. The layered background consists of a dielectric slab ($\varepsilon_r = 2.25$) bounded by air, with interfaces located at $z_1 = 0$ nm and $z_2 = 50$ nm.

Acknowledgement: This research was supported by the Swiss National Science Foundation (SNSF) under project 200021 212758.

References

[1] P. S. Mavrikakis, O. J. F. Martin, "Surface Integral Equations in Computational Electromagnetics: A Comprehensive Overview of Theory, Formulations, Discretization Schemes and Implementations", Appl. Comput. Electromagn. Soc. J. **40**, 279 (2025).
[2] S. Pratama, D. van Oosten, "Efficient and versatile surface integral approach to light scattering in stratified media", Opt. Express **23**, 21741 (2015).
[3] U. Hohenester, "Nanophotonic resonators in stratified media with the nanobem toolbox", Comput. Phys. Commun. **294**, 108949 (2024).
[4] W. C. Chew, J. L. Xiong, M. A. Saville, "A Matrix-Friendly Formulation of Layered Medium Green's Function", IEEE Antennas Wirel. Propag. Lett. **5**, 490 (2006).

Imaging of degenerate and hybridized plasmonic modes by cathodoluminescence spectroscopy

V. Myroshnychenko [1,*], N. Nishio [2], N. Yamamoto [2], J. Förstner [1]

[1] *Theoretical Electrical Engineering & CeOPP, Paderborn University, Warburger Straße 100, D-33098 Paderborn, Germany*

[2] *Department of Materials Science and Engineering, School of Materials and Chemical Technology, Institute of Science Tokyo, Kanagawa, 4259 Nagatsuta, Midori-ku 226-8503, Yokohama Japan*

[*] *viktor.myroshnychenko@uni-paderborn.de*

Metal nanoparticles host localized plasmon excitations that enable the manipulation of optical fields at the nanoscale. Detailed knowledge of the electromagnetic field distribution associated with surface plasmons (SP) at nanometer spatial resolution is of fundamental importance for a wide range of applications [1, 2]. Here, we present a theoretical and experimental investigation of plasmonic-state symmetries in individual gold nanoprisms and coupled nanoprism pairs arranged in a bow-tie antenna configuration using cathodoluminescence (CL) spectroscopy. Specifically, we use a focused 80 keV electron beam to excite multiple localized SPs over a broad spectral range. The induced optical radiation emitted from the structures is detected and imaged through angle-, polarization-, and space-resolved CL measurements (Fig. 1a). This combined technique grants access to both spectral information (Fig. 1b) and spatially resolved maps (Fig. 1c) of multipolar SP modes localized on the nanoprisms with nanometer spatial resolution. Remarkably, we reveal the spatial distribution of energetically degenerate SP states in a single nanoprism and hybridized SP states in a coupled nanoprism pair. We demonstrate that both degeneracy and hybridization can be unveiled through examination of the symmetry in the s- and p-polarized photon emission maps. Our approach enables a systematic study of plasmonic states in high-symmetry nanostructures. Finally, we analyse our findings by comparing full-wave electromagnetic simulations with experimental results.

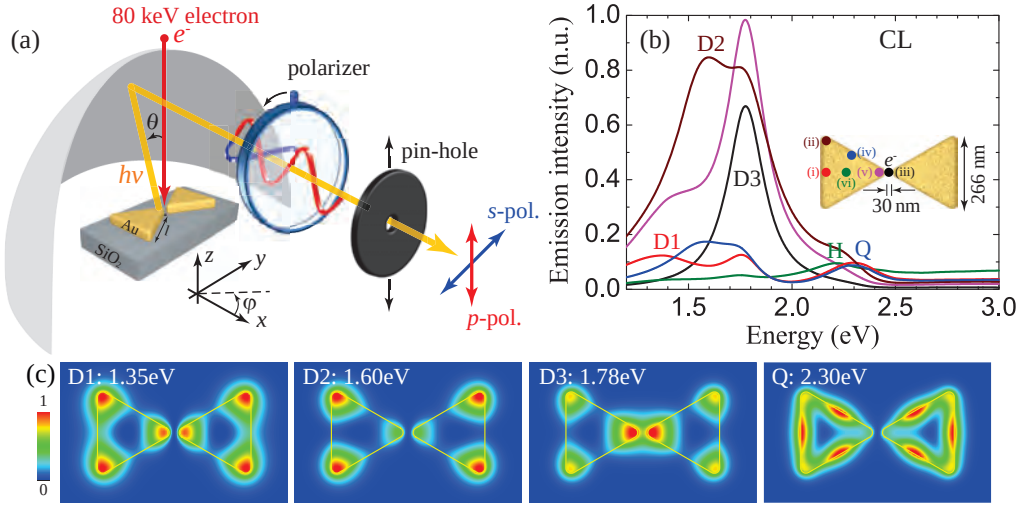

Fig. 1. (a) Schematic of our angle- and polarization-resolved CL setup. (b) Calculated photon-emission spectra collected at different electron-beam probe positions, shown in the inset. (c) Photon-emission maps of the modes, marked by colored letters in (b), as a function of electron probe position.

References

[1] F. J. García de Abajo, "Optical excitations in electron microscopy", Rev. Mod. Phys. **82**, 209 (2010).

[2] V. Myroshnychenko, N. Nishio, F. J. García de Abajo, J. Förstner, N. Yamamoto, "Unveiling and imaging degenerate states in plasmonic nanoparticles with nanometer resolution", ACS Nano, **12**, 8436 (2018).

All-Dielectric Photo-thermo-optical Metasurfaces for Thermal Landscaping at the Nanoscale

GOPAL NARMADA NAIDU,* OMER CAN KARAMAN, GIULIA TAGLIABUE

Laboratory of Nanosciene for Energy Technologies, EPFL, Switzerland
**gopal.naidu@epfl.ch*

Abstract

Precisely shaping temperature fields at the micro- and nanoscales is a key challenge in nanotechnology, with applications in photonics, nanochemistry, biology, and microfluidics.[1], [2], [3], [4] Unlike electromagnetic fields, thermal fields are diffusion-driven, which makes spatial control difficult and pose challenges for applications requiring uniform or complex temperature distributions.[5] Thermonanophotonics, the study of photothermal effects in optical nanoantennas, has garnered significant attention in addressing this challenge. Most research to date has focused on thermoplasmonic systems, where metallic nanoparticles strongly absorb light and dissipate the energy as heat.[6] However, recent advances in all-dielectric nanophotonics provide a compelling alternative for photothermal control.[7] Resonant high-index dielectric and semiconductor nanostructures exhibit low-loss resonances below the bandgap, and strong absorption above the bandgap. Moreover, many of these materials have large thermo-optical coefficients (TOC) = dn/dT, enabling efficient light–matter interactions along with substantial thermal tunability of their optical response. Furthermore, their low thermal capacity also leads to rapid photothermal responses. Notably, silicon nanoresonators have demonstrated exceptionally strong thermo-optical nonlinearities, in some cases surpassing plasmonic counterparts in terms of localized heating efficiency. [8]

While single dielectric nanoresonators have been studied in detail, extending thermo-optical control to large arrays remains challenging due to inter-resonator interactions and collective heating effects. In such systems, collective heating alters local absorption cross-sections and modifies individual resonator responses.[9] Recent work demonstrates that optimizing parameters such as resonator size, array periodicity, and illumination wavelength, yield non-trivial thermal profiles. For instance, spatially flat temperature distributions in heterogeneous arrays of silicon nanoresonators.[10] However, such brute-force parametric optimization is computationally expensive and impractical for designing metasurfaces with tailored temperature landscapes, motivating the need for inverse-design strategies.[11] Beyond static optimization, thermo-optical resonators also offer opportunities for dynamic thermal reconfiguration. Because their optical response depends on both geometry and temperature, a single nanoresonator can, in principle, support multiple thermal output patterns. By changing the illumination wavelength or intensity, one nanoresonator could produce different heating effects, eliminating the need for complex multi-resonator unit cells to achieve tunability. Despite this potential, such tunable nanoscale thermal control remains largely unexplored.

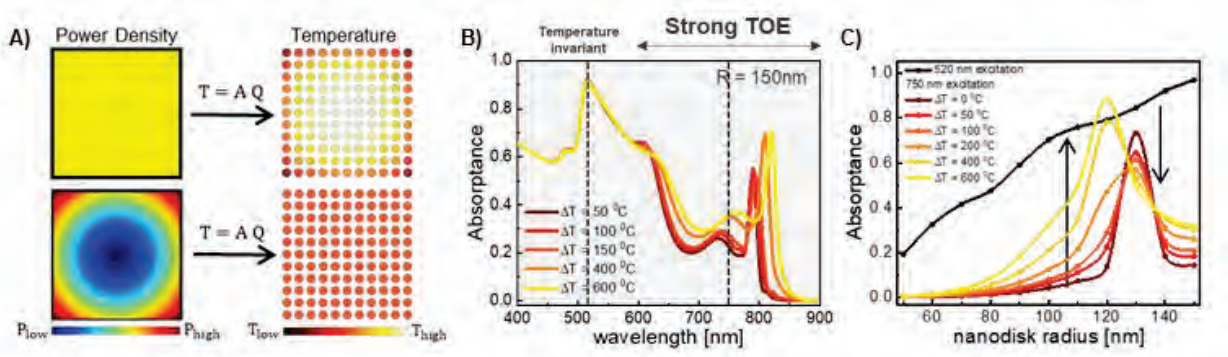

Figure 1. A) Uniform and inverse-gaussian thermal power density distributions and their corresponding temperature distributions obtained over a 4 µm x 4 µm a-Si metasurface composed of a-Si nanodisks (R = 150 nm, H = 100 nm, P = 350 nm) on a silica substrate. B) The calculated absorptance spectra of a-Si nanodisk array (R = 150 nm; H = 100 nm; P = 350 nm) at different temperatures (70, 120, 170, 400 and 6000C). C) The absorptance of the a-Si nanodisks of varying radii at 520 nm and 750 nm excitation as a function of temperature increase (ΔT).

In this work, we introduce the first inverse-design framework for shaping temperature fields in all-dielectric metasurfaces with strong thermo-optical response. Our approach combines a library of absorption spectra of amorphous silicon (a-Si) nanodisks - parameterized by geometry and temperature - with a matrix formulation of self- and collective heating to inversely map target temperature profiles to nanopattern designs. This framework enables a direct computational mapping of an arbitrary target temperature profile onto a spatially varying nanoresonator distribution (Figure 1. A). We demonstrate metasurfaces that produce either uniform or spatially complex thermal fields under uniform illumination thanks to the versatility of our static thermal shaping approach. Furthermore, by exploiting the wavelength-dependent TOC of a-Si, we achieve temperature-invariant operation at a wavelength (~500 nm) where the thermo-optical coefficient is negligible, and intensity-dependent thermal tuning at wavelengths where the TOC is appreciable (Figure 1. B). In other words, the same

Extraction of intrinsic chiral effects via Mueller matrix polarimetric decomposition

Jeeban Kumar Nayak[1]*, Olivier J.F. Martin[1]

1. Nanophotonics and MetrologyLaboratory (NAM), Swiss Federal Institute of TechnologyLausanne (EPFL), Lausanne 1015, Switzerland

*jeeban.nayak@epfl.ch

Chiral light–matter interactions are of fundamental importance in biomedicine and photonics, enabling enantiomer-specific detection of biomolecules, controlling light–matter coupling at the nanoscale, and realizing spin-dependent phenomena in chiral nanophotonic structures with direct implications for quantum optics. In chiral nanophotonics, broken mirror symmetry allows for directional emission, spin–momentum locking, and enhanced optical activity, which are central to emerging platforms for quantum light sources and integrated quantum photonic circuits [1]. However, real biological and nanostructured media are inherently complex and often exhibit multiple coexisting anisotropic effects such as linear diattenuation, linear birefringence, and depolarization, which can mask or mimic genuine chiral signatures. Under such conditions, conventional chiro-optical techniques, including circular dichroism spectroscopy and optical rotatory dispersion, fail to reliably isolate intrinsic chiral responses. In this work, we present a polarization Mueller matrix–based framework combined with a differential decomposition approach that enables the separation and quantitative extraction of true chiral effects from concurrent linear and circular anisotropies (Fig. 1). The Mueller matrix [2] provides a complete polarimetric description of the medium, while the differential decomposition yields physically meaningful generator parameters associated with diattenuation, birefringence, and optical activity, offering a robust pathway for studying chirality in complex photonic systems.

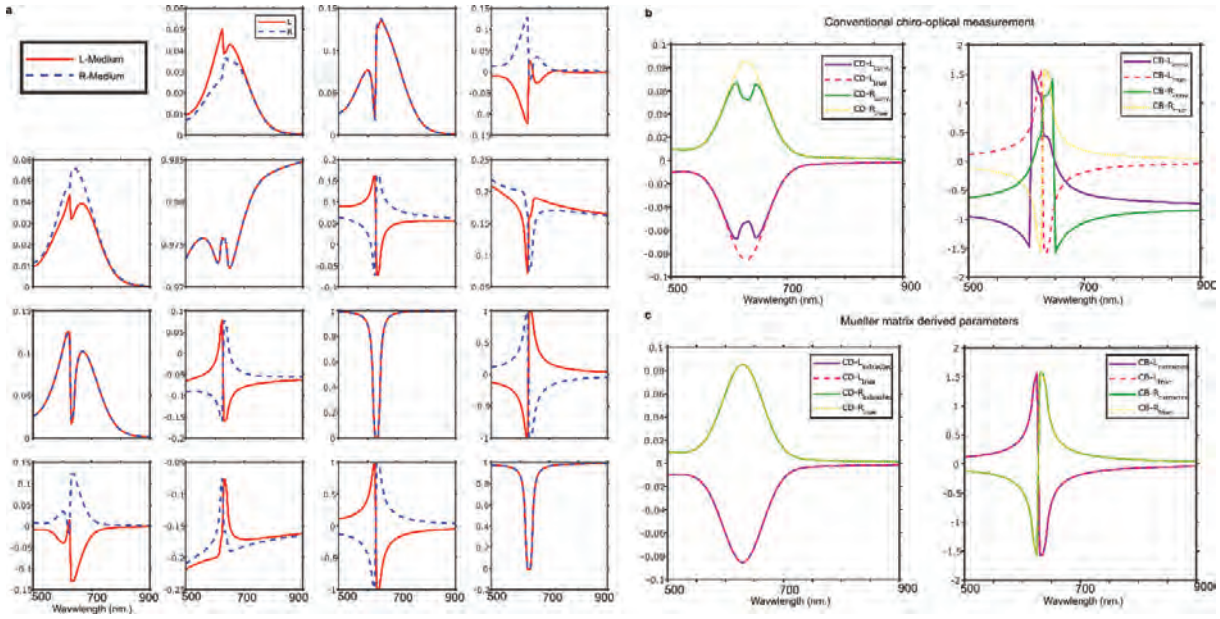

Fig. 1. Polarization Mueller matrix of a system exhibiting simultaneous linear and circular anisotropic effects(a). Circular anisotropy parameters obtained using conventional chiro-optical measurements (b) and those extracted via the Mueller matrix–based approach incorporating differential decomposition (c), presented for quantitative comparison.

References

[1] Mun, J., Kim, M.., ... & Rho, J. (2020).. *Light: Science & Applications*, *9*(1), 139.

[2] Azzam, R. M. A. *Journal of the Optical Society of America* 68, no. 12 (1978): 1756-1767.

How to Build a Scattering Code with Mathematically Guaranteed Convergence

Alexander I. Nosich
Lab. of Micro and Nano Optics, Institute of Radio-Physics and Electronics NASU, Kharkiv 61085, Ukraine
anosich@yahoo.com

Abstract. We review basic ideas, implementations, and merits of the method of analytical regularization (MAR) as a systematic approach to build the computational electromagnetics codes, which have mathematically guaranteed convergence. MAR uses explicit inversion of the most singular part of the full-wave scattering operator and results in well-conditioned Fredholm 2-nd kind matrix equation.

In the wave scattering theory, integral equation (IE) methods have well-known advantages: their solutions "automatically" satisfy the radiation condition at infinity and exist on bounded supports. However, any IE should be discretized, i.e. cast to the infinite-matrix equation, which should be truncated before feeding a computer. Therefore, additional computational parameter appears - truncation order, also called discretization order. Here, the question arises of the *accuracy* of the solution of truncated equation with respect to the exact solution of the infinite equation and how it can be improved. The answer is based on the presence or absence of *convergence*, understood as the possibility of minimizing computation error, in a certain norm, by increasing the discretization order.

Although rarely recognized in the engineering community, if IE discretization does not lead to the matrix equation with the diagonal predominance, then the convergence is absent and accuracy of the solution is uncertain. As a result, there is no instrument to improve the accuracy of the obtained approximations systematically. This is a common defect of general-purpose commercial software.

Fortunately, all these troubles can be completely overcome using the Method of Analytical Regularization, which encompasses techniques aimed at transforming various strongly singular and weakly singular 1-st kind IEs into the IEs of the Fredholm 2-nd kind, ensuring well-posedness and guaranteed convergence [1]. The underlying idea is conceptually straightforward yet mathematically elegant: isolate a suitably chosen most singular part of the integral operator and invert it analytically.

This reference operator is always tailored to the specific problem - it can be taken as either the static, or high-frequency, or canonical-geometry component of the original full-wave operator. To carry out its inversion, powerful tools from functional analysis exist, such as the Carleman formula, Titchmarsh theorem, Wiener–Hopf factorization, Cauchy and Abel transforms, and Sokhotski–Plemelj theorem in the Riemann–Hilbert Problem theory. In the problems involving arbitrary smooth shapes, separation of variables can be applied to derive explicit solutions to the invertible canonic-shape reference equations. The obtained 2-nd kind Fredholm IEs can be converted to the Fredholm 2-nd kind matrix equations by various conventional local and global discretization schemes. Then, the convergence of the truncated equation solutions is guaranteed by the Fredholm theorems.

In a broad class of problems, analytical regularization and discretization of IEs can be carried out simultaneously, giving rise to what is known as method of analytical preconditioning [2]. This needs selecting the eigenfunctions of the singular part of the full-wave integral operator as the expansion functions. In such a case, the Galerkin projection works as a perfect preconditioner, resulting in a Fredholm 2-nd kind matrix equation. More generally, Fredholm theory remains applicable if the discretized operator can be written as the sum of an invertible operator (with a continuous inverse on both sides) and a compact (completely continuous) operator. If the convergence is guaranteed, numerical accuracy can be easily controlled by the matrix truncation order. In principle, the error can be reduced to machine precision, which is unthinkable for today's popular commercial codes.

References

[1] A. Nosich, "Method of analytical regularization in computational photonics," Radio Sci., **51**, 1421 (2016).
[2] M. Lucido, et al., "MAR for new frontiers of applied electromagnetics," IET MAP, **15**, 1127 (2021).

Utilization of a Pair of Matched Dielectric Mirrors for Modes Filtering in Open Resonators

V. Pazynin [1,*], K. Sirenko [2], K. Makhanov [3], W. Keusgen [1]

[1] *Department of High Frequency Systems, Technical University of Berlin, Berlin, Germany*
[2] *Department of mathematical physics, O.Ya. Usikov Institute for Radiophysics and Electronics, Kharkiv, Ukraine*
[3] *Department of radio engineering, electronics and telecommunications, L.N. Gumilyov Eurasian National University, Astana, Kazakhstan*
[*] *vadim.pazynin@gmail.com*

We propose using a pair of multilayer dielectric mirrors to filter the eigenmodes of open resonators (ORs). For this purpose, the thicknesses of the dielectric layers in each mirror are chosen so that their reflection windows overlap within a narrow frequency band, thereby providing effective suppression of OR modes whose frequencies lie outside this band (or bands). This effect was investigated using a rigorous numerical 2D model of a Fabry-Perot OR with two multilayer dielectric mirrors, each composed of 15 sapphire plates separated by air gaps, see Fig. 1(a). The plates thicknesses and the spacings between them are chosen so that the first reflection windows of each mirror overlap in the frequency range from 32.364 to 33.237 GHz, see Figs. 1(b) and 1(c). The second overlapping band is in the range from 65.613 to 66.476 GHz. The designed OR supports only two eigenmodes in the 0–105 GHz range (Fig. 1(e)), which is in the full agreement with the expected $TE_{1,11}$ and $TE_{1,22}$ modes. The finite-difference time-domain (FDTD) method [1] and the transfer matrix method [2] were used for numerical simulations the resonator characteristics.

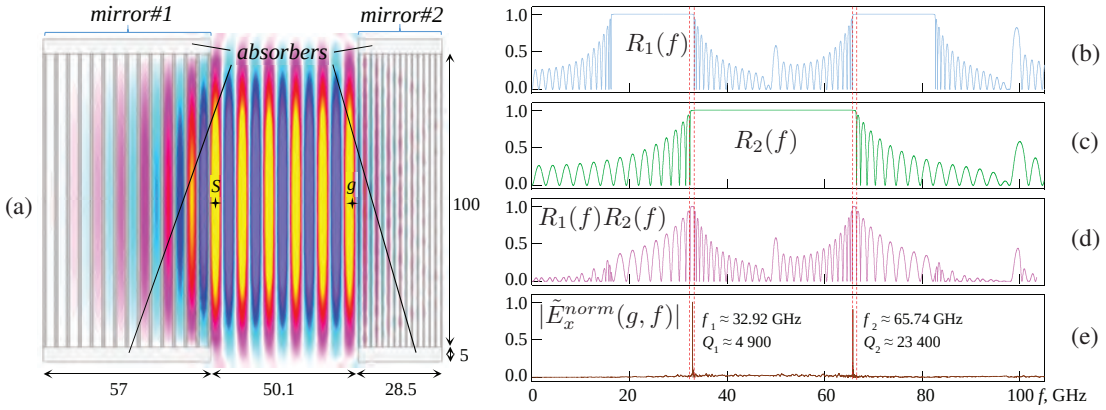

Fig. 1. (a) OR geometry and electric field distribution of the $TE_{1,11}$ mode; reflection coefficients of the first (b) and second (c) mirrors; (d) double reflection coefficient from two mirrors; (e) normalized pulse response of the OR at point g under excitation by external current filament at point S. Dielectric layers are made of sapphire ($\varepsilon = 9.4$, $\tan\delta = 5 \cdot 10^{-5}$); layer thickness and spacing are 1 mm and 3 mm for the first mirror, and 0.5 mm and 1.5 mm for the second mirror. Absorber parameters $\varepsilon = 3.5$, $\tan\delta = 1.5$. All dimensions are in millimeters.

References

[1] A. Taflove, S.C. Hagness, "Computational Electrodynamics: The Finite-Difference Time-Domain Method", Artech House (2000).
[2] M. Born, E. Wolf, "Principles of optics", – 4-th ed. Pergamon Press (1968).

A model of a quasi-single-mode Fabry-Perot resonator incorporating a tilted high-k frequency-selective dielectric plate

V. Pazynin [1,*], M. Maiboroda [2], G. Veselovska-Maiboroda,[2], K. Makhanov [3], N. Burambayeva [3], W. Keusgen [1]

[1] *Department of High Frequency Systems, Technical University of Berlin, Berlin, Germany*
[2] *Department of mathematical physics, O.Ya. Usikov Institute for Radiophysics and Electronics, Kharkiv, Ukraine*
[3] *Department of radio engineering, electronics and telecommunications, L.N. Gumilyov Eurasian National University, Astana, Kazakhstan*
[*] *vadim.pazynin@gmail.com*

A 2D model of a composite Fabry-Perot open resonator (OR) is considered. In this model (Fig. 1(a)), the region between the OR mirrors has a permittivity $\varepsilon = 2.2(1 - i \cdot 10^{-4})$ (Teflon or polyethylene) and contains a high-k plate (layer) with $\varepsilon = 25(1 - i \cdot 10^{-4})$ ($LaAlO_3$ or $LaGaO_3$), 0.6 mm thick, positioned at an angle of $45°$ to the mirrors. The transmission coefficient of plane waves through such a plate [1] for an angle of incidence of $45°$ (Fig. 1(b), black line) exhibits several resonance peaks in the frequency range from 0 to 220 GHz. Since the waves reflected from the plate leave the OR without additional reflections from the metal mirrors, the plate acts as an effective filter of the OR eigenmodes. FDTD simulation [2] of the OR excitation by an external current filament with constant spectral amplitude demonstrates a significant reduction in the number of OR eigenmodes (Fig. 1(b), blue line). Introducing an additional scatterer inside the OR design in the form of a thin metal strip placed at a standing-wave node leaves only a single dominant mode in the range from 0 to 200 GHz at a frequency of approximately 102.1803 GHz with a quality factor of $Q = 3900$ (Fig. 1(b), red line).

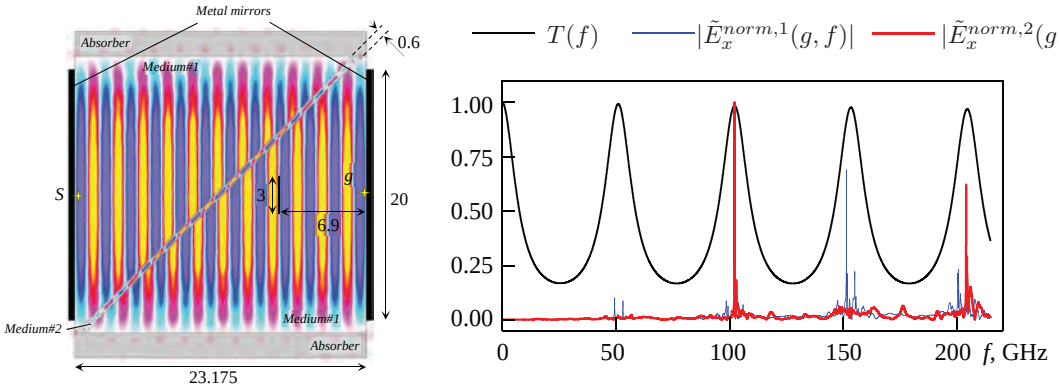

(a) (b)

Fig. 1. (a) Geometry of the OR and the electric field distribution of the operating mode; (b) Transmission coefficient $T(f)$ of a plane wave through a plate with $\varepsilon = 25$ at an angle of incidence $\theta_i = 45$ (black line), the normalized impulse response at point g of the OR without the metal strip $|\tilde{E}_x^{norm,1}(g,f)|$ (blue line) and with it $|\tilde{E}_x^{norm,2}(g,f)|$ (red line). Absorber, media#1 and #2 have $\varepsilon = 3.5(1 - 0.2i), 2.2(1 - 10^{-4}i), 25(1 - 10^{-4}i)$ correspondingly. All dimensions are in millimeters.

References

[1] M. Born, E. Wolf, "Principles of optics", – 4-th ed. Pergamon Press (1968).
[2] A. Taflove, S.C. Hagness, "Computational Electrodynamics: The Finite-Difference Time-Domain Method", Artech House (2000).

Bound states in the continuum for guiding light

J. Petráček [1,2,*], J. Čtyroký [3,4], K. Krajíčková [1], V. Kuzmiak [3], I. Richter [4]

[1] *Institute of Physical Engineering, Faculty of Mechanical Engineering, Brno University of Technology, Technická 2, 616 69 Brno, Czech Republic*

[2] *Central European Institute of Technology, Brno University of Technology, Purkyňova, 656/123, 612 00 Brno, Czech Republic*

[3] *Institute of Photonics and Electronics, Academy of Sciences of the Czech Republic, v.v.i., Chaberská 57, 182 51 Praha 8, Czech Republic*

[4] *Department of Physical Electronics, Faculty of Nuclear Sciences and Physical Engineering, Czech Technical University in Prague, Břehová 7, 115 19 Prague 1, Czech Republic*

[*] *petracek@fme.vutbr.cz*

Bound states in the continuum (BICs) are the confined states with isolated eigenvalues embedded in the continuum of free states. The concept of BICs, first proposed nearly 90 years ago in quantum physics as a theoretical construction, has become the subject of an intensive investigation in the realm of photonics. The majority of studies on photonic BICs focused on periodic structures, such as gratings, photonic crystals slabs, metasurfaces, and waveguide arrays. In this talk, we report on our recent studies on BICs which appear in photonic waveguides. The "propagating" BICs are usually formed from quasi-TM leaky modes in rib waveguides exhibiting the effect of lateral leakage when the latter is suppressed due to destructive interference of radiating TE waves [1, 2, 3]. However, the conventional propagating BICs have some limitations: they are localized inside or in the vicinity of high-refractive-index materials, they are observed as quasi-TM polarized waves, and they appear only for certain "magic" sets of parameters. Here, we focus on two systems that support alternative mechanisms of BIC formation. In contrast to the previously described configurations, the first geometry, consisting of a rectangular waveguide coupled to a planar waveguide, facilitates genuine guiding of quasi-TE modes in the core with the lower refractive index [4]. The TE BICs appear when the coupling between the bound and radiation modes is suppressed due to accidental orthogonality of modes. The second system, proton exchanged waveguide in Z-cut thin-film lithium niobate, can support very low-loss TM-polarized quasi-BIC modes for a range of waveguide widths not limited to "magic widths" [5]. This is because the system exhibits a very small change of the ordinary refractive index between the core and substrate, which enables formation of polarization-protected quasi-BICs. We discuss the potential advantages of these configurations for the design of practical integrated amplitude modulators. We believe that the presented approaches well illustrate rich physics associated with BICs and offer new possibilities in their technical applications.

The authors acknowledge the support of the Czech Science Foundation project 26-21651S.

References

[1] M. A. Webster, R. M. Pafchek, A. Mitchell, T. L. Koch, "Width dependence of inherent TM-mode lateral leakage loss in silicon-on-insulator ridge waveguides", IEEE Photonics Technol. Lett. **19**, 429 (2007).

[2] C.-L. Zou, J.-M. Cui, F.-W. Sun, X. Xiong, X.-B. Zou, Z.-F. Han, G.-C. Guo, "Guiding light through optical bound states in the continuum for ultrahigh-Q microresonators", Laser Photonics Rev. **9**, 114 (2015).

[3] T. G. Nguyen, A. Boes, A. Mitchell, "Lateral Leakage in Silicon Photonics: Theory, Applications, and Future Directions", IEEE J. Sel. Top. Quantum Electron. **26**, 8200313 (2020).

[4] J. Petráček, V. Kuzmiak, J. Čtyroký, I. Richter, "Guiding light through quasi-TE modes embedded in the radiation continuum", Opt. Lett. **48**, 3463 (2023).

[5] J. Čtyroký, J. Petráček, V. Kuzmiak, I. Richter, "Bound modes in the continuum in integrated photonic $LiNbO_3$ waveguides: are they always beneficial?", Opt. Express **31**, 44 (2023).

GPU-Accelerated Graph-Based Maxwell Solver for Large-Scale Nanophotonic Simulations

Lorenzo Piatti[1,], Pawan Ratra[1], Davide Cassarà[1], Murat Yessenov[1], Federico Capasso[1]*

[1]*Harvard John A. Paulson School of Engineering and Applied Sciences, Harvard University, Cambridge, Massachusetts 02138, USA*

*lpiatti@seas.harvard.edu

The numerical solution of Maxwell's equations remains a major computational bottleneck in large-scale nanophotonic simulations. Graph-based electromagnetic methods (GEM) have recently shown that finite-difference time-domain (FDTD) update equations can be exactly reformulated as fixed-weight message passing on a graph, enabling efficient GPU execution while preserving the physical fidelity of the Yee discretization [1]. In this work, we present a two-dimensional graph-based electromagnetic solver extended from the original GEM formulation into a fully operational simulation framework. Specifically, we implement planar-wave excitation, periodic boundary conditions encoded directly in the graph topology, frequency-domain field extraction via discrete Fourier transform (DFT) monitors, and an energy-based auto-shutoff criterion. To enable simulations over large computational domains, we introduce a domain-decomposition strategy in which the simulation region is partitioned and distributed across multiple GPUs. Using two GPUs approximately doubles the accessible domain size, enabling simulations spanning several thousand wavelengths in the transverse (non-propagation) direction while preserving numerical consistency.
The method is validated against an in-house FDTD implementation and rigorous coupled-wave analysis (RCWA), showing excellent agreement across multiple geometries. Representative error maps for a periodic photonic structure are shown in Fig. 1(a)–(b), where the normalized root-mean-square error (NRMSE) between GEM and FDTD solutions, and between single-GPU and multi-GPU GEM simulations, remains low, with a coefficient of determination $R^2 \approx 0.9$. Benchmark results in free-space simulations demonstrate favorable scaling with domain size compared to FDTD (Fig. 1(c)), with a speed-up of approximately 40 times (and about 20 times compared to MEEP) [2].
These results indicate that the proposed solver provides a promising framework for accelerating large-scale electromagnetic simulations in nanophotonics, while its graph-based structure and GPU-native implementation enable direct integration into optimization pipelines for inverse photonic design.

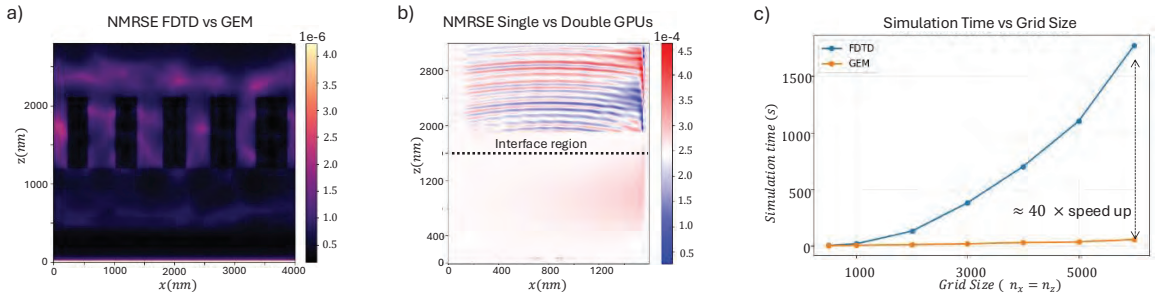

Fig. 1 (a) (b) Spatial distribution of the normalized root mean square error (NRMSE) respectively between the GEM and FDTD and between GEM on a single and a double GPUS of a periodic supercell simulation. (**c)** Computational performance comparison between the FDTD (blue) and the GEM solver (orange).

References

[1] Stefanos Bakirtzis et al. "Solving Maxwell's Equations with Non-Trainable Graph Neural Network Message Passing". In: arXiv preprint arXiv:2405.00814. 2024.

[2] David Roundy et al. "MEEP: MIT Electromagnetic Equation Propagation" Manual. Mar. 2005.

Optical Magnetic-Field-Gated Criticality in Photon Avalanching Processes

Benoît Reynier[1*], Natalie Fardian-Melamed[2], Eric Charron[1], Filippo Calavaro[1], Bleuenn Blez[1]
Artiom Skripka[3], Sébastien Bidault[4], Emory M. Chan[3], P. James Schuck[2] and Mathieu Mivelle[1]
[1]*Sorbonne Université, CNRS, Institut des NanoSciences de Paris, 75005 Paris, France*
[2]*Department of Mechanical Engineering, Columbia University, New York, New York 10027, USA*
[3]*The Molecular Foundry, Lawrence Berkeley National Laboratory, Berkeley, California 94720, USA*
[4]*Institut Langevin, ESPCI Paris, Université Paris Sciences et Lettres, CNRS, 75005 Paris, France*

*benoit.reynier@unifr.ch

Avalanche processes—ranging from stadium waves to landslides—transform weak stimuli into disproportionately strong responses. In nanophotonics, this dynamic offers powerful opportunities for signal amplification and extreme sensitivity. Among these phenomena, photon avalanching (PA) in lanthanide-doped nanocrystals stands out due to its sharp thresholds and extreme nonlinearity. However, achieving optical control of this process at the nanoscale has remained a major challenge.

Here, we demonstrate the active "gating" of this criticality in thulium-doped quantum processes by exploiting the optical magnetic field. We reveal that while the self-sustaining avalanche cycles are electrically driven (Excited State Absorption), the ignition step (Ground State Absorption) possesses a mixed magnetic-dipole character. By positioning a monolayer of emitters within a nanofabricated standing-wave cavity, we spatially partition the electromagnetic field to regulate this ignition probability (**Fig. 1a**). This allows us to decouple the system's threshold from its cooperativity, achieving a giant, reversible tuning of the nonlinearity order from s = 15 to a record s = 62 (**Fig. 1c**).

The experimental observations are reproduced using a Differential Rate Equation (DRE) and an adapted analytical model, in which the multi-parameter landscape governing photon-avalanche dynamics is systematically tuned. This is achieved by coupling, for the first time, finite-difference time-domain (FDTD) simulations with optical DREs, explicitly incorporating the influence of the nanomirror on both excitation (change in local electric and magnetic field) and emission (change in electric and magnetic LDOS) processes (**Fig. 1b**). Based on this framework, we also proposed a corrected theoretical description of photon-avalanche DREs, thereby capturing the full complexity of this optically driven, highly nonlinear process. This work demonstrates, for the first time, the critical role of magnetic light–matter interactions in the photon-avalanche mechanism. Our results open new routes for harnessing extreme light–matter interactions and engineering tailored nonlinear responses in future photonic architectures.

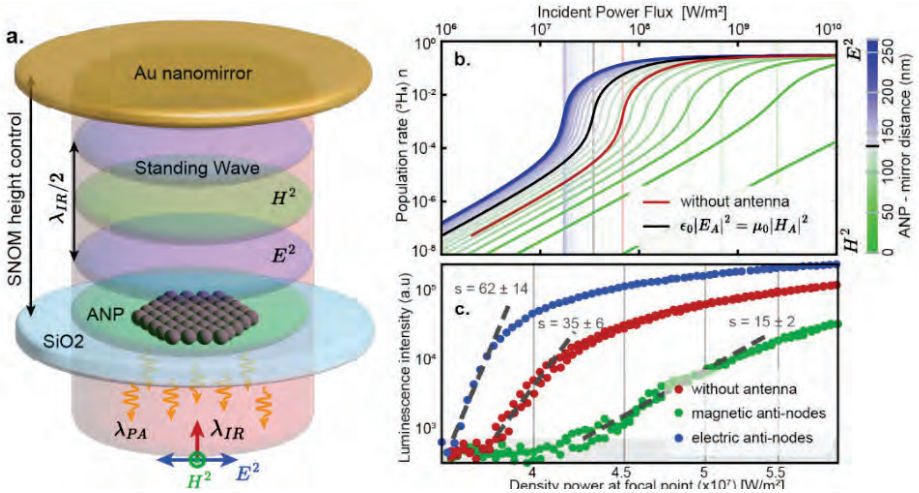

Fig. 1. (a) Nanophotonic standing-wave setup featuring a gold mirror nanofabricated at the apex of a near-field probe. (b) Theoretical and (c) experimental photon-avalanching behavior within the standing wave. Electric anti-nodes (blue) amplify nonlinearity, while magnetic anti-nodes (green) suppress it.

A Magnetic Monopole Antenna

Benoît Reynier[1*], Xingyu Yang[1], Bruno Gallas[1], Sébastien Bidault[2], and Mathieu Mivelle[1]

[1]*Sorbonne Université, CNRS, Institut des NanoSciences de Paris, INSP, 75005 Paris, France*

[2]*Institut Langevin, ESPCI Paris, PSL University, 75005 Paris, France*

*benoit.reynier@unifr.ch

Magnetic monopoles are hypothetical particles which, similarly to the electric monopoles that generate electric fields, are at the origin of magnetic fields. Despite many efforts, to date, these theoretical particles have yet to be observed. Nevertheless, many systems or physical phenomena mimic the behavior of magnetic monopoles.

Here, we propose a new type of photonic nanoantenna behaving as a radiating magnetic monopole [1]. We demonstrate that a half-nanoslit in a semi-infinite gold layer generates a single pole of an enhanced magnetic field at the nanoscale and that this single pole radiates efficiently in the far field (Figure 1). We also introduce an effective magnetic charge using Gauss's law of magnetism, in analogy to the electric charge, which further highlights the monopolar behavior of this new antenna.

Finally, we show that different plasmonic and metallic materials can provide magnetic monopole antennas covering the visible to near infrared range, and even down to GHz frequencies. This original antenna concept opens the way to a new model system to study magnetic monopoles and a new optical magnetic field source to study the "magnetic light-matter coupling". Furthermore, it opens potential applications at lower frequencies, such as in magnetic resonance imaging.

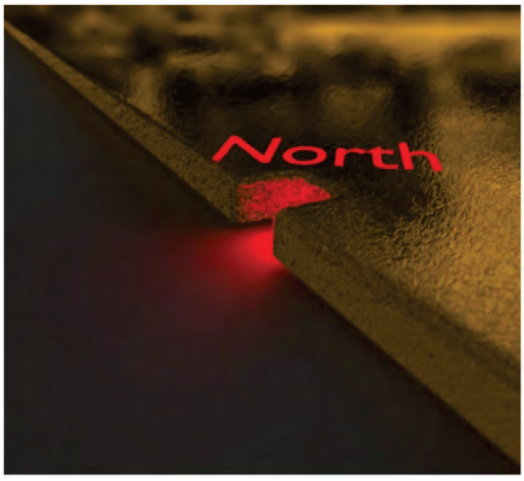

Fig. 1. Illustration of a magnetic monopole nanoantenna made in a semi-infinite gold layer.

References

[1] B. Reynier et al. "A Magnetic Monopole Antenna", ACS Photonics 10, 3070-3076, (2023)

Magnetoelectric Nonreciprocal Metasurfaces with Spontaneous Magnetization: Measurements and Analysis

S. Safaei Jazi[1,*], I. Faniayeu[2], R. Cichelero[2], N. Kuznetsov[3], S. van Dijken[3], S. Fan[4], A. Dmitriev[2], V. Asadchy[1]

[1] *Department of Electronics and Nanoengineering, Aalto University, Espoo, 02150, Finland*

[2] *Department of Physics, University of Gothenburg, Gothenburg, 41296, Sweden*

[3] *Department of Applied Physics, Aalto University, Espoo, 02150, Finland*

[4] *Department of Electrical Engineering, Stanford University, Stanford, 94305, US*

*shadi.safaeijazi@aalto.fi

Magnetoelectric nonreciprocity, commonly associated with the Tellegen effect, constitutes a central mechanism in axion-inspired electrodynamics and magnet-free optical nonreciprocal devices [1,2]. Despite its significance, an experimental realization at optical frequencies has remained elusive due to the intrinsically weak response of natural materials. In this contribution, we present the first experimental observation of an optical Tellegen metasurface. The metasurface is formed by randomly distributed cobalt-silicon nanocones exhibiting pronounced shape anisotropy and spontaneous magnetization, enabling a sizable Tellegen response without the need for an external magnetic field. Large-area samples are fabricated using hole-mask colloidal lithography [2]. Owing to symmetry, the structure simultaneously supports gyroelectric and gyromagnetic responses, which together with the magnetoelectric coupling contribute to nonreciprocal cross-polarized reflection. To disentangle these contributions, we analyze three metasurfaces with identical meta-atoms and surface densities but different dielectric spacer thicknesses backed by a metallic reflector. Polar magneto-optical Kerr measurements provide three independent cross-polarized reflection coefficients, allowing the magnetoelectric, gyroelectric, and gyromagnetic polarizabilities to be uniquely extracted [2]. The measured magnetoelectric response exhibits a pronounced optical resonance and is approximately two orders of magnitude stronger than that reported for any known natural material.

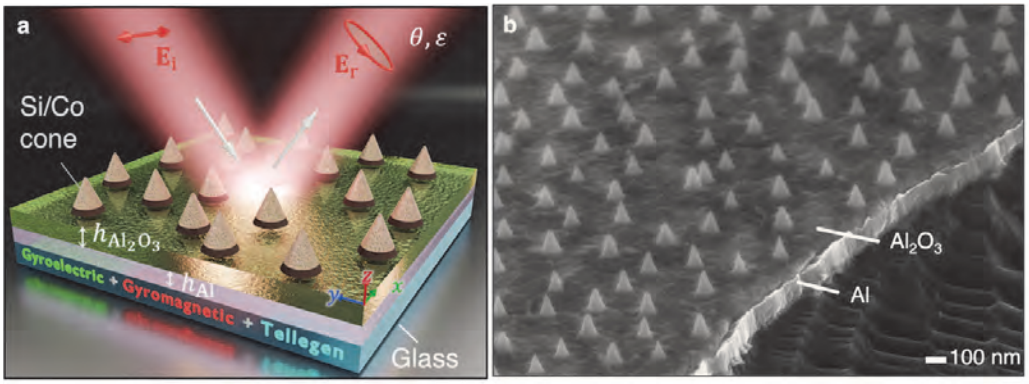

Fig. 1. Optical magnetoelectric metasurface based on cobalt-silicon nanocone meta-atoms: (a) schematic of the layered structure and (b) tilted-view SEM image of the fabricated sample.

References

[1] S. Safaei Jazi *et al.*, "Optical Tellegen metamaterial with spontaneous magnetization", *Nat. Commun.* **15**, 1293 (2024).

[2] S. Safaei Jazi *et al.*, "Realization of the Tellegen Effect in Resonant Optical Metasurfaces", *arXiv* **2503.22184**, DOI: 10.48550/arXiv.2503.22184 (2025).

Enhanced Molecular Chiral Response Driven by Crosstalking Quasi-Bound States in the Continuum

D. Shakirova [1,*], A.C. Valero [1,2], D. Riabov [3], H. Altug [3], A. Bogdanov [4,5], and T. Weiss [1]

[1] *Institute of Physics, University of Graz, and NAWI Graz, Graz, 8010, Austria*
[2] *Institute of Telecommunications, Riga Technical University, Riga, 1048, Latvia*
[3] *Laboratory of Bionanophotonic Systems, Institute of Bioengineering, École Polytechnique Fédérale de Lausanne (EPFL), Lausanne, 1015, Switzerland*
[4] *Qingdao Innovation and Development Center of Harbin Engineering University, Qingdao, 266500, China*
[5] *School of Physics and Engineering, ITMO University, St. Petersburg, 191002, Russia*
[*] *diana.shakirova@uni-graz.at*

Identifying the handedness of chiral molecules is of fundamental importance in chemistry, biology, pharmacy, and medicine. In this work, we predict the chiroptical response of a dielectric metasurface engineered to amplify molecular circular dichroism (CD) using a general electromagnetic theory of chiral light-matter interaction in arbitrary resonators [1,2]. The idea behind this theory is the ability to reconstruct the optical response (i.e., transmission, reflection and absorption) from a system via its resonant states. We derive a recipe to maximize a particular mechanism of chiral light-matter interaction, namely, the modal crosstalk, by supporting two nearly degenerate, high-quality-factor resonant states known as quasi-bound states in the continuum. Our theoretical and numerical analysis predicts a pronounced differential transmittance ΔT that exceeds the detection threshold of standard spectrometers. For the proposed metasurface, the differential transmittance approximately equals CD and can be measured in experiment directly. Moreover, we provide several strategies to decrease the computational time of numerical simulations without loss of physics.

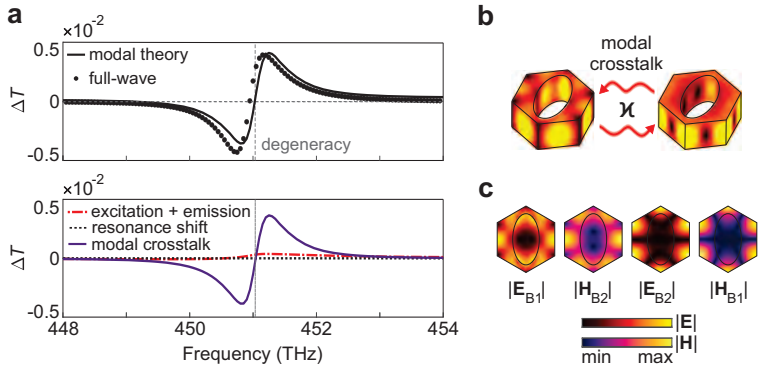

Fig. 1. (a) Modal theory calculations. The upper plot shows ΔT predicted by modal theory and full-wave calculation. In the lower plot, all mechanisms contributing to the ΔT are presented separately. (b) Scheme of the modal crosstalk between the considered quasi-BICs. (c) Field distribution in the unit cell. Two colormaps are associated with absolute values of electric and magnetic fields.

References

[1] S. Both, M. Schäferling, F. Sterl, E. A. Muljarov, H. Giessen, T. Weiss "Nanophotonic Chiral Sensing: How Does It Actually Work?", *ACS Nano*, 16, 2, 2822–2832.

[2] D. Shakirova, A.C. Valero, D. Riabov, H. Altug, A. Bogdanov, T. Weiss "Molecular Chiral Response Enhanced by Crosstalking Quasi-Bound States in the Continuum", *ACS Photonics*, 2025, 12, 11, 6011–6018.

From Maxwell to Effective Hamiltonians: a Reduced-Order Framework for Layered Photonic Cavities

P. Oliwa[1], H. Sigurdsson[1], W. Bardyszewski[2], Jacek Szczytko[1,*]
[1]*Institute of Experimental Physics, Faculty of Physics, University of Warsaw, Poland*
[2]*Institute of Theoretical Physics, Faculty of Physics, University of Warsaw, Poland*
*Jacek.Szczytko@fuw.edu.pl

Accurate modeling of layered photonic cavities relies on Maxwell-based formalisms such as the transfer matrix method, which require repeated calculations over many in-plane wavevectors and polarization states, making the exploration of complex dispersion landscapes computationally demanding. While transfer matrix approaches provide rigorous optical solutions, extracting physical insight and efficiently scanning parameter spaces remain significant challenges, particularly in cavities exhibiting strong birefringence, optical activity, and non-Hermitian behavior [1].

We introduce a symmetry-guided optimization framework that reconstructs effective photonic Hamiltonians directly from measured or transfer-matrix-derived Stokes fields (Fig. 1). By fitting the effective non-Hermitian Hamiltonian with polynomial expansions to arbitrary order, the method determines complex coefficients with high precision while dramatically reducing the number of full electromagnetic simulations required. Once obtained, the effective Hamiltonian provides rapid and predictive access to the polarization-resolved band structure across momentum space.

This reduced-order description enables efficient investigation of higher-order photonic spin-orbit coupling, exceptional points, Fermi arcs, and polarization singularities without exhaustive numerical sampling. Applicable to a wide class of layered systems – including cavities with quantum wells, perovskites, organic materials, and liquid crystals [2] – the approach establishes a practical bridge between rigorous Maxwell solvers and compact analytical models. More broadly, the framework is applicable to band-structured systems in which polarization or other internal degrees of freedom are intrinsically linked to the dispersion. It therefore offers a powerful computational tool for studying complex photonic and topological phenomena [3] and for steering the design of next-generation anisotropic cavity platforms.

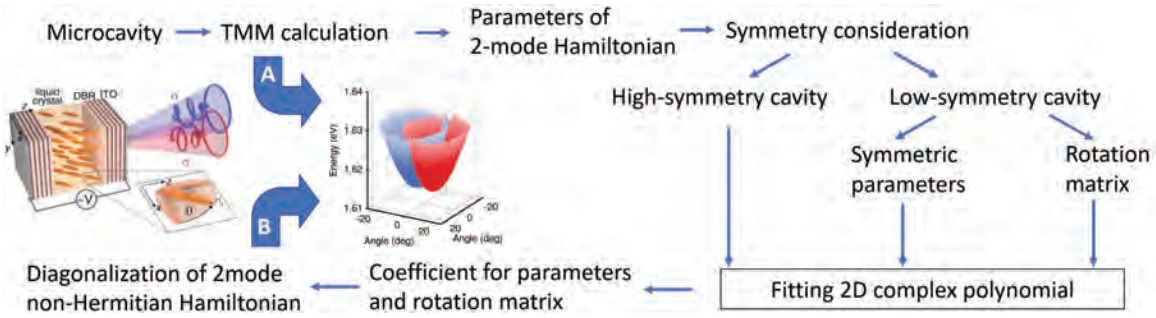

Fig. 1. Schematic illustration of the method. The images show a sketch of a liquid-crystal microcavity and the dispersion relation $E(k)$ for circularly polarized emission in the Rashba-Dresselhaus spin-orbit coupling regime [2]. Numerical **method A** (Transfer Matrix Method) is exact but computationally demanding. **Method B** requires the calculation of only a few points in parameter space while providing accurate estimates of $E(k)$ and optical losses.

References

[1] P. Oliwa, W. Bardyszewski, and J. Szczytko, "Quantum mechanical-like approach with non-Hermitian effective Hamiltonians in spin-orbit coupled optical cavities", Phys. Rev. Research 6, 013324 (2024)
[2] K. Rechcińska, et al., "Engineering spin-orbit synthetic Hamiltonians in liquid-crystal optical cavities", Science 366, 727-730 (2019)
[3] P. Oliwa, et al. "Electrically Tunable Momentum Space Polarization Singularities in Liquid Crystal Microcavities", Advanced Science 12, 2500060 (2025)

Freeform light routing in photonic integrated circuits using hyperuniform disordered structures

T. Amoah[1], A. Vafa[1,*], G. Gkantzounis[1], C. Wan[1], M. Milosevic[2], K. Debnath[2], F. Gardès[2], W. Man[3], M. Florescu[2]

[1]*Advanced Technology Institute, University of Surrey, Guildford, GU2 7XH, United Kingdom*

[2]*Optoelectronics Research Centre, University of Southampton, SO17 1BJ, United Kingdom*

[3]*Department of Physics and Astronomy, San Francisco State University, San Francisco, CA 94132, USA*

*a.pourmohammadqolivafa@surrey.ac.uk

Most existing photonic integrated circuit design strategies lie at opposite ends of the complexity spectrum: they are either highly simplified, such as strip and photonic crystal (PC) interconnects, or rely on computationally intensive and often unintuitive structural optimization schemes [1]. Recent studies have shown that large photonic band gaps (PBGs) can arise not only in periodically structured PCs but also in disordered photonic materials, provided that the disorder is appropriately constrained to exhibit hyperuniformity [2]. Hyperuniform disordered (HUD) materials lack preferential directions and are statistically isotropic. This allows light to be guided along arbitrary pathways.

In this work, we present a pathway-first approach to design freeform planar photonic interconnects implemented in nearly HUD photonic slabs. Rather than optimizing a predefined lattice or topology, we prescribe the desired optical pathway and construct the surrounding dielectric environment locally to support PBG-guided transport.

Figures 1 presents the guided field profile and transmission spectra for a freeform interconnect designed to mimic the shape of a tanh function, embedded in a near-hyperuniform background in a planar silicon slab. The spectrum is compared against a straight W1 waveguide in a honeycomb structure of the same dimensions and material. We use a slab thickness of 0.48a and a wall width of 0.4a. Across the low-loss transmission window, our interconnect design exhibits substantial transmission, reaching values comparable to those attained by the straight photonic crystal waveguide.

These results demonstrate that the pathway-first near-hyperuniform design strategy preserves the guided-mode manifold of the reference photonic crystal waveguide over a broad spectral range, enabling efficient freeform routing without catastrophic degradation of transmission.

We note that the curved interconnects exhibit additional resonant features in their transmission spectra, which can be mitigated through further local optimization of the interconnect environment.

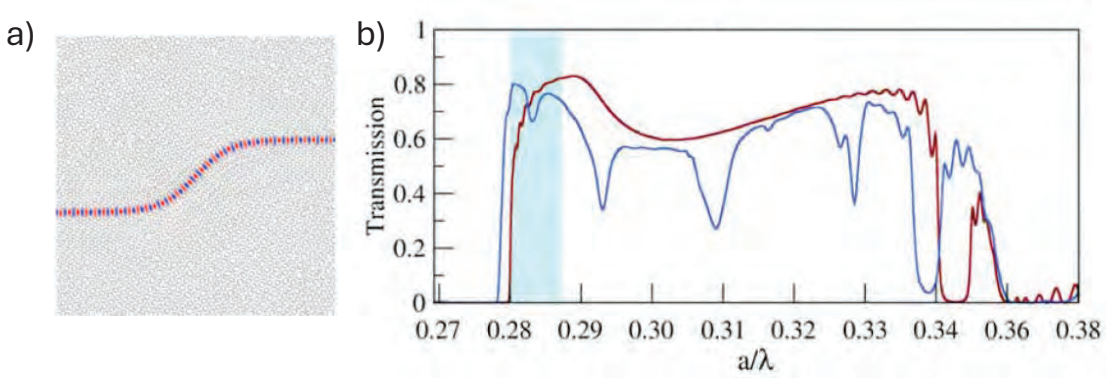

Fig. 1. a) The guided field of a freeform tanh-shaped interconnect, and b) its transmission spectrum (blue) compared to a straight PC waveguide (red). The shaded area denotes the low-loss transmission window.

Fano resonances in deep subwavelength gratings

S.J. Verwer,[1,2] I. D. Setija,[2,3] A.F. Koenderink,[1]

[1]*AMOLF, center for Nanophotonics, Amsterdam*
[2]*Eindhoven University of Technology*
[3]*ASML*

Fano resonances arises from the interference of broad and narrow spectra of radiation and becomes an important tool for many applications in the physical, chemical, and biological sciences [1]. Research has shown that these resonances can be found within dielectric structures by interference between the broad Fabry-Perot resonance and the narrow guided mode resonance (GMR) [2]. Further research has shown that dimerization of gratings opens up a quasi-Bound state in the continuum (qBIC) and increases the wavelength at which the Fano resonances show up [3]. Within this study we will extend these previous works and show that using the concept of band folding we can obtain Fano resonances at larger relative wavelengths by tuning the asymmetry within deep subwavelength gratings.

[1] Limonov, M., Rybin, M., Poddubny, A. et al. Nature Photonics 11, 543–554 (2017).
[2] C. Chang-Hasnain, 2010 23rd Annual Meeting of the IEEE Photonics Society, Denver, CO, USA, 2010, pp. 467-468
[3] Overvig, Adam C., Shrestha, Sajan and Yu, Nanfang. Nanophotonics, vol. 7, no. 6, 2018, pp. 1157-1168.

Passive and Active Plasmonic Metafiber Devices

J. Wang[1,*], L. Zhang[2], M. Qiu[2]

[1]*Ministry of Education Engineering Research Center of Smart Microsensors and Microsystems, School of Electronics and Information, Hangzhou Dianzi University, Hangzhou 310018, China*

[2]*Key Laboratory of 3D Micro/Nano Fabrication and Characterization of Zhejiang Province, School of Engineering, Westlake University, 18 Shilongshan Road, Zhejiang Province, Hangzhou 310024, China*

*jiyongwang@hdu.edu.cn

Metafibers expand the functionalities of conventional optical fibres to unprecedented nanoscale light manipulations by integrating metasurfaces on the fibre tips, yielding a variety of advanced applications such as ultrafast fiber lasers[1,2], planar waveshaping[3,4], and ultracompact sensing[5]. Current metafibers remain proof-of-concept demonstrations that mostly explore isolated bare fibres owing to the lack of standard interfaces with universal fiber networks. Here I will first introduce the methodologies for fabricating well-defined plasmonic metasurfaces directly on the end facets of commercial single-mode fibre jumpers using standard planar technologies. After that I will demonstrate two practical applications of our metafibers in the regimes of passive and active plasmonic devices.

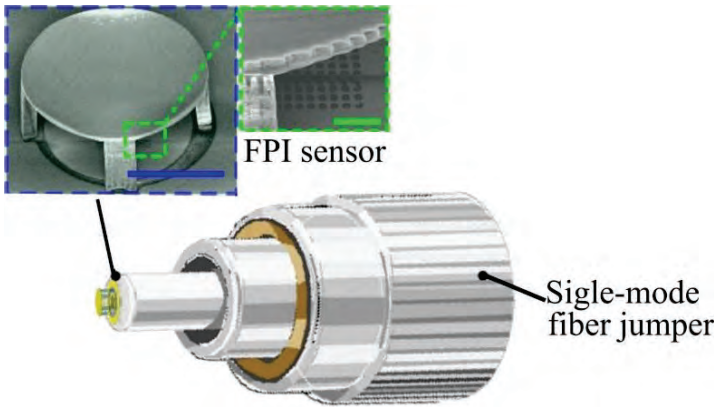

Fig. 1. A metafiber Fabry-Perot interferometer (FPI) is integrated on the facet of commercial single-mode fiber jumper. The blue and green scale bars represent 38 μm and 3.5μm, respectively.

References

[1] C. Zhang, L. Zhang, H. Zhang,B. Fu, J. Wang, M. Qiu, “Pulsed Polarized Vortex Beam Enabled by Metafiber Lasers” , PhotoniX, 5, 36 (2024).

[2] L. Zhang, H. Zhang, X. Chen, F. Liu, X. Sun, H. Yu, X. Sun, Q. Jia, B. Chen, B. Cluzel, P. Grelu, A. Coillet, F. Qiu, L. Ying, W. Sha, X. Liu, J. Qiu, D. Zhao, W. Yan, D. Wu, X. Shen, J. Wang, M. Qiu. ’Plug-And-Play’ Plasmonic Metafibers for Ultrafast Fibre Lasers. Light Adv. Manuf., 3, 45(2022).

[3] C. Zhang, L. Cong, J. Zhang, H. Meng, S. Peng, S. Li, H. Zhang, Y. Wang B. Fu, J. Wang, M. Qiu, Advanced Metasurfaces: Precise Modulations of Light in Space and Time Domains, Adv. Photonics, 8,14003(2026).

[4] L. Zhang, X. Sun, H. Yu, N. Deng, F. Qiu, J. Wang, M. Qiu, Plasmonic Metafibers Electro-Optic Modulators, Light Sci. Appl., 12, 198(2023).

[5] L. Zhang, X. Shang, S. Cao, Q. Jia, J. Wang, W. Yan, M. Qiu, Optical Steelyard: High-Resolution and Wide-Range Refractive Index Sensing by Synergizing Fabry–Perot Interferometer with Metafibers, PhotoniX, 5, 24(2024).

Opto-mechanical analogue of Peierls transition

Torgom Yezekyan*, Sergey I. Bozhevolnyi
Centre for Nano Optics, University of Southern Denmark, Odense, 5230, Denmark
*ty@mci.sdu.dk

The Peierls transition is a fundamental phenomenon in condensed-matter physics, where a one-dimensional periodic system undergoes a spontaneous structural distortion that opens a band gap and lowers the system's energy, leading to a phase transition from metal to insulator [1]. In this work, we present an opto-mechanical analogue of the Peierls transition realized in a diffraction grating waveguide coupler [2]. When illuminated by light, optical gradient forces act on the grating ridges and can drive a symmetry-breaking deformation of the structure. At certain wavelengths, the initially uniform grating becomes unstable and relaxes into a configuration with a doubled spatial period, closely mirroring the lattice dimerization characteristic of the Peierls transition.
This mechanically induced structural change has a pronounced impact on the optical response of the system (Fig. 1). In particular, the period-doubled configuration allows for normally incident radiation to efficiently excite waveguide modes that were inaccessible in the symmetric structure, resulting in strongly modified transmission. Our results demonstrate how classic concepts from solid-state physics can be translated into nanophotonic systems and suggest new routes toward optomechanically controlled photonic devices, such as all-optical switches and reconfigurable filters.

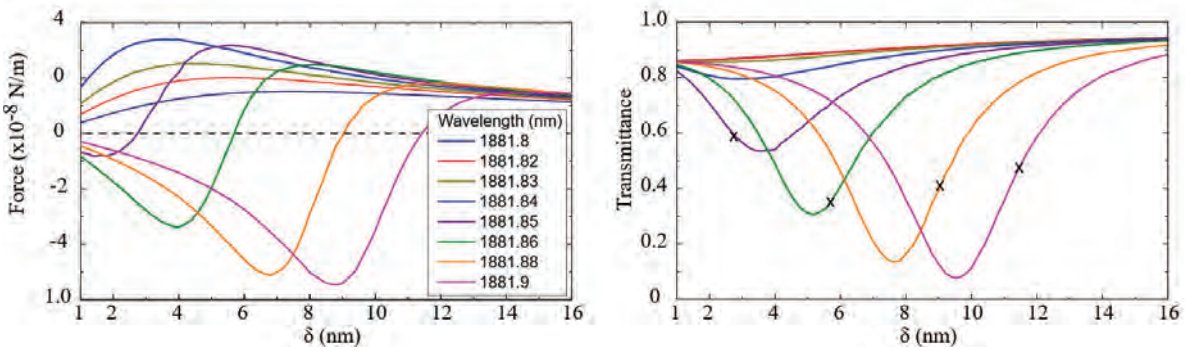

Fig. 1. Optical force (left) and transmission (right) dependences on the ridge displacement δ calculated for different wavelengths, with the crosses indicating the zero-force ridge displacements.

References

[1] R. Peierls, "More surprises in theoretical physics", Princeton University Press (2020).
[2] T. Yezekyan, S. I. Bozhevolnyi, "Opto-mechanical analogue of Peierls transition", New J. Phys. **27**, 122002 (2025)

Angle Invariant Scattering in Metasurfaces

M. Yücel [1,*], F. S. Cuesta [1], K. Achouri [1]

[1] *Laboratory for Advanced Electromagnetics and Photonics, École Polytechnique Fédérale de Lausanne (EPFL), Lausanne, 1015, Switzerland*

[*] *mustafa.yucel@epfl.ch*

Metasurfaces are an emerging technology in various fields due to their ability to easily control and shape incident waves. Nevertheless, angular dispersion and its link to nonlocality remain underexplored. To analyze metasurfaces with different shapes and symmetries, we use the Generalized Sheet Transition Conditions (GSTCs) as a mathematical framework [1].

$$\hat{z} \times \Delta\mathbf{H} = j\omega\mathbf{P}_{\parallel} - \hat{z} \times \nabla_{\parallel} M_z, \tag{1a}$$

$$\hat{z} \times \Delta\mathbf{E} = -j\omega\mu_0\mathbf{M}_{\parallel} - \hat{z} \times \nabla_{\parallel} \left(\frac{P_z}{\epsilon_0}\right). \tag{1b}$$

Based on this formalism, we derive equations and conditions under which the response remains unchanged with respect to variations in the angle of incidence. As examples, we investigate angle-invariant co- and cross-polarized transmission and reflection, where the amplitude, phase, or both remain unchanged. We also show explicitly that nonlocality enables the suppression of angular dispersion, leading to angle-invariant scattering. We further show that a pseudochiral metasurface enables efficient extrinsic chirality in a semi–angle-invariant system. These results clarify our understanding of angular dispersion and open new opportunities for applications sensitive to dispersion effects.

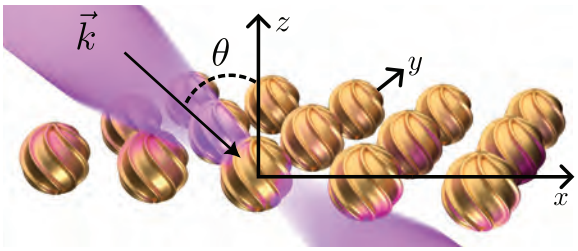

Fig. 1. **Generalized sheet transition conditions on a metasurface**. The period of the array is small enough compared to the wavelength so that the scattering response of the metasurface may be modeled by homogeneous effective material parameters.

References

[1] K. Achouri, C. Caloz Electromagnetic metasurfaces: Theory and applications 2021, John Wiley & Sons

[2] M. Yücel, F. S. Cuesta, K.Ãchouri Angle-invariant scattering in metasurfaces Phys. Rev. B, vol. 111, p. 235448, Jun 2025

Low-frequency electromagnetic forces for bio-nanoparticle manipulations

S. Zavatski [1,*], O.J.F. Martin [1],

[1] *Nanophotonics and Metrology Laboratory, Swiss Federal Institute of Technology Lausanne (EPFL), Lausanne, 1015, Switzerland*

[*] *siarhei.zavatski@epfl.ch*

Manipulation of matter by electromagnetic forces and torques is at the forefront of various research fields spanning from nanotechnology to medicine. While optical tweezers have traditionally been viewed as the standard tool for generating them, there are other approaches that enable electromagnetic manipulation of nanoscale entities. One of them is dielectrophoresis (DEP), which operates in a lower frequency range of electromagnetic fields, yet stands on the same physical principles: the interaction of matter with gradients of the field intensity or phase [1].

Here, we address the long-standing challenge of accurately predicting the DEP response of bio-nanoparticles, which has previously been identified by observing the discrepancy between simulations and experimental measurements of their DEP polarizability (Clausius-Mossotti) factor [2]. To do this, we depart from the assumptions of the standard DEP model, which considers a thin electrical double layer surrounding the particle in aqueous conductive buffers. Since no analytical DEP models exist for this case, we calculate DEP polarizability factors numerically using the Poisson-Nernst-Planck equations. The simulation results show that the polarizability factor can significantly exceed the theoretical bound of unity defined by the Clausius-Mossotti relation (Fig. 1a), which may explain previous experimental observations of nanoparticle trapping by applying lower DEP forces than the minimum required by the standard DEP theories [2]. We also observe good agreement between the simulated and experimentally measured polarizability values for 50-60 nm diameter polystyrene beads and the bovine serum albumin (BSA) immersed in aqueous buffers of 0.5-8 mM ionic strength (Figs. 1b, c). These findings emphasize the importance of accounting for electrical double layer polarization at the nanoscale and shall accelerate further research toward developing novel DEP theoretical models.

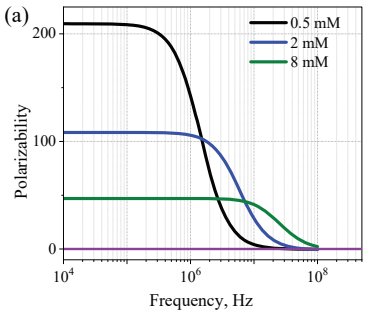

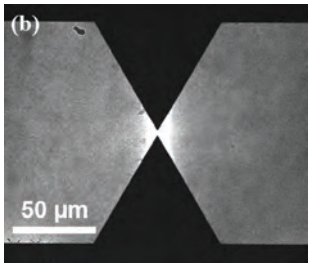

(c)

I, mM	Simul.	Exp.
0.5	201.2	122 ± 14.1
2	108.2	96.8 ± 4.3
8	48.3	67.0 ± 3.3

Fig. 1.: (a) Simulated DEP polarizability factors for BSA in a liquid of various ionic strength, I. (b) Fluorescent microscopy image of BSA after DEP trapping. (c) Comparison of simulated and experimentally measured DEP polarizability factors for BSA

References

[1] M. Riccardi, O. J. F. Martin, "Electromagnetic forces and torques: From dielectrophoresis to optical tweezers", Chem. Rev., **123(4)**, 1680 (2023).

[2] S. Zavatski, H. Bandarenka, O. J. F. Martin "Protein dielectrophoresis with gradient array of conductive electrodes sheds new light on empirical theory", Anal. Chem. **95(5)**, 2958 (2023).

Designing optical metagrating for total internal reflection

Mads LArsen, Emil Priergaard, Vladimir A. Zenin*
Center for Nano Optics, University of Southern Denmark, Odense, DK-5230, Denmark
*zenin@mci.sdu.dk

The are optical setups where illumination of the sample creates unwanted background, which obscures a study of the sample (Fig. 1). There exist many ways to mitigate this background by modifying the illumination (for example, dark-field and phase contrast optical microscopy). However, sometimes there is little room for modification of the illuminating beam (e.g., in transmission-mode scattering-type Scanning Near-field Optical Microscopy). A proposed solution is to use a metagrating, which will bend a normally incident light to the angle beyond the critical angle, prohibiting it from escaping a glass substrate of the sample. This metagrating is designed to be reusable by employing immersion oil to attach it to any sample substrate.

Here we study different designs of metagratings based on Si nanostructures, deposited on a glass substrate and encapsulated into a glass-like polymer (Fig. 1). The grating was designed to operate at telecom wavelengths (around 1500 nm). When fabrication limitations were taken into account (minimum edge-to-edge distance was set to be 100 nm), then the best performance was achieved for a simple design with two cylinders, resulting in more than 70% of incident light being bent into the first diffraction order. Next step would be to verify this performance in the experiment.

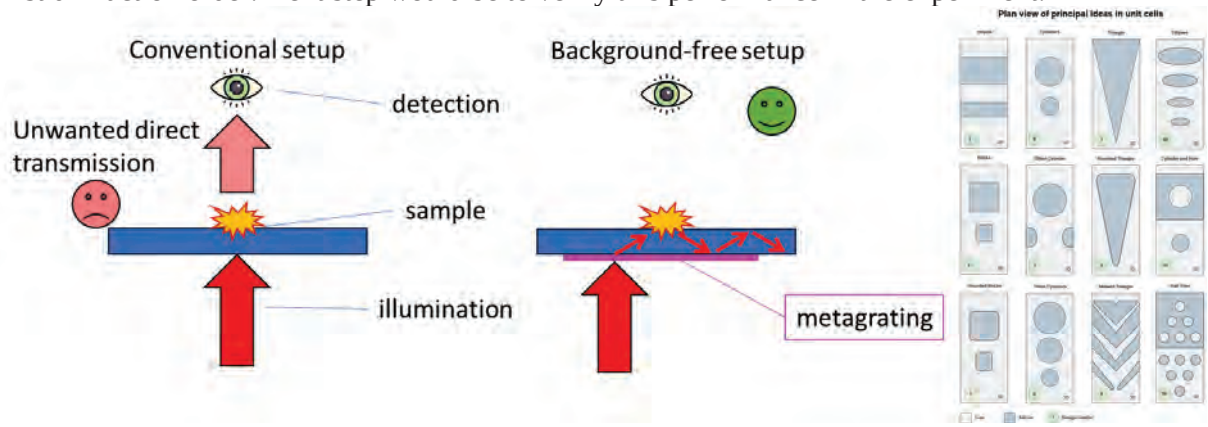

Fig. 1. Left: how metagrating can help to eliminate unwanted background. Right: different designs of Si metagratings studied here. A metagrating with two Si cylinders (design 2) was found to be optimal, when limitations of the fabrication were taken into account.